UNCLASSIFIED

AD 295 490

Reproduced
by the

ARMED SERVICES TECHNICAL INFORMATION AGENCY
ARLINGTON HALL STATION
ARLINGTON 12, VIRGINIA

UNCLASSIFIED

63-2-3

ASD-TDR-62-899

CAVITY VAPOR GENERATOR PROGRAM

TECHNICAL DOCUMENTARY REPORT No. ASD-TDR-62-899

DECEMBER 1962

FLIGHT ACCESSORIES LABORATORY
AERONAUTICAL SYSTEMS DIVISION
AIR FORCE SYSTEMS COMMAND
WRIGHT-PATTERSON AIR FORCE BASE, OHIO

Project No. 8173, Task No. 817305-14

NOTICES

When Government drawings, specifications, or other data are used for any purpose other than in connection with a definitely related Government procurement operation, the United States Government thereby incurs no responsibility nor any obligation whatsoever; and the fact that the Government may have formulated, furnished, or in any way supplied the said drawings, specifications, or other data, is not to be regarded by implication or otherwise as in any manner licensing the holder or any other person or corporation, or conveying any rights or permission to manufacture, use, or sell any patented invention that may in any way be related thereto.

Qualified requesters may obtain copies of this report from the Armed Services Technical Information Agency, (ASTIA), Arlington Hall Station, Arlington 12, Virginia.

This report has been released to the Office of Technical Services, U.S. Department of Commerce, Washington 25, D.C., in stock quantities for sale to the general public.

Copies of this report should not be returned to the Aeronautical Systems Division unless return is required by security condiderations, contractual obligations, or notice on a specific document.

200 - January 1963 - 3-24

FOREWORD

This report was prepared by the General Electric Company, Missile and Space Division, on Air Force Contract Number AF 33(616)-8394, Project Number 3145, Task Number 60962; "Cavity Vapor Generator Development Program." The work was administered under the guidance of Directorate of Aeromechanics, Deputy for Technology, Aeronautical Systems Division.

This report covers work initiated in June of 1961 and completed in September of 1962.

The personnel who actively participated in the generator development were:

D. L. Purdy	Systems Project Engineer, GE-MSD
J. J. Guy	Program Development Office, GE-MSD
E. W. Williams	Generator Design and Fabrication Engineer, GE-MSD
R. C. Keyser.	Generator Fabrication and Test Engineer, GE-MSD
F. A. Blake	Collector System Engineer, GE-MSD
J. F. Williams	Generator and System Technician, GE-MSD
E. F. Batutis	Thermal Energy Storage Chemist, GE-MSD
J. C. Danko	Manager, Advanced Space Power Engineering, GE-MSD
H. Kitson, Jr.	Manager, Advanced Design and Development, GE-MSD
D. Jones.	Converter Development Engineer, GE-Power Tube Department

The following paper was presented in connection with this contract:

Purdy, D. L. "Thermionic Cavity Generator Development," American Rocket Society Space Power Systems Conference, September 25-28, 1962. Paper #2572-62.

ABSTRACT

A description of the theoretical study, design, and test of a thermionic generator utilizing solar energy concentrated by means of a parabolic collector. The generator produced 21.25 watts at a cathode temperature of 1773°K in solar test with a five foot diamter, sixty degree rim angle, parabolic collector.

Expected future performance of solar thermionic systems are discussed.

PUBLICATION REVIEW

Publication of this technical documentary report does not constitute Air Force approval of the report's findings and conclusions. It is published only for the exchange and stimulation of ideas.

TABLE OF CONTENTS

LIST OF ILLUSTRATIONS

LIST OF ILLUSTRATIONS (Cont'd)

LIST OF ILLUSTRATIONS (Cont'd)

LIST OF TABLES

1.0 INTRODUCTION AND SUMMARY

The Cavity Vapor Generator (CVG) Program successfully demonstrated the feasibility of operating a multiple vapor-converter generator at the focus of a parabolic solar collector. A peak power of 21.25 watts, at 1.21 volts and 17.50 amps, was obtained at a cathode temperature of 1773°K, with all 3 converters operating in series. At a cathode temperature of 1668°K, 14.54 watts, at .97 volts and 15 amps, was obtained with 3 converters operating in series. A generator efficiency of 3.89%, excluding aperture losses was recorded at 1663°K cathode temperature, close to the design point of 1650°K.

A corresponding efficiency of 2.02%, including aperture losses, was recorded. All data points were obtained at steady-state electrical and thermal equilibrium. No dynamic electrical testing was employed.

The test system is shown in Figure 1. It consists of a series of venetian blind type shutters that control the amount of solar energy impinging on the collector, a 5' diameter, 60° rim angle collector with a highly reflective coating, and a 12" diameter vacuum tank with a quartz faceplate through which the solar energy is transmitted. A vacuum, during operation of the generator, on the 10^{-6} scale is supplied by a diffusion pump backed up by a roughing pump. The diffusion pump passes through a rotating "O" ring joint to allow it to remain vertical during tracking of the sun in elevation, by the antenna drive system. This drive and tracking system was developed for operation of the STEPS I* system, and was modified to accommodate the present system. Silicon solar sensors provide the input error signal to allow a sun tracking error of less than two minutes of arc. The entire platform on which the instrumentation, operating personnel, and roughing pump are located rotates in azimuth, whereas the vacuum tank, collector, and collector support structure rotate in elevation. Instrumentation leads pass from the generator, through the vacuum baseplate, to the recorders on the platform rear.

The CVG, shown in Figures 2 and 3, is placed within the vacuum tank with its aperture positioned at the focal point of the parabolic collector. It consists of 3 vapor converters positioned radially around axis of the collector, forming a cavity for solar energy absorption by means of shoes welded to the converter cathodes. The concentrated energy from the solar collector passes through the aperture and impinges on the cathode shoes. Insulation surrounds each converter, consisting of 60 layers of machined and dimpled tantalum foil, effectively forming a series of radiation shields. A front aperture cone protects the insulation and generator body from over-temperature due to collector accuracy or orientation system misalignment.

---

*See Final Report on Solar Thermionic Electrical Power System Technical Documentary Report ASD-TDR-62-74, March 1962.

NOTE: Manuscript released by the authors Nov. 1962 as an ASD Technical Documentary Report.

Figure 1. CVG Test System

2

Figure 2. CVG Detail Drawing
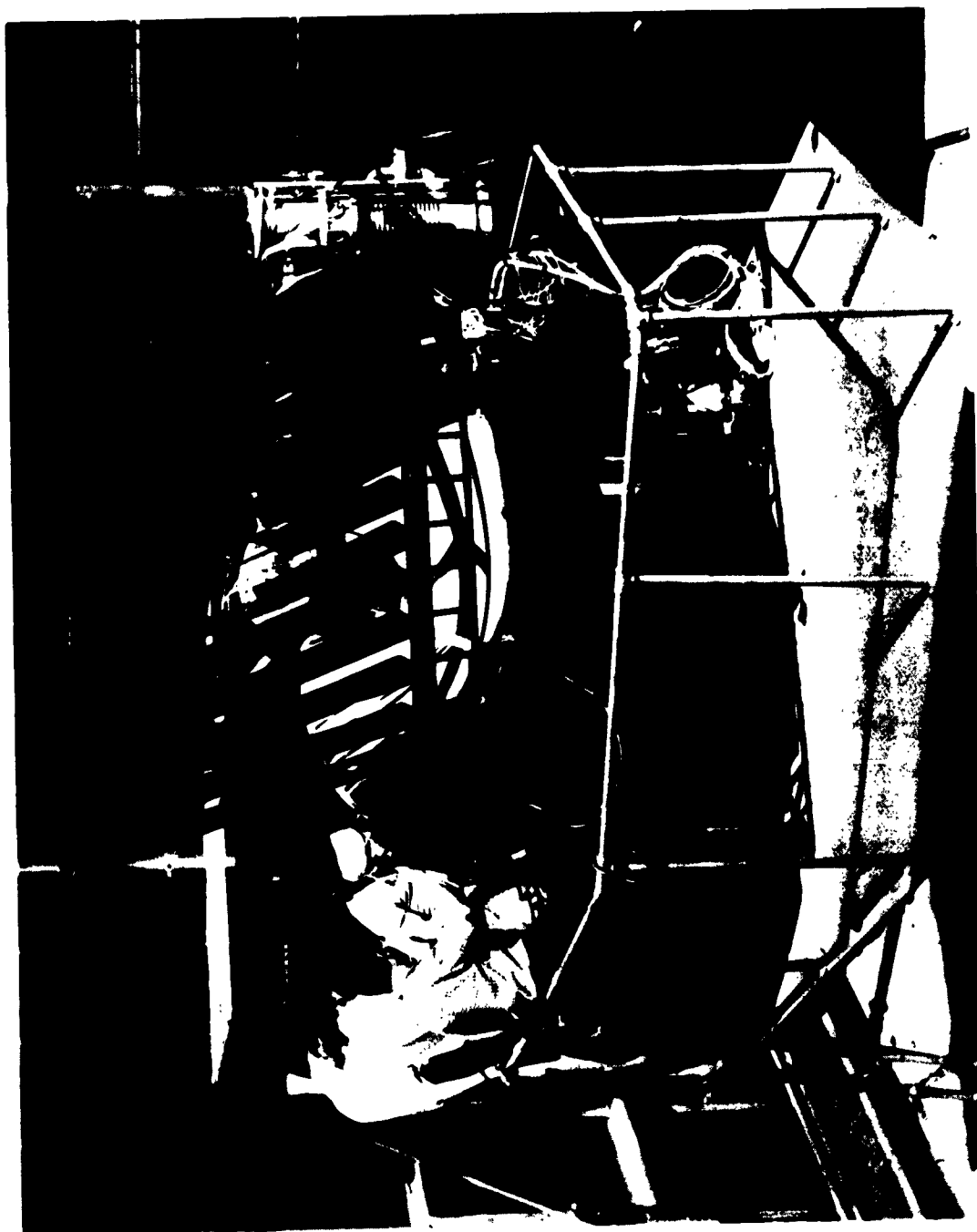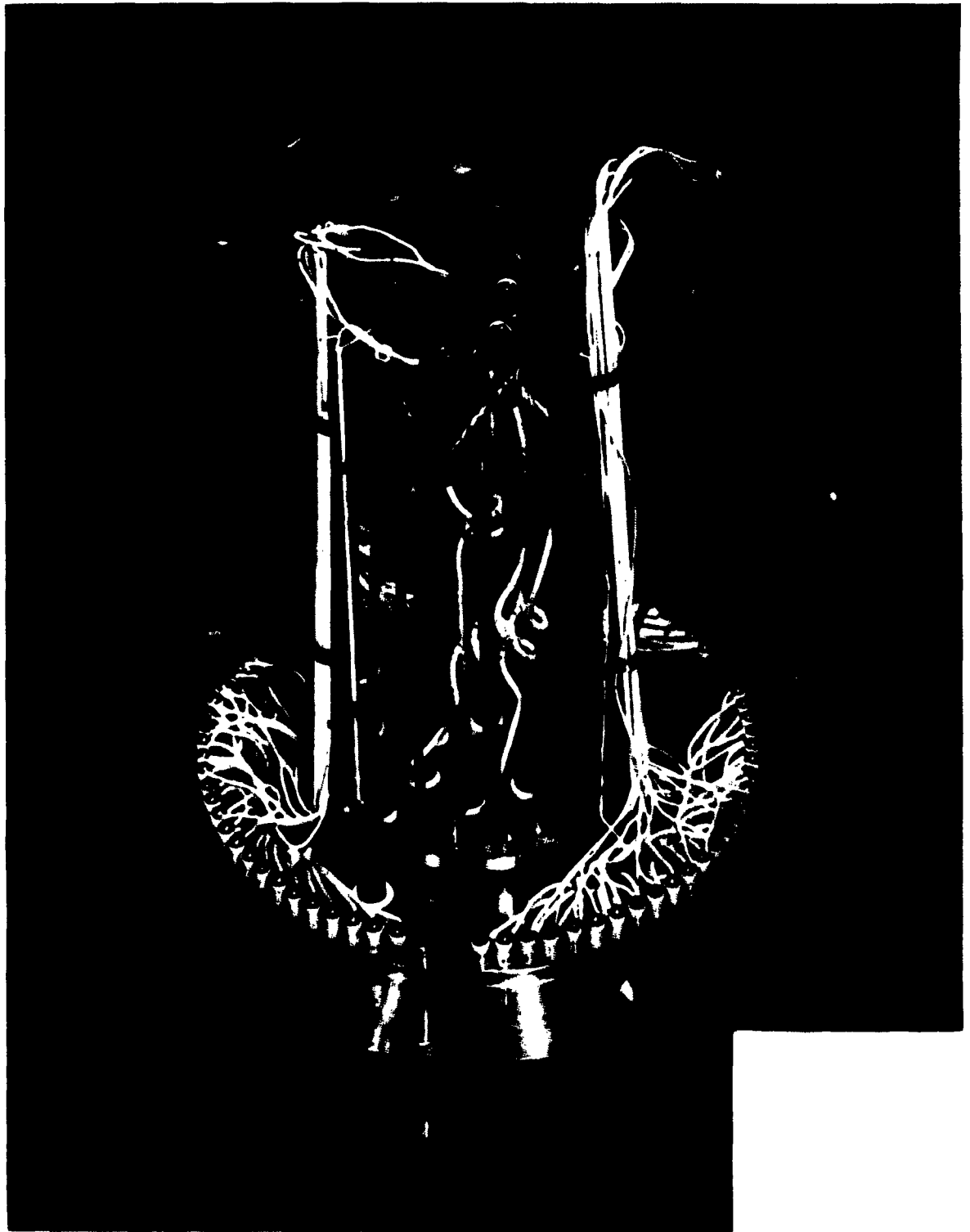
Figure 3. CVG on Vacuum Chamber Mounting Stand

4

Each converter is electrically insulated from the heat shield type insulation by ceramic spacer rings encircling the cylindrical envelope, and by ceramic bushings that hold the radiating fin to the generator exterior. The cathode shoes are also prevented from touching by thoria spacers between the shoes.

The molybdenum cathode is welded to the cathode pickup shoe and to a cylindrical tantalum envelope. This envelope provides an electrical conducting path to the cathode, and contains the cesium. The cool side of the envelope is attached to a ceramic seal, the other side of which is attached through a semi-flexible member to the anode slug. The heat is rejected via a circular anode radiating fin. Exterior to this fin is the cesium reservoir tube. Its temperature is controlled at an optimum value by means of an electrical resistance heater, controlled from the exterior of the tank.

Detailed performance information and system descriptions appear in the body of this report.

2.0   PROGRAM OBJECTIVES

The primary objective of the CVG Program was to prove the feasibility of a multi-vapor converter solar generator, designed to operate at the focus of a parabolic collector. Operation of the converters in series was considered necessary to prove this feasibility. This feasibility was proven. In addition, the program was intended to define various component and system interactions, collect technical data useful for generator redesign, and establish and verify analytical techniques used in generator design.

The feasibility of thermal storage systems was also to be investigated by means of the construction and test of an integral thermal storage container and converter. This objective was not met when the container of the thermal storage material failed under test.

To accomplish the overall objectives, a series of system and component design objectives were formulated as follows:

Converter Objectives

1)   Cathode temperature - Based on a thermal energy requirement for the generator of 1/2 that available from the collector.

2)   Converter efficiency - 11%

3)   Seal temperature - 600°C maximum

4)   Converter type - Cesium vapor filled planar converters.

5)   Converter temperature range - 1400-1850°K

6)   Cesium temperature - low enough to allow for a 30% increase in power upon heating by an external resistance heater.

7) Anode heat rejection - by radiation only.

8) Anode temperature control - sufficient to increase the anode temperature by 100°C.

Generator Objectives

1) Aperture diameter - sufficient to provide a maximum of energy available for the generator structure after re-reflection and re-radiation losses have been accounted for.

2) Insulation requirement - maximum insulating capability in a minimum height and chemically stable up to 1900°K.

3) Three converters to be utilized.

4) Off - orientation protection.

5) Instrumentation - Electrical measurement $\pm$ 1%. Temperature measurement - $\pm$ 5°C.

6) Generator efficiency of 10%, excluding re-radiation and reflection losses.

System Objectives

1) Vacuum system surrounding the generator for simulation of space and environmental protection of the generator.

2) Vacuum requirement - 10^{-7} to 10^{-6} mm of Hg during operation.

3) Collector Diameter - sufficient to provide twice the energy required for the generator at its design point.

4) Collector Reflectivity - maximum .8 - 1.0

5) Energy Input control - 0 watts to maximum

6) Collector Rim Angle - 45° - 60°

7) Collector accuracy - Less than 4 minutes of slope error.

8) Vacuum Chamber cooling water cooled.

9) Instrumentation - sufficient to provide electrical and thermocouple feedthroughs for complete temperature and electrical performance definition.

10) Tracking accuracy - Less than six minutes of angular error.

11) Focal spot adjustment - Possible after generator mounting.

6

3.0 ACCOMPLISHMENTS AND RECOMMENDATIONS

Accomplishments include:

1) Successfully designed, built and tested a vapor converter generator operating with 3 converters in series, delivering 21.25 watts at 1.21 volts output.

2) Built and successfully tested a vacuum system for solar testing of thermionic generators. This vacuum system with generator temperatures of approximately $1750^{\circ}K$ operates between 5×10^{-7} and 2×10^{-6} mm of Hg.

3) Successfully built and tested a collector system utilizing a searchlight mirror with a highly reflective coating and louvre shutters for energy input control. This system automatically tracks the sun at less than 2 minutes of orientation accuracy.

4) Developed calorimetric, accuracy, and flux density measuring techniques to explicitly define the performance of solar collectors. These parameters were successfully measured on a 60" collector.

5) Successfully instrumented and obtained thermocouple data on the CVG generator, including thermal gradients within the cavity, on the converters and on the generator exterior.

6) Developed calorimetric techniques and measured the thermal characteristics, individual converters, the generator, insulations and coatings. This includes converter and generator efficiency measurements.

7) Developed analytical techniques and correlated these with experimental facts for the design and construction of solar thermionic generators, converters and systems.

Recommendations based on the cavity vapor program analytical and test results, both laboratory and solar are:

1) The converter efficiency must be improved. Possible methods would be to reduce spacing, investigate new emission metals, modify envelope structure, and investigate molybdenum poisoning prior to or during operation.

2) The problem of cracking at the cathode-envelope interface should be examined. Embrittlement and cracking occurs which possibly could be corrected by proper material selection.

3) Converter fabrication techniques should be examined with the intent of improving reproducibility of performance, reliability, and less susceptibility to thermal cycling failures.

4) The envelope length area and anode choke dimensions should be modified to conform to a new design-point and insulation characteristic. Trade-offs between insulation and envelope thermal losses, as a function of envelope length and efficiency, should be prepared and a new envelope length and insulation thickness determined.

5)   The cesium regulator must be capable of regulating at different cesium temperatures, since the optimum reservoir values vary from converter to converter.

6)   The design-point should be re-evaluated. The cathode temperature is felt to be too low and a more ideal temperature would be in the range of $1750^\circ K$ to $1850^\circ K$.

7)   The cathode shoe and cathode should be made of the same material, if possible, to eliminate thermal expansion mismatches and subsequent cracking.

8)   The external heaters on the anode fin and cesium reservoir should be omitted. Self-regulating controls operating on the thermal waste heat should be developed.

9)   The converter fin, now only a thermal structure, would be integrated with the generator structure to conserve weight.

10)   Converter life tests in a thermal environment similar to that used in the operable generator should be undertaken.

11)   Thermocouple improvements would be to use alumina rather than beryllia as protective shields on the cathode couples, and to adopt the policy of never re-using a W-Re couple due to its fragility under thermal stress after initial thermal cycling.

12)   Laboratory testing of a complete generator with resistive, or electron bombardment, heating should be performed prior to sun testing.

13)   The radiation shield design should be re-evaluated. Molybdenum should be investigated as a replacement for tantalum, and a separation approach utilizing ceramic spacers should be investigated. Other insulations, such as powders, cloth, wool, fibers and flakes should be investigated.

14)   Experimental and theoretical studies should be made of the aperture diameter size variation. The one inch aperture on the present CVG generator is too large, and results in excessive aperture losses.

15)   Studies should be made to determine more accurately the need for and thermal characteristics, including system degradation, of the front aperture cone.

16)   The cavity optics, including re-radiation and re-reflection characteristics should be more carefully evaluated. The computation of re-reflection loss, when compared to calorimeter data, results in a high loss due to the assumption of diffuse reflection from the cavity wall. Specular reflection has a dominant effect.

17)   A means for eliminating the large insulation crack losses should be included in the generator redesign.

18)   The spacers within the generator were not satisfactory. A more reliable approach is needed.

8

4.0 PRELIMINARY SYSTEM DESIGN

4.1 Collector Size and Type

Due to the difficulty in obtaining complete performance data on the STEPS I system, it was established early in the program that the collector for the CVG program should be over-sized by a factor of 2, i.e., twice the energy required for operation of the generator at its design point should be available from the collector. This safety factor would provide for over-temperature capability of the generator to obtain complete performance information as a function of cathode temperature and would also provide some leeway for the errors that always exist between preliminary design estimates and final performance characteristics of any system. Since the vapor generator for the CVG program was expected to operate at a higher cathode temperature than the STEPS design point of $1423^{\circ}K$, a more accurate collector than the STEPS I collector would be required. A smaller one would also be required since the total number of converters would be between three and five for the CVG Program, whereas 105 were used in the STEPS I program. Since five foot diameter Army searchlight collectors were readily available, an investigation was conducted to determine the suitability of this collector for the cavity vapor generator. This collector was expected to have a slope error of less than 4 minutes which was within the accuracy tolerance required. Estimates were then made of window transmissivity, collector reflectivity, collector performance, and shadow area. The total available energy at the focal point of the system was then computed and compared to generator requirements.

Estimates made in June of 1962 of the converter performance are shown in Table 1. Utilizing the values of thermal energy required for operation of the cathode of the converter from this table, and by selecting a 3 cm^2 cathode area, with 3 converters in series the factor-of-2 safety factor could be maintained at a cathode temperature of $1650^{\circ}K$. This operating temperature was also consistent with the design objectives of a ten percent-efficiency generator. Although a 45 to 50 degree rim angle mirror would have been preferable, the ready availability of the 5 foot diameter mirror coupled with the fact that its accuracy was much greater than had previously been produced, confirmed the selection of the collector.

TABLE 1

CONVERTER PERFORMANCE COMPUTED JUNE 1962

Cathode Temperature, $^{\circ}K$	1400	1700	2100	2500
Thermal Energy Input, watts/cm^2 of cathode	14.37	27.3	68.28	122.2
Converter Efficiency	4.46	12.3	17.9	23.5
Electrical Power Output, watts/cm^2	.603	3.37	12.2	28.7
Current, amps/cm^2	2.7	6.4	13.0	21.0

4.2 Vacuum Chamber Type and Selection

A majority of the problems on the STEPS I Program were due to operating the generator in the oxidizing atmosphere of air. Since a large factor in the design of a solar thermionic system for space operation is the necessity to transfer heat by radiation, the selection of a vacuum environment surrounding the generator was made. As was discussed under the objectives of the vacuum system, a number of performance and design parameters had to be met. The chief objective was obtaining a vacuum of less than 10^{-5} mm of mercury during hot operation of the generator. This low vacuum was felt to be necessary because most of the refractory materials, particularly tantalum, will react with water vapor, oxygen, or other mixed gases within a vacuum system, causing deterioration of their material properties. Tantalum for example, is extremely active and will getter oxygen from the system. This gettering of the oxygen (or hydrogen) can cause embrittlenent, change of thermal characteristics, such as emissivity, change in grain structure by attack along the grain boundaries, and could cause failure of the very thin converter envelope.

Another problem considered was that the vacuum system had to operate at varying angles as the collector tracked the sun. The first vacuum pump selected was an ion pump operating at the base of the vacuum tank and attached to it. This pump can operate at varying angles with respect to the horizontal. Preliminary estimates of the outgassing rate, the shadow area and the weight of this ion system, however, indicated that its pumping speed would be insufficient. Also its weight would approximate 500 pounds, causing strain on the support structure. Furthermore, its location at the base of the vacuum system would unduly complicate the problem of passing leads from the vacuum system to the exterior recording instruments. Based upon this investigation, a diffusion pump was then considered. The diffusion pump was lightweight, could obtain large pumping speeds at low pressures with the use of liquid nitrogen trapping, but unfortunately could not deviate from the vertical by more than $15°$. The Tri-Metals Corporation of New Jersey, therefore, undertook a program to develop a rotating joint which would allow the diffusion pump to remain vertical. It is this design which was subsequently selected and used, and has been shown in Figure 1.

4.3 Converter Size and Performance

In June of 1962 the expected converter performance was as illustrated in Table 1. These estimates have been subsequently proven to be optimistic. The performance was measured on molybdenum cathode and anode converters of 5 cm^2 area and sufficient data on the continued performance at these high levels of electrical power output were not available. In addition, the information at that time indicated that an extremely sensitive condition with regard to spacing existed and that the optimum spacing of the device was in the vicinity of .009 inches. This is now felt to be too large. Also, in order to estimate the insulation performance, a degradation of the converter performance of 10% was assumed based upon calculations made on the area of insulation required within a typical generator assuming emissivities of 0.1 and a series of heat shields which were not thermally connected by conduction paths. This assumption was assumed to be realistic and subsequently has been shown to be also optimistic. With three 3 cm^2 cathode converters a converter thermal requirement of 234 watts at a cathode temperature of $1650°$K was

computed. The converter size was reduced from the standard 5 cm^2 converters in use at that time to 3 cm^2 in order to provide for the factor of 2 safety margin. As can be seen from Table 1, at this operating temperature a converter efficiency of 11% could be expected resulting in an overall generator efficiency of 10%, excluding re-radiation and re-reflection losses. Standard planar converters were selected since in the design of a multiple element generator, they provide a maximum of flexibility. They were also undergoing development at the General Electric Power Tube Department thus providing for reliance upon past experience.

4.4 Insulation Selection

Preliminary layouts of three 3 cm^2 converters indicated that to utilize a cylindrical converter geometry and a planar cathode structure there would be a large amount of space between the converters, particularly if a cavity of sufficient dimensions to properly entrap solar flux was required. The two possible solutions to this geometric problem were: 1) to design the individual converters such that they were in close contact along the envelope length, which would mean a trapezoidally shaped pyramid envelope structure or 2) to fill voids with insulation. Since it was recognized that the converter development and construction was in itself a complicated manufacturing process, the selection of the latter approach was necessary.

The problem, then, was to develop an insulation. Radiation shield insulation is the best known insulation for high vacuum application. This radiation shield approach can take the form of fibers, powders, cloth, mesh, or metal sheets. Since the emissivity and workability characteristics of tantalum, as well as its gettering characteristics, were known, insulation development was pinpointed toward the development of tantalum heat shields utilizing smooth foils. Tantalum is also easy to work, can be cold formed, is manufactured with a high surface finish and low emissivity, and getters oxygen and impurities quite rapidly at high temperatures. This possibly would ensure an entrapment and containment of gases which might attack the converter envelope, resulting in embrittlement and subsequent converter failure. Tantalum also has a high vapor pressure which would result in low material losses and deposition, important in preventing contamination of the vacuum system and window. The development program which was undertaken, is described in more detail under the insulation section.

4.5 Generator Design Approaches

After preliminary sizing of the converter and collector, preliminary geometric layouts of generator approaches could be made. Representative types of generator approaches are shown in Figures 4 through 11. These approaches represent a variety of design attempts to reconcile the system and component tradeoffs. Figure 4 shows a three-converter generator with a very large and deep cavity. A cathode pickup shoe is attached to the cathode to pick the thermal energy from the cavity and transmit it to the converter cathode. The anode radiating fin radiates waste energy to space. In this design, a deep cavity is used in the hope that the re-radiation and reflection losses will simulate a black body. Preliminary studies of the cavity indicated that as far as reflection was concerned a large percentage of the re-reflection would occur in the front part of the cavity and that a cavity of less depth would provide efficiencies comparable to a deep cavity. In addition, a deep cavity requires a

Figure 4. Hexagonal Body – Deep Cavity
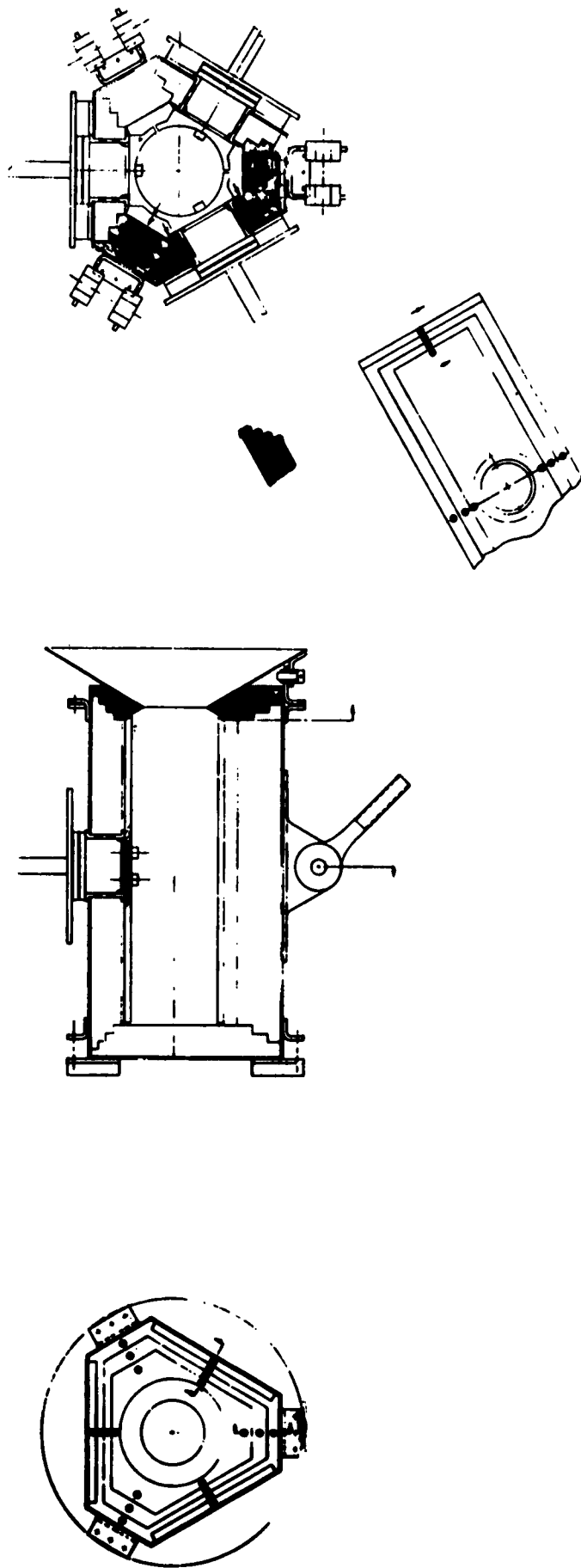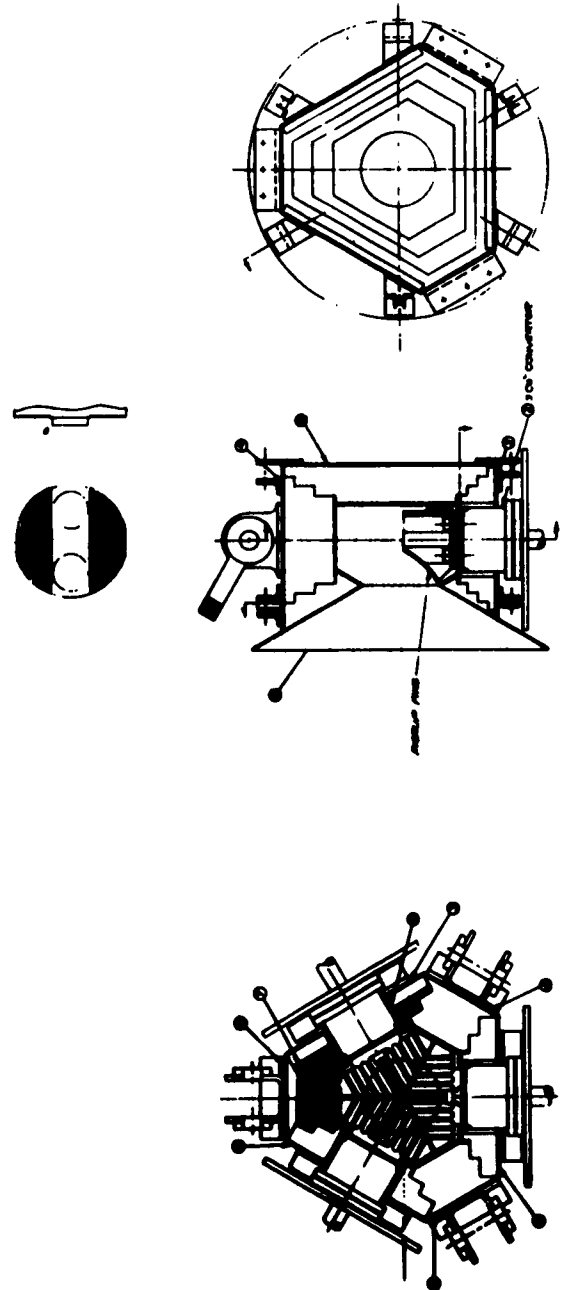

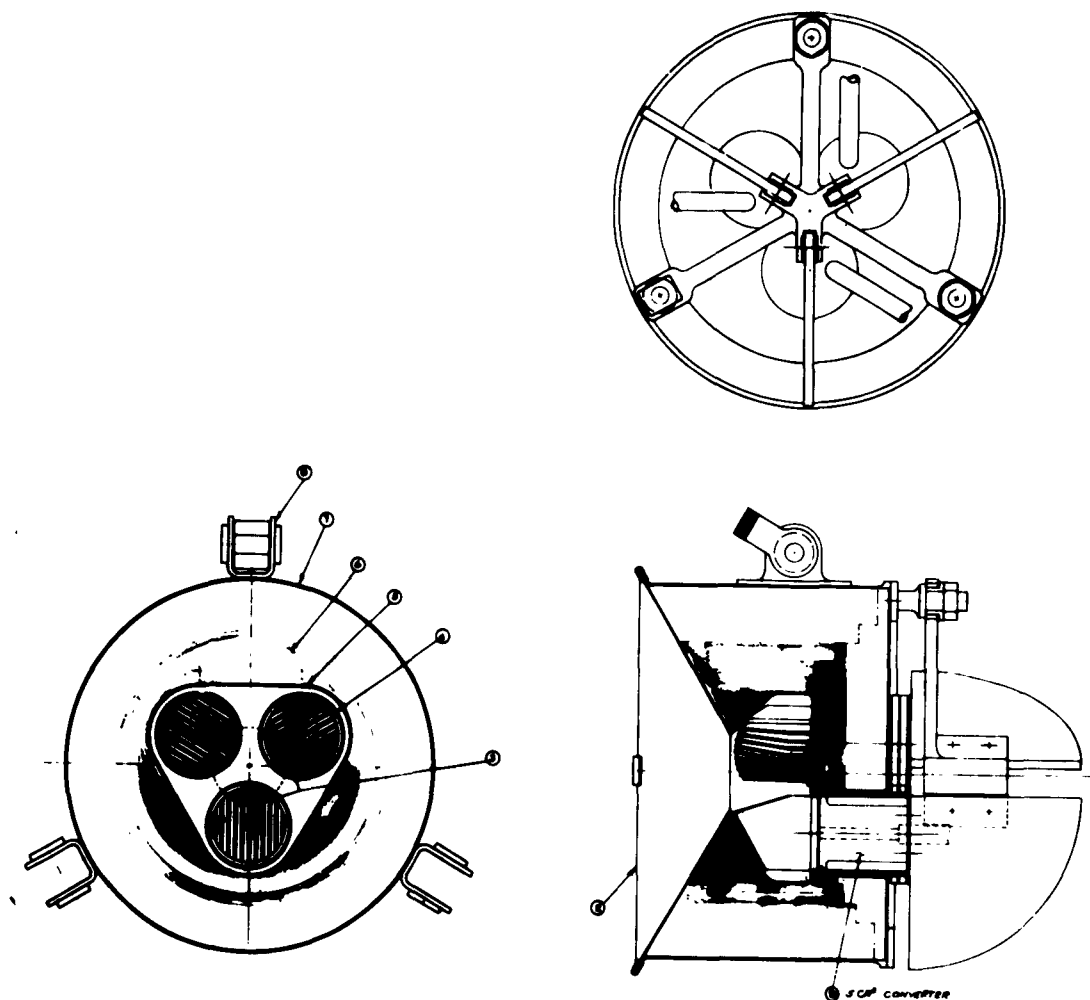**Figure 5. Hexagonal Body – Pickup Fins**

12

Figure 6. Round Body with Pickup Fins and
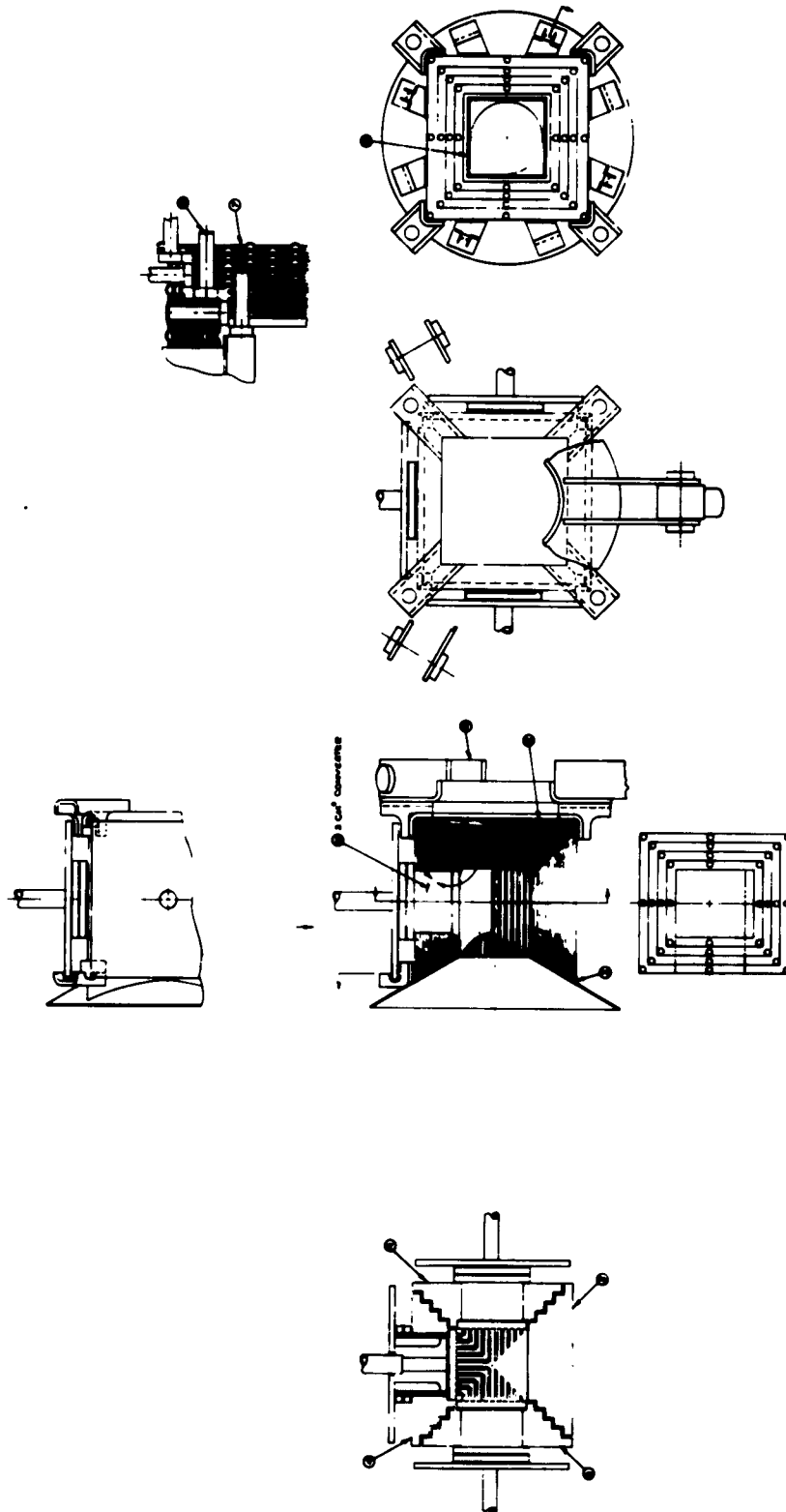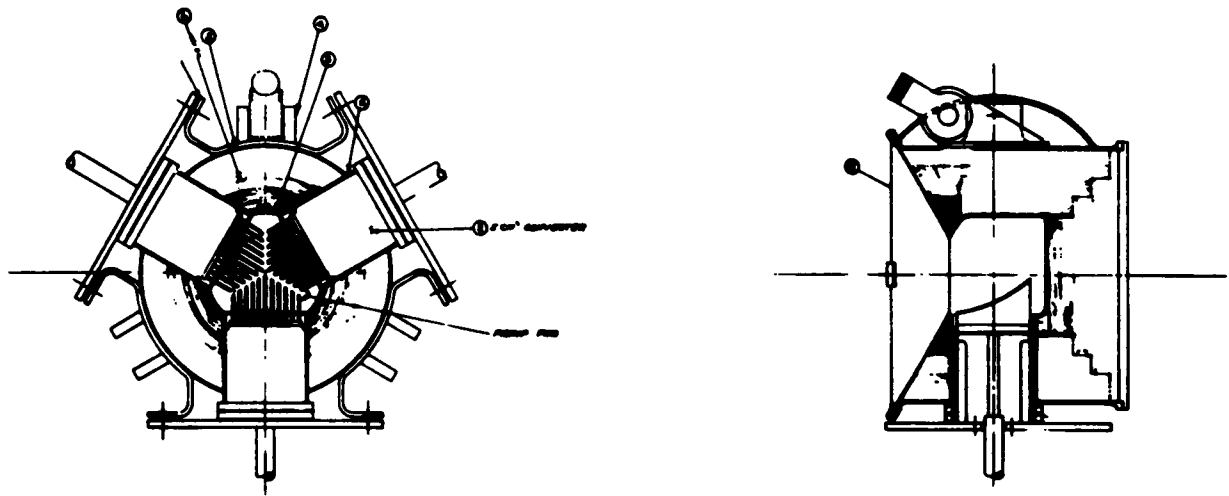Axially Supported Converters

Figure 7. Cubic Body – Pickup Fins

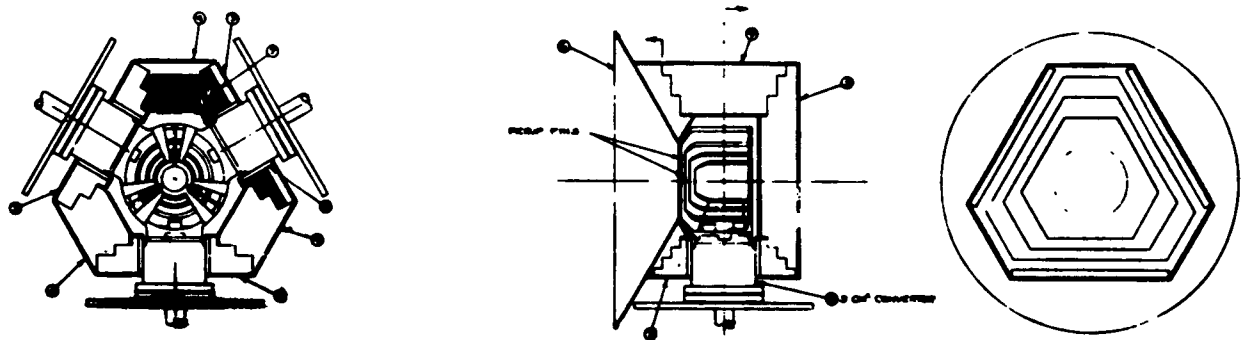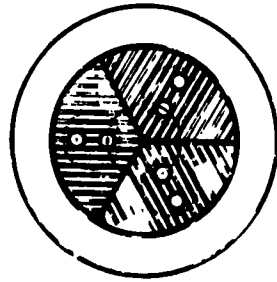Figure 8. Round Body - Pickup Fins

Figure 9. Hexagonal Body
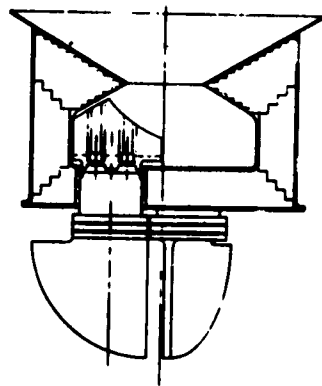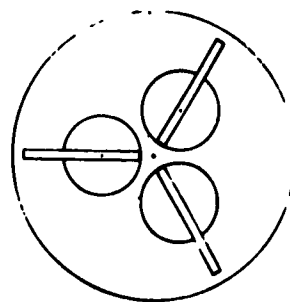
Figure 10. Round Body with Pickup Fins and Axially Supported Converters
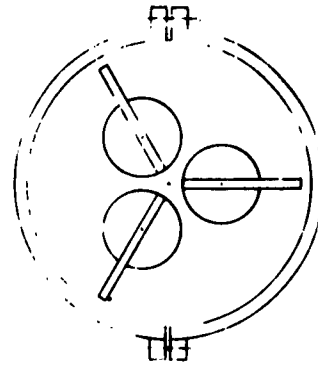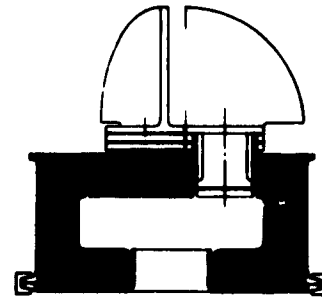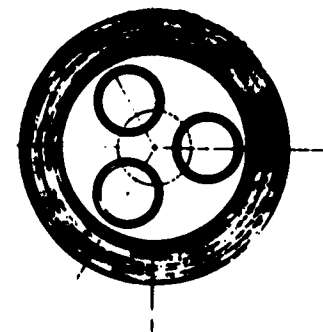
Figure 11. Round Body with Wide Aperature and Axially Supported Converters

large amount of insulation resulting in large insulation losses. It would be an extremely high weight design due to the amount of insulation compared to the amount of converter cathode area. Figure 5 shows a cavity in which the size is reduced but pickup fins have been placed extending into the cavity interior of the generator. These slotted pickup fins are designed to channel the solar energy into the cathode and provide a minimum of re-radiated area due to knife edges facing the incoming energy. This cavity would approximate a black body cavity, but no benefit is gained by the fact that tantalum absorbs energy at a greater rate than it emits it, i.e., its absorptivity is greater than its emissivity at the design temperature. Figure 6 is an attempt to locate the converters at the rear of the cavity with pickup fins to simulate a black body cavity. The disadvantage of this approach is the large amount of insulation which would be required, and the fact that the waste thermal radiation from the anode fins is less effective due to the high energy density at the rear surface. In addition, there are problems in obtaining a sufficiently low cesium reservoir temperature due to the high emitting area. Figure 7 is a design which utilizes 4 converters in place of three. This design would be superior to the selected one except that 4 converters with a total cathode area of 12 cm^2 would be required and the thermal losses might be increased. This increased thermal utilization would possibly eliminate a portion of the safety margin in the existent generator design, and should be considered seriously as a follow-on approach. Thermal symmetry for converters is maintained in all designs, i.e., all converters experience identical thermal input distribution in identical re-radiating environment. A converter is not placed at the rear of the cavity thus maintaining this principle of thermal symmetry in Figures 5 and 7.

In Figure 8 a design similar to the selected one is shown with exception that tantalum foil shields are spirally wrapped around the converters. This design is of value with the exception that the problem of winding the foils spirally and the machining of the holes with accurate tolerances for the insertion of the converters appears to be overly complicated. For this reason, this approach was discarded. In Figure 11 an approach is shown that illustrates the problem of the front entrance aperture. The cavity in this case consists of two cylindrical cavities. In this design, the first cavity would cause a maldistribution of thermal energy since energy impinging at the very front edge of the cavity would cause overheating of the front surface.

In Figure 9, the hex body with cathode pickup fins is shown with a different method of inserting the fins. This approach might provide additional light trapping since the circular rings correspond to circular light patterns entering the aperture and would possibly cause a larger absorptivity than the design shown in Figure 5.

In Figure 10 a round body generator is shown with a circular foil wrapped around the exterior. In this design the converter shoe is designed to fill the entire cavity but would have to be bolted to the cathode surface. In all of the designs shown, a ceramic insulation would surround each converter.

Figure 2 shows the geometry selected and is a compromise between many of the geometries shown in this last section. Its basic features are that it provides a cavity which capitalizes on the absorptivity - emissivity ratio of tantalum for solar and thermal energy, and it has converters that are easily removed. The insulation sections are staggered to minimize losses and are also designed for ease of fabrication. The insulation sections machining method was developed during the program. Further details on the design are given in the generator section.

4.6 Instrumentation Selection

Since one of the objectives of this program was to obtain technical information for redesign, a large amount of instrumentation was designed into the system. Based on lessons learned in STEPS I testing, it was decided early in the program to design the instrumentation as part of the generator structure, and careful attention was given to minimizing losses which could have been introduced by improper instrumentation design. Due to the inaccuracy and unreliability of pyrometric measurements, particularly with a number of reflecting surfaces between the point being observed and the pyrometer, as well as the non-blackness of the selected cavity, thermocouple instrumentation was selected as the only valid way of obtaining sufficient technical information. A program was undertaken to determine the best thermocouple materials for vacuum and high temperature use, resulting in the selection of chromel-alumel couples for the surfaces cooler than 900°C and for tungsten-rhenium couples for surfaces hotter than 900°C. Instrumentation and meters were ordered to properly record the couples and calibration procedures were used on all thermocouples and instruments to ascertain their accuracy during the course of the program. Ceramics, such as the segmented beryllia sections for the interior of the generator to eliminate heat losses, were used to provide insulation for the couples.

4.7 Dummy Generator and Heater

It was decided early in the program that to ascertain the reliability of the instrumentation, to obtain technical information such as the drop across some of the impedances in the generator interior, and to obtain estimates of the insulation losses, a generator was built with dummy insulation sections in place of converter sections. These dummy insulation sections were then inserted in testing in the Philadelphia Laboratory in place of the converters. A bombardment heater and I^{2}R were designed to replace the front aperture cone and to fit into the cavity of the generator. The heater was designed for growth potential so that it could be used with 3 converters although during the course of the testing only one converter at a time was introduced. This was done to measure the characteristics of each converter as well as to ascertain the losses in the insulation and to obtain sufficient technical data for correlation with later tests in Phoenix.

18

5.0 SUB-SYSTEM DETAILED DESCRIPTION

5.1 Collector

5.1.1 Preliminary Design Analysis

Energy requirements for the Cavity Vapor Generator were initially established at 500 watts. Sizing of the solar concentrator was based on a requirement of concentrating 1000 watts thru the generator aperture. The 2:1 margin covered expected insulation, re-radiation, and re-reflection losses and provided a margin needed to permit utilization of an input energy control.

An Army searchlight with a reflective coating of aluminum and a transparent protective coating, both applied under vacuum, was selected based on the design analysis. Energy vs. aperature performance predicted for the design parameters is shown on Figure 12. Geometry of this mirror is:

Diameter	60.0	Inches
Focal Length	42.56	Inches
Rim Angle (θ)	60.56	Degrees
Gross Mirror Area	19.635	Ft^2
Central Shadow Diameter	15.0	Inches

Figure 13 shows the mirror installed in the calibration testing assembly.

5.1.2 Calibration Testing of Mirror

Inspection and performance testing were performed with the CVG mirror to define: 1) mirror optical accuracy, 2) mirror efficiency with cold cavity, 3) mirror efficiency with quartz-plate and pyrex-dome windows, and 4) misorientation degradation effects on performance.

OPTICAL ACCURACY

A general geometric error of 0.125 degree was used for the design analysis. The actual error distribution measured by Hartman testing is shown in Figures 14 and 15. The effect on performance is generally improved over that expected from the design analysis. The performance with the Hartman error pattern is shown in Figure 16.

MIRROR EFFICIENCY-OPEN CALORIMETER

Initial open-calorimeter testing was performed to empirically establish the energy collection pattern with apertures of 0.6, 0.8, 1.0, 1.2, and 1.4 inch diameters. The peak energy capture points for each of the apertures are plotted in Figure 17. For the generator aperture size (1.0 inch) 1193 watts were obtained. Several months later the 1.0 inch diameter test was rerun with the final vacuum system installed and this value was reduced to 1041, principally due to the increased shadow. All calorimeter data reported has been standardized for a solar insolation intensity of 80 watts per square foot.

Correlation of the open-calorimeter data with the Hartman geometric data, revealed an effective mirror reflectivity of 0.83.
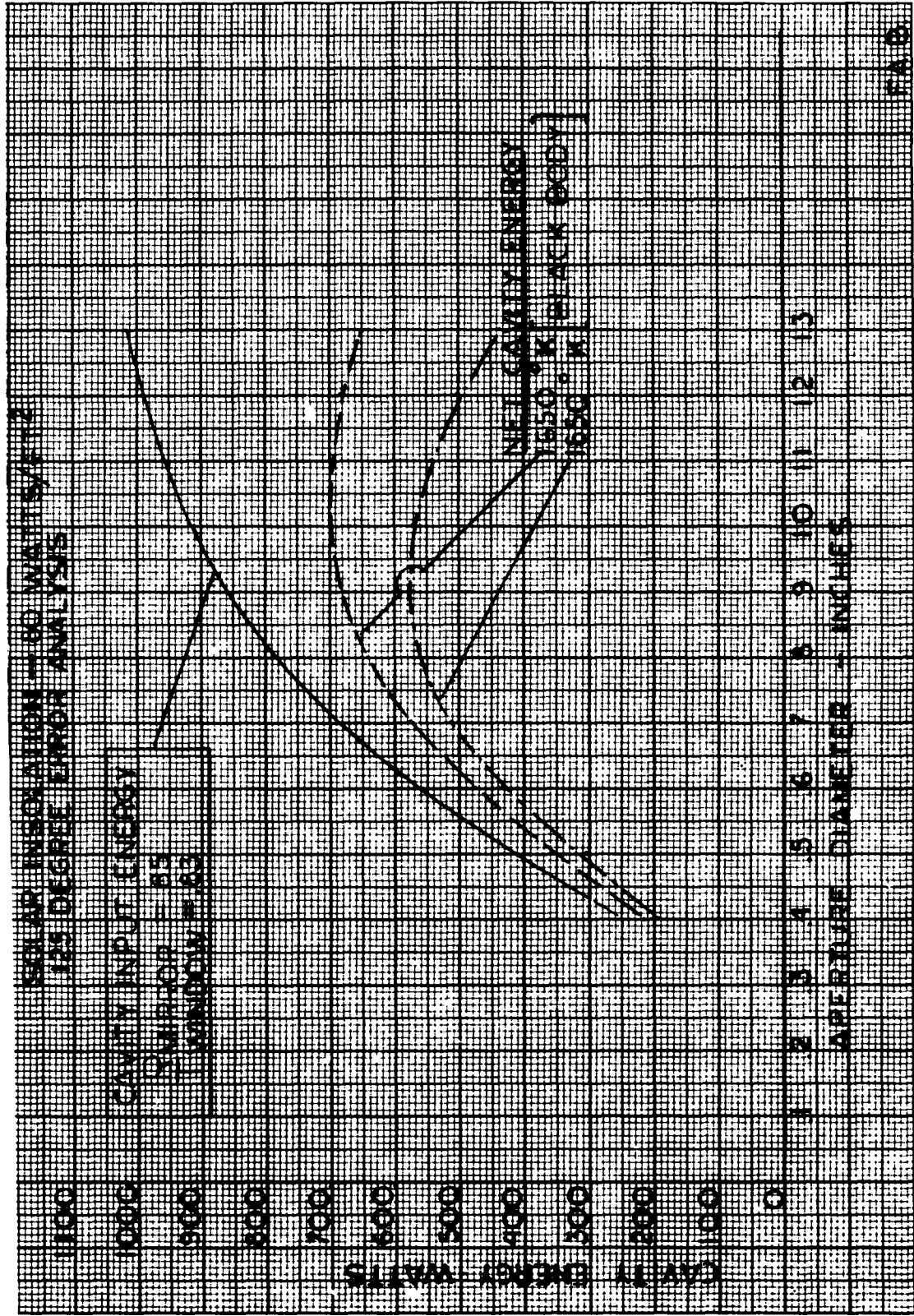
Figure 12. Cavity Energy vs. Aperture Size

20

Figure 13. CVG Mirror Installation

Figure 14. CVG Mirror Tangential Error - Minutes
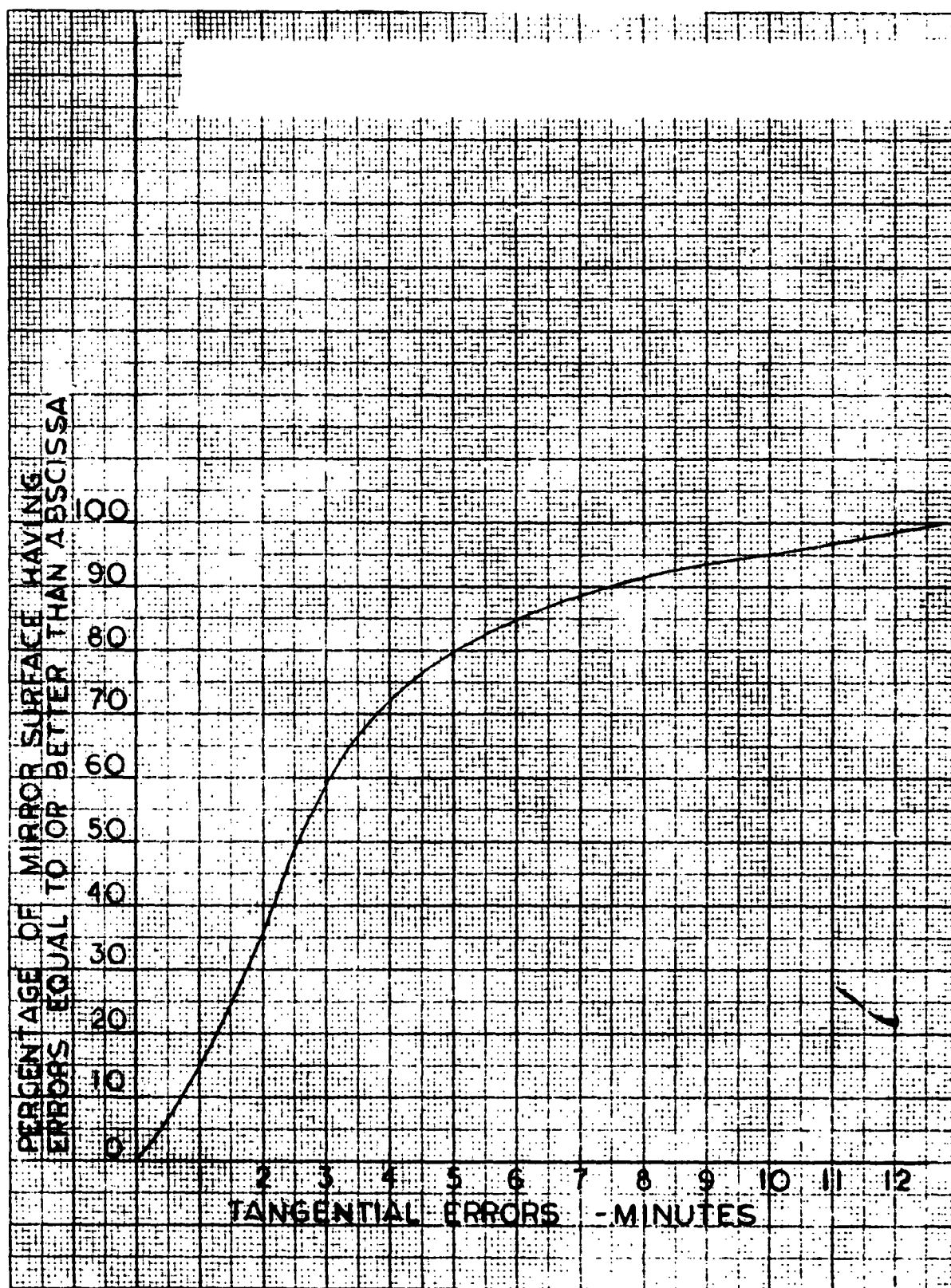
Figure 15. CVG Mirror Tangential Error Distribution
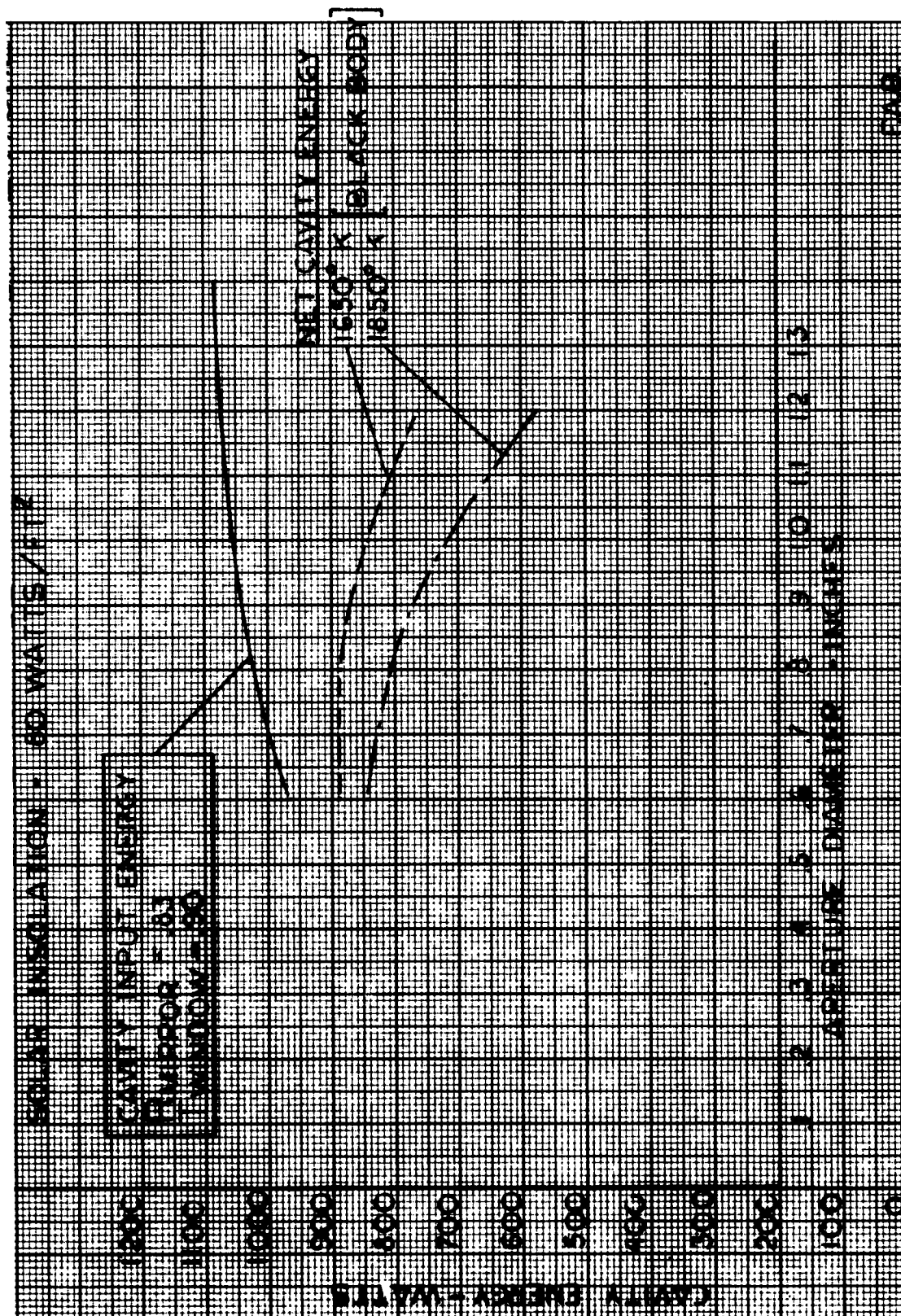
Figure 16. Hartman Performance Pattern vs. Aperture Diameter

24
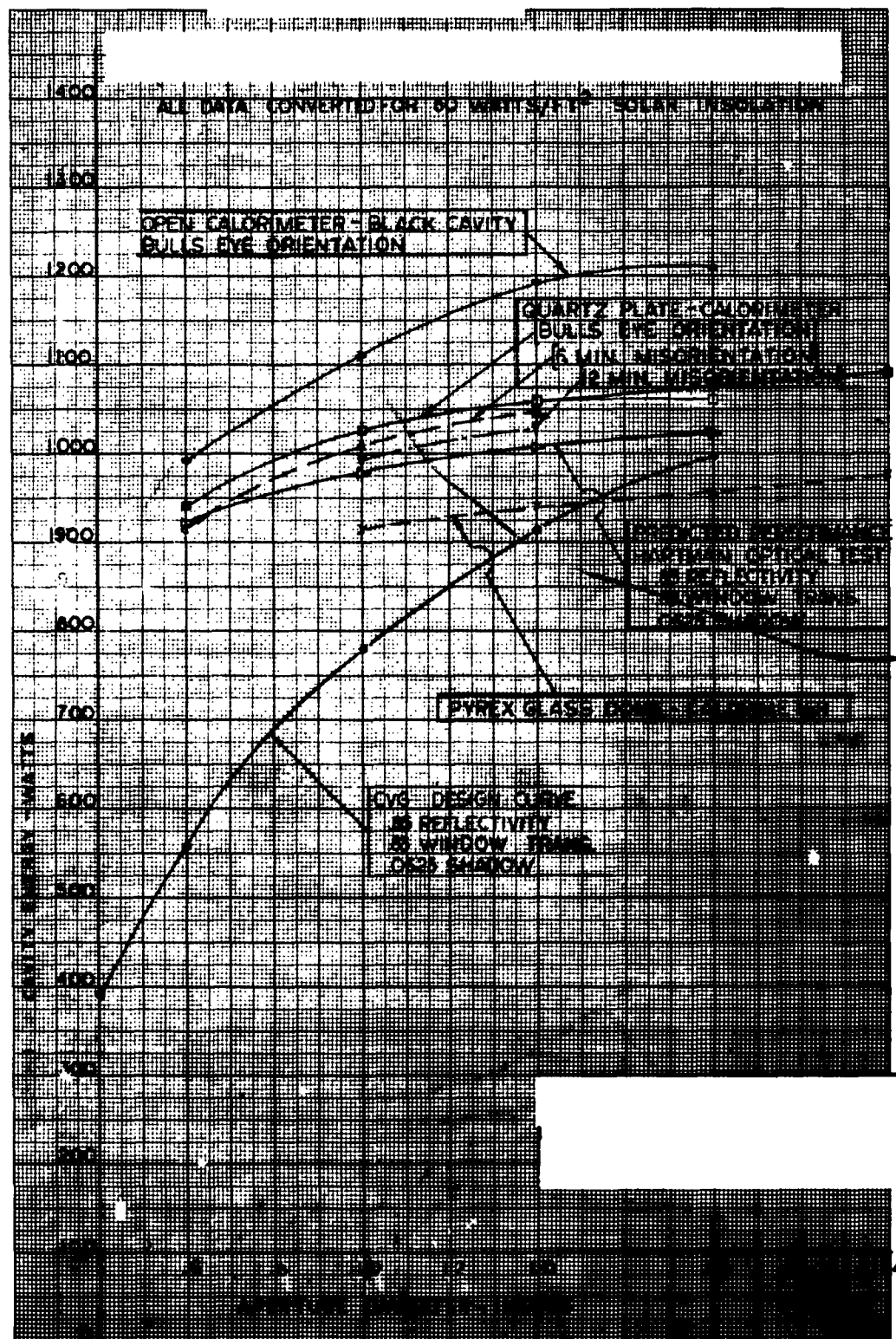
Figure 17. CVG Solar Concentrator Performance

25

QUARTZ PLATE-PYREX DOME

It was realized from the outset of the program that the final high tempera-
ture testing must be performed in a vacuum chamber to eliminate oxygen attack
on the generator and to eliminate the convective heat transfer. Candidate windows
for the vacuum chamber were finally reduced to a flat quartz plate and a pyrex
dome. The dome was the preferred geometric shape as it least affected the focused
energy pattern. Tests were performed on both windows (Figures 18, 19, and 20).

Energy capture thru the quartz plate was significantly higher than the pyrex
dome (Figure 17), 1060 watts vs. 942 watts for the 1.0 inch aperture. For the
final generator testing, the available energy thru the quartz plate was reduced to
887 watts due to the combined shadow increase of the vacuum system and the
control shutters. Figure 21 shows the final system calorimeter test in operation.

MISORIENTATION TRACKING

Calorimetric testing with the quartz window at controlled misorientation
angles up to 24 minutes was performed. Average results of these test runs are
shown on Figure 17 and Figure 22. In general these results were encouraging
as the rate of performance degradation with increasing misorientation was lower
than expected. The 1.0 inch aperture data is:

Misorientation Angle	Energy Captured In Cavity-1.0 Aperture (Watts)
Bulls Eye	1060
6 Min.	1048
12 Min.	1028
18 Min.	1010
24 Min	972

Figures 23 and 24 show the Hartman test patterns for the zone 5 lights for
Bullseye and 6-minutes-low orientation, respectively.

FLUX INTENSITY-CAVITY WALLS

Design point diameter for the generator cavity is 1.4 inches. Since it was
highly desirable to establish the energy pattern impinging on the cavity wall,
traverses were made with a 1.4 inch aperture thru a distance corresponding to
the cavity length. The energy increment striking the wall between points one and
two, was determined by the decrease of energy captured at position two, compared
with that of position one. At position two, the increment passing the 1.4 inch
diameter strikes the face plate frontal surface and bounces out. Figure 25 shows
the flux distribution curves obtained in this manner, for both the open-calorimeter
and the quartz plate-calorimeter. The curves of Figure 25 are an average of the
energy striking the wall, and locate peak axial patterns.
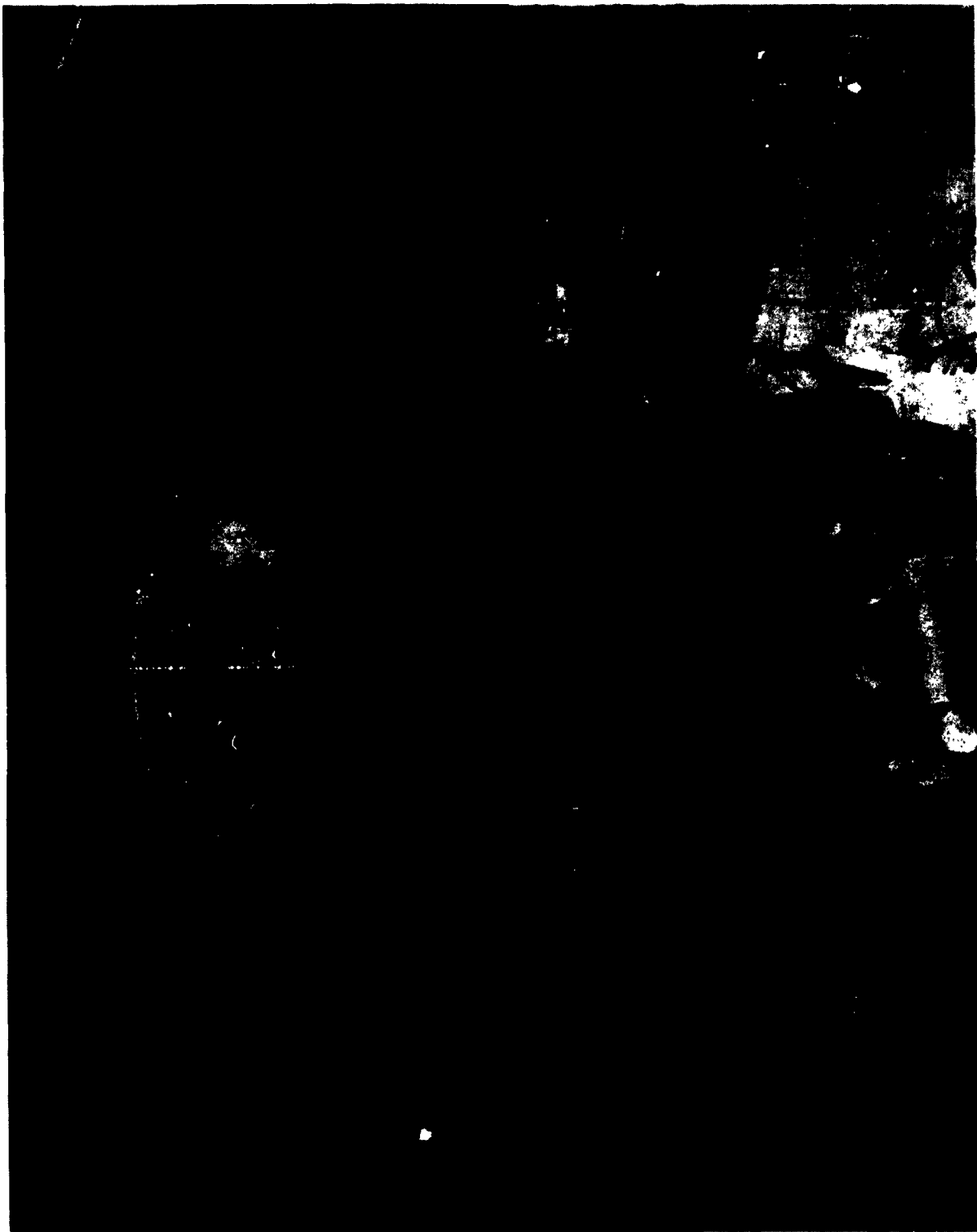
Figure 18. Calorimeter Test Operation, Quartz Plate Installation

Figure 19. Quartz Plate Calorimeter Assembly During Solar Test

Figure 20. Pyrex Dome Calorimeter Assembly During Test
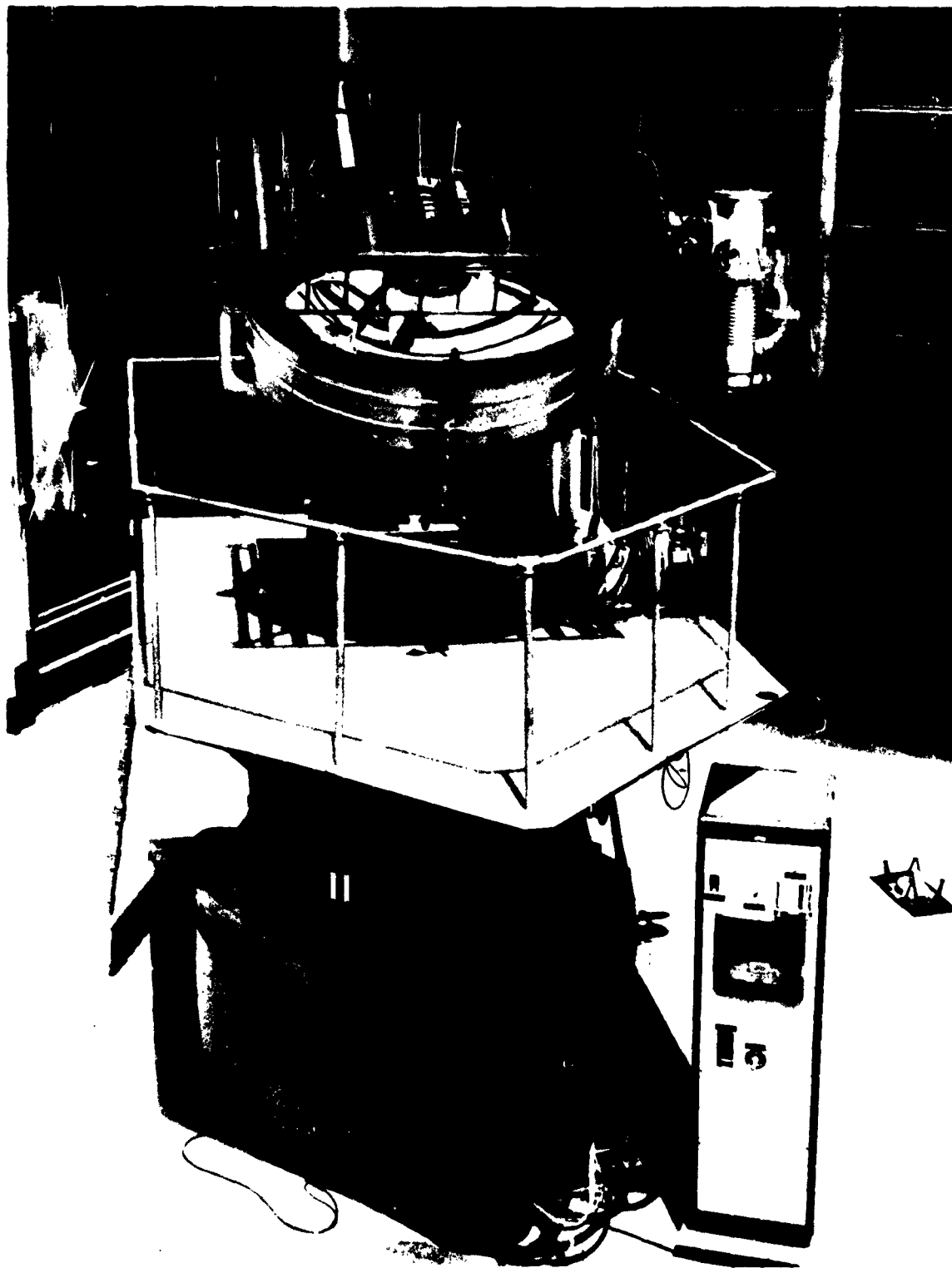
Figure 21. Calorimeter Test of Final CVG Test Installation
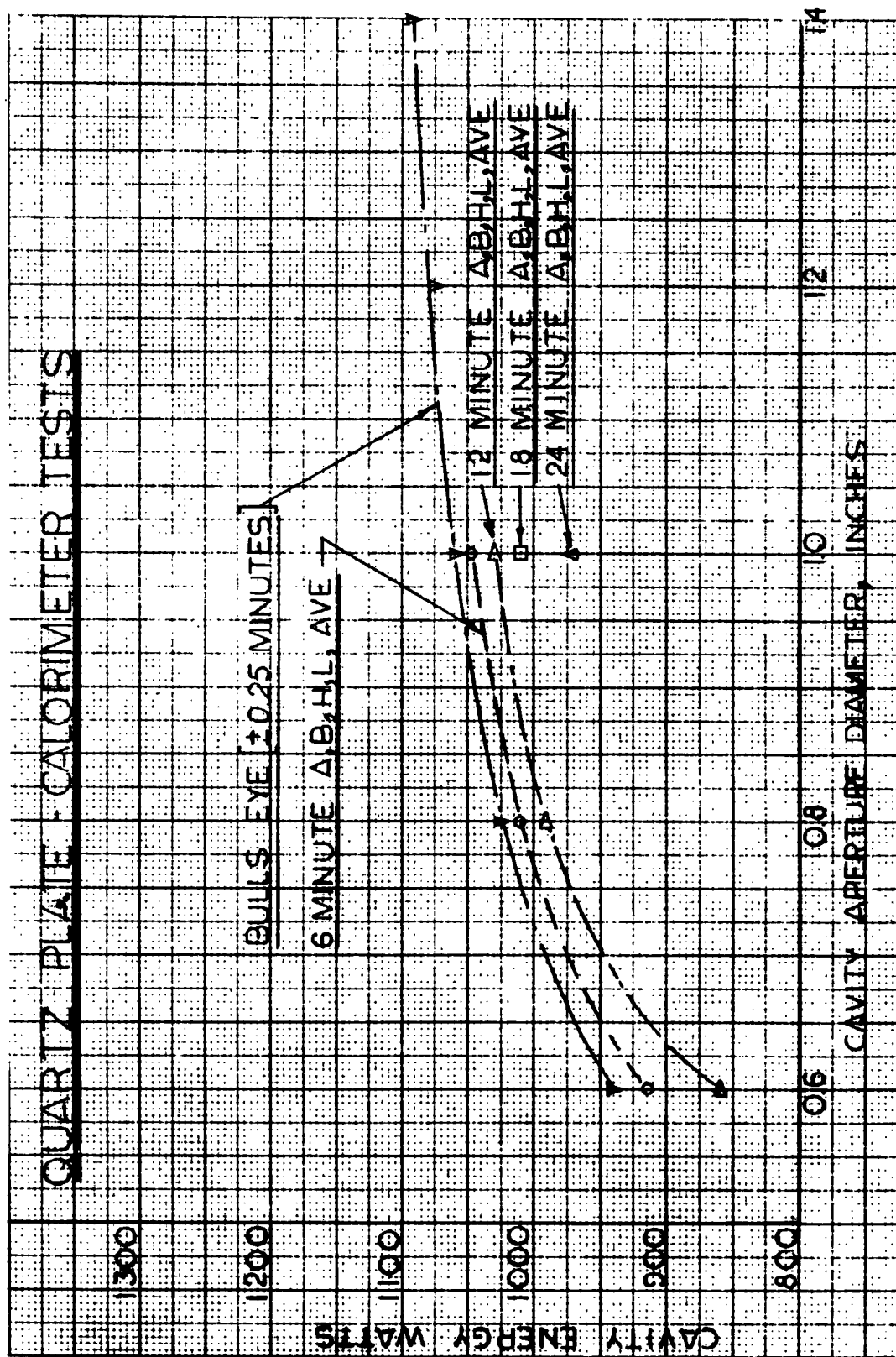
Figure 22.   CVG Concentrator – Misorientation Performance

Figure 23. All Zone-5 Lights, Bullseye Orientation

Figure 24. All Zone-5 Lights, Six-Minutes - Low Orientation
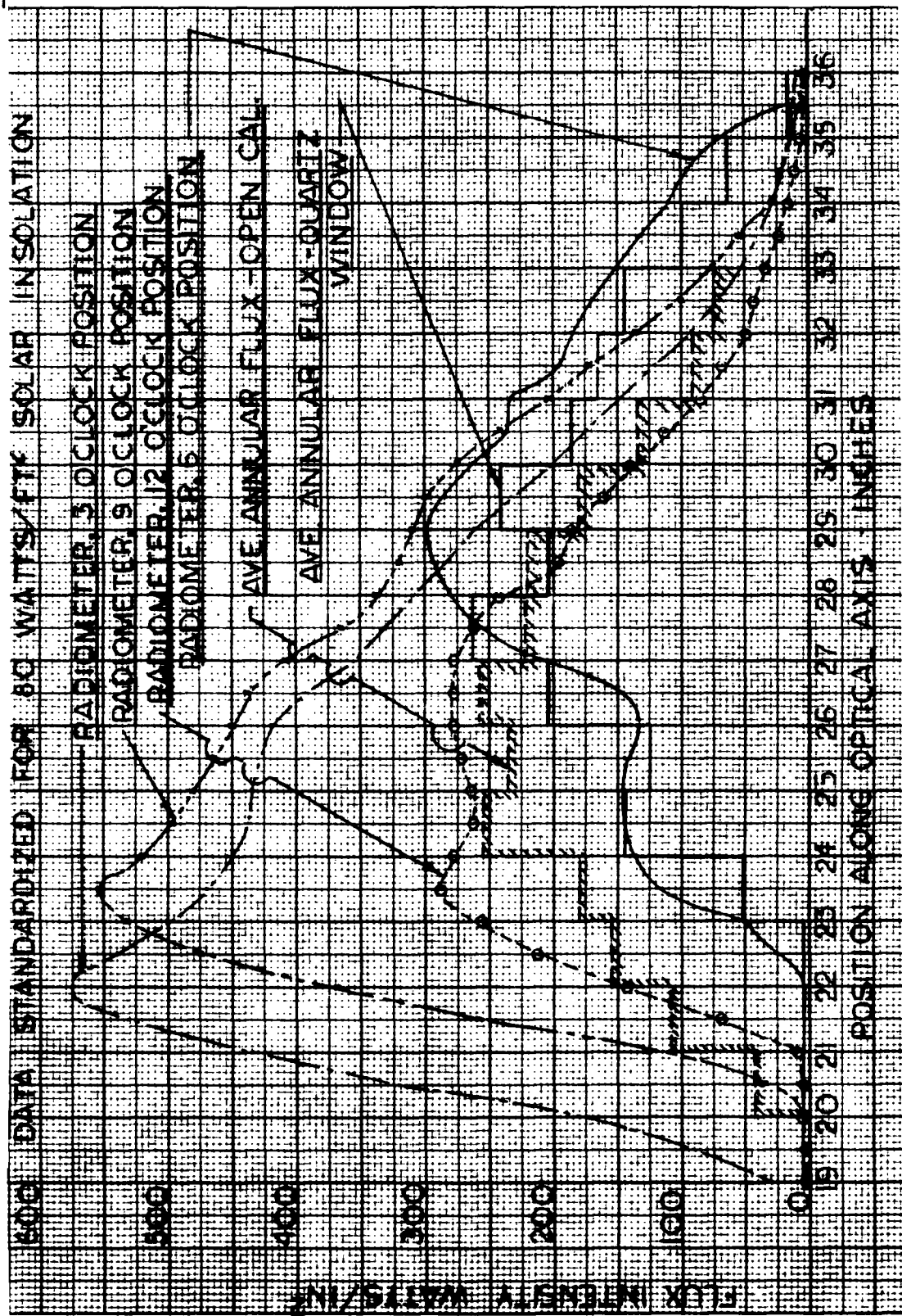
Figure 25. CVG Cavity Flux Intensity Distribution – 1.4 in. Dia. Cyl.

34

It was desirable to verify the flux distribution by an independent method, and if possible detect any circumferential variations. Traverses were run at twelve positions around the 1.4 inch diameter with an RdF miniature radiometer. This instrument samples the flux thru a 0.01 inch diameter aperture. Figure 22 shows four of these flux patterns plotted against the average intensity obtained by incremental calorimetry. These curves highlight that circumferential variations of a significant magnitude do exist.

5.1.3 Collector Alignment

Alignment of the optical axis of the collector with the tracking telescope, sensors, and focal plane equipment, was accomplished by use of the Hartman test. Alignment of the target with the optical axis is performed thru simultaneous use of lights from each quadrant of the mirror. Criteria for establishment of the reference focal plane was the most symmetrical light pattern from zone 1 lights (Figure 26).

5.1.4 Calorimetric Test-CVG System Installation

A final calorimetric test was performed on the complete CVG system, just prior to the generator testing. The major objective of this test was to calibrate the energy being supplied to the generator. A secondary objective was the determination of the effects, on collector performance, of the increased shadow and the thicker quartz plate. A plot of the solar concentrator efficiency based on total intercepted energy for shutter closing angles from 0 to 30 degrees closed, is shown on Figure 27. This efficiency, multiplied by the 19.635 square foot intercepted area and by the solar insolation in watts per square foot, establishes the energy being supplied to the generator.

The efficiency fraction for the quartz window in the final setup (0.96 inch thick plate) was 927/1041 = .8902, which compares closely with 1060/1193 = .8883, obtained with the early testing using the 0.5 inch plate.

5.2 Vacuum System

Basic objectives to be fulfilled with the vacuum system design, were to provide a 1×10^{-6} mm. Hg. vacuum chamber around the focal zone of the mirror constructed to minimize the performance effect of its shadow. The final system consisted of a 12 inch diameter by 15 inch length chamber, tri-strut supported from the mirror rim, with one of the struts doubling as the connecting duct to the vacuum equipment. Frontal closure of the chamber was a 1.0 inch thick quartz window selected after results of both calorimetric tests and flux intensity tests indicated its suitability. Aft closure is the 304 stainless steel plate to which the generator is mounted and thru which all electric power and instrumentation lea leads pass. Sealing of both ends is accomplished by a double face type, O-ring design, which utilizes a mechanical vacuum pump pump-down between the rings to minimize the ΔP across the inner seal ring.

Vacuum below one micron is provided by a diffusion pump-liquid nitrogen trap combination linked to a two stage mechanical fore-pump. Figure 28 shows the vacuum system in operation during a test of the Dummy cavity vapor generator. This picture highlights one of the critical design problems which had to be overcome, the need to keep the diffusion pump axis vertical while the optical axis of the mirror to which it is mounted is variable from vertical to within approximately ten degrees of horizontal. The solution involved incorporation of a double sleeve rotary joint between the chamber connecting duct and the liquid nitrogen trap. The inner sleeve is flange mounted to the duct.

Figure 26. Zone-1 Lights, Bullseye Orientation, Criteria for Focal Plane Location
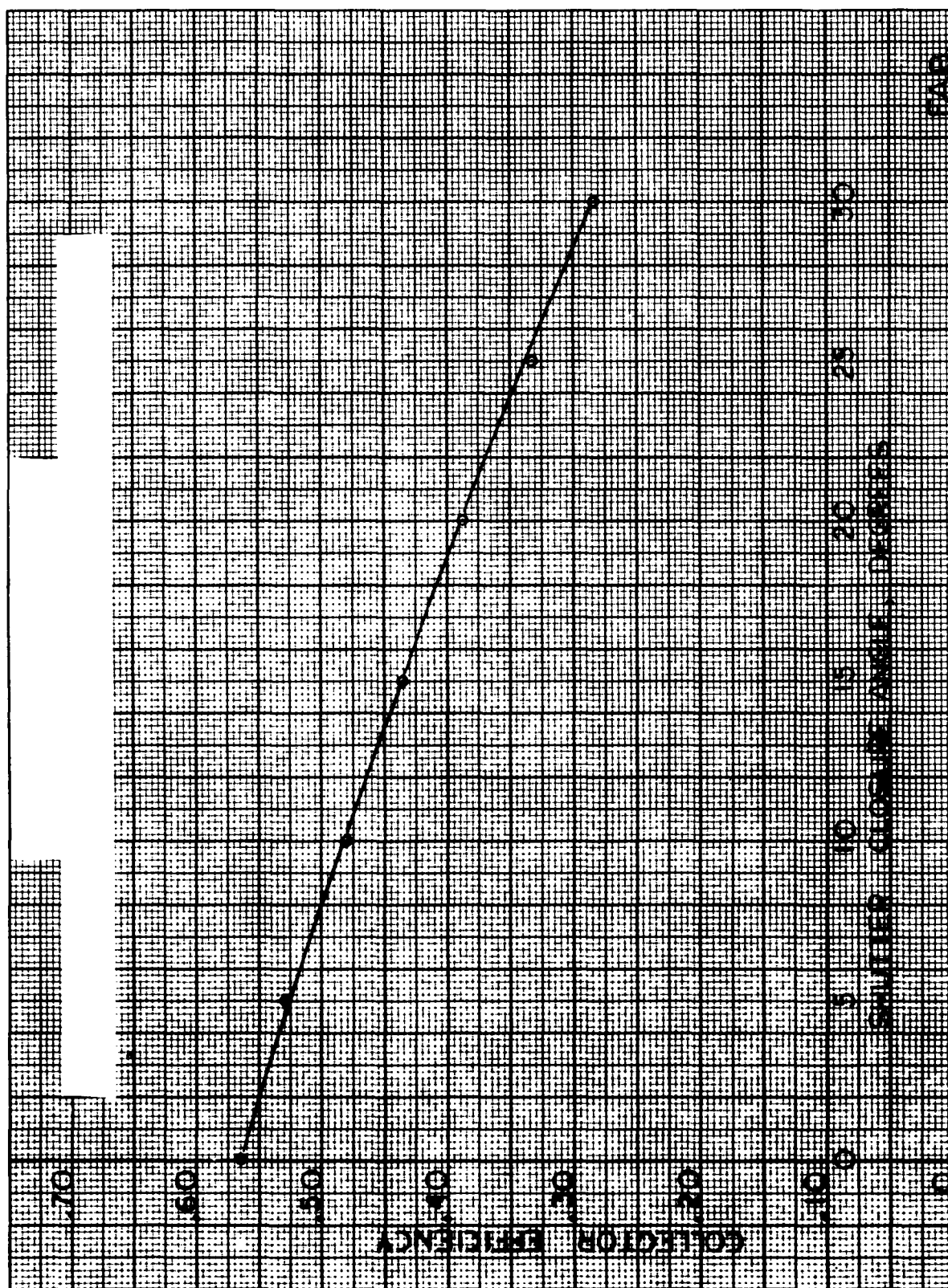
Figure 27. Cavity Energy vs. Shutter Angle
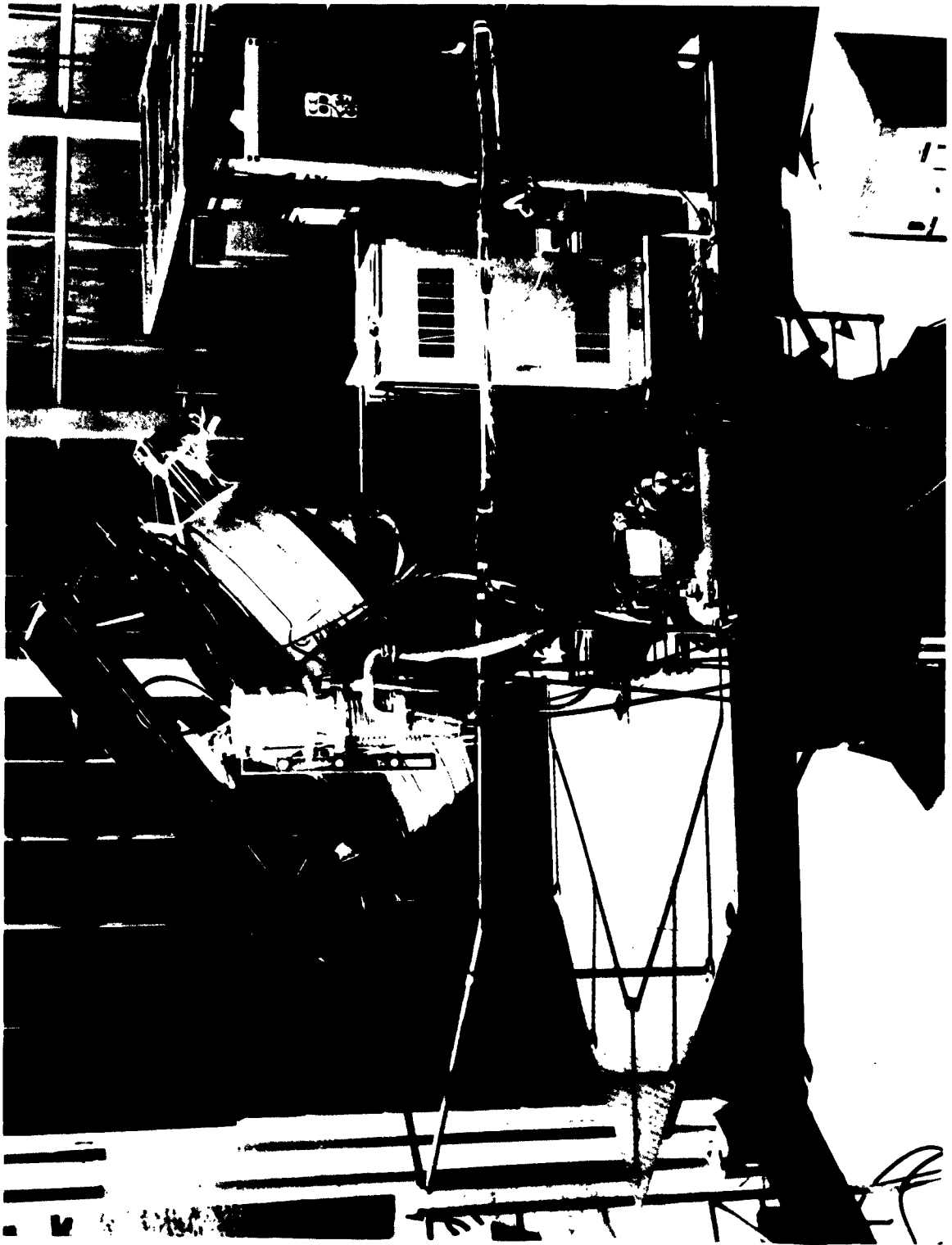
Figure 28. Vacuum System Installed on CVG Solar Test Pedestal

38

The outer sleeve is axially positioned along the inner by a thrust collar and is radially sealed by two O-rings. As in the chamber front and aft closures, a vacuum pump-down is performed between the two O-rings. Functional integrity of the rotary joint has been repeatedly demonstrated by position adjustments being made without observable pressure changes while operating on the 10^{-6} range.

Diffusion pumping is performed by a Consolidated Vacuum Corp. Model PMC 1440 (6 inch dia.) pump rated at 590 liters/sec. at 1.0×10^{-6}, when used in conjunction with a liquid nitrogen trap.

Performance of the vacuum system operating cold with a blank aft cover is illustrated by the curves of Figure 29. The lowest pressure attained during these check out test runs, is the end point of the 8/22/62 Solar Facility Test, 3.8×10^{-7} mm. Hg.

Performance during hot-operation is illustrated by Figure 30 which is the pressure profile for the pump-down and test periods of CVG generator test runs No. 4 and No. 5.

Instrumentation monitoring the vacuum system consists of thermocouple gauges for pressures above one micron and Bayard-Alpert type ionization gauges for pressures in the $10^{-8} - 10^{-4}$ mm. Hg. range. Thermocouple gauge taps are located in three positions: 1) chamber duct, 2) forepump inlet, and 3) seal pump header. Ionization gauge taps are located in the chamber duct and at the diffusion pump inlet.

Chamber cooling provision was made during design with the incorporation of a concentric water jacket around the 12 X 15 chamber. Inlet water to the chamber is maintained below $70^{\circ}F$ and the effect of this cooling on chamber outgassing is evident from the 8/22/62 curve on Figure 29.

The high absorptivity coating required for the chamber interior was provided by application of Cathode Ray Tube Coating #117 manufactured by the Joseph Dixon Crucible Company.

Dow Corning Silicone High Vacuum Grease was used for lubrication of the chamber O-rings and the teflon insulating washers used on the power lead feed throughs. Insulation of the power feed throughs from the base plate was provided by a teflon sleeve and teflon washers under the axial clamping collar and washer.

Initial testing of the quartz face plate in the sun, revealed that a loose mounting was necessary to allow use of padded sheet metal clamps having sufficient strength to provide the initial sealing force, while still being light enough to yield with thermal expansions. One question which needed answering prior to system testing, was that of the structural integrity of the vacuum chamber window under vacuum with high radiant energy concentration in the central zone. Tests were performed with a radiant heater positioned two inches from the plate center (corresponding to aperture position) with satisfactory results. Stress analysis of the plate indicated a 627 psi. level present from the vacuum load allowing a safety factor of 11.1 using the 7,000 psi. tensile strength property.

Confidence in the quartz window was further strengthened by testing in Phoenix where the focal point of the mirror was passed thru the window with no ill effect. The Phoenix test was non-vacuum, while the radiant test was vacuum loaded. The flux level passed thru the plate is shown on Figure 31.
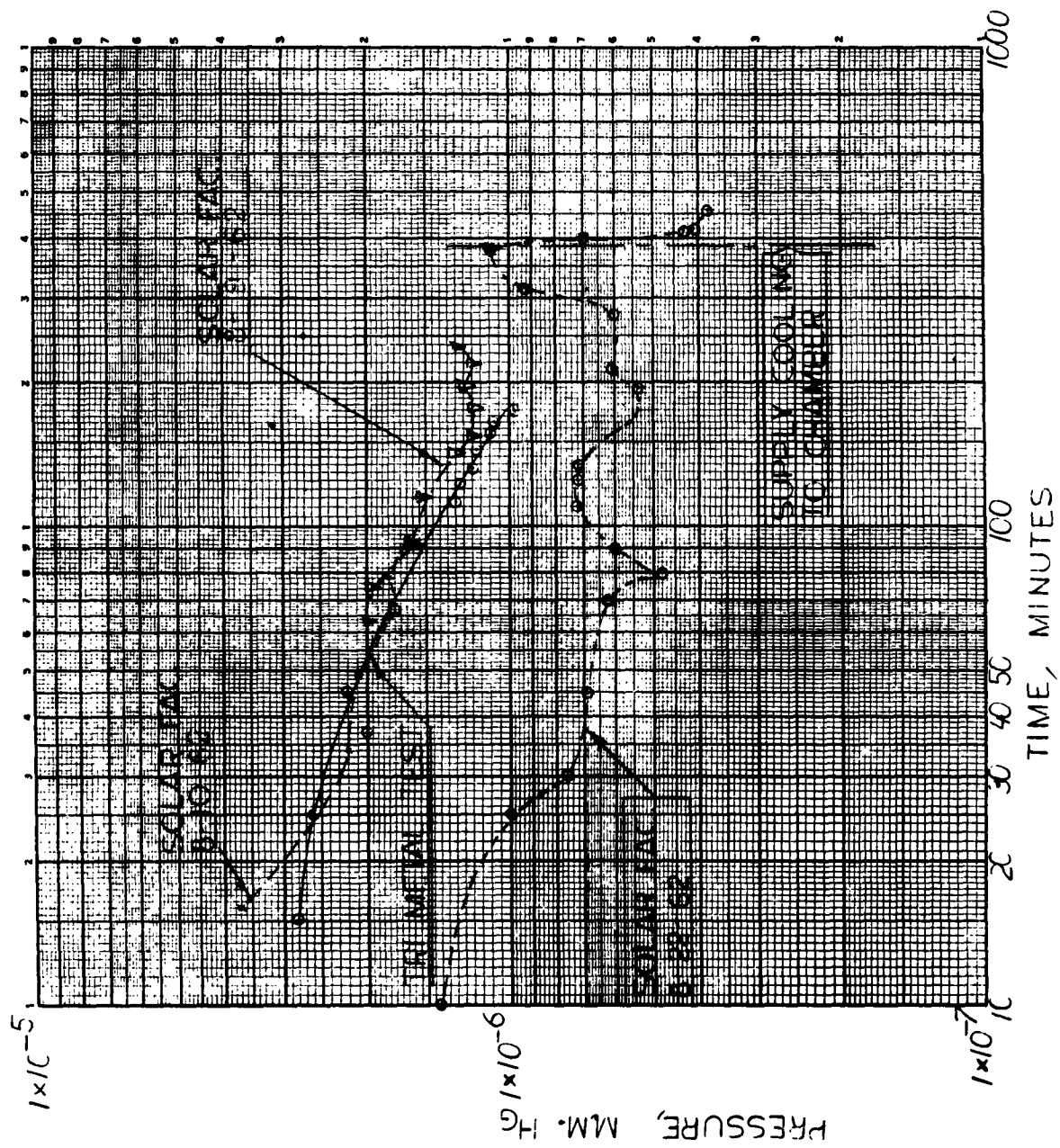
Figure 29. CVG Vacuum Chamber Checkout Tests

40
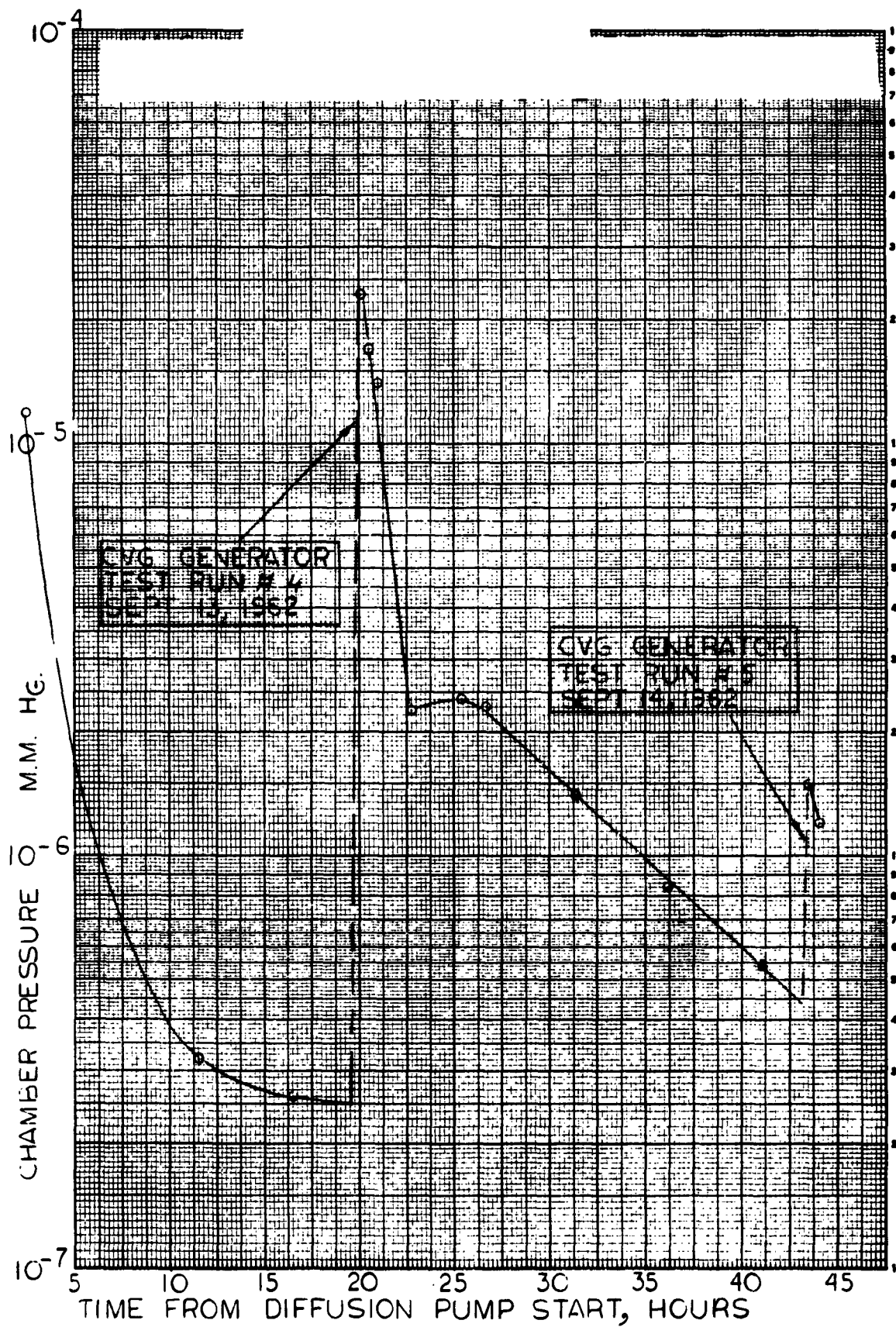
Figure 30. Vacuum Chamber Pressure Profile, CVG Runs 4 and 5
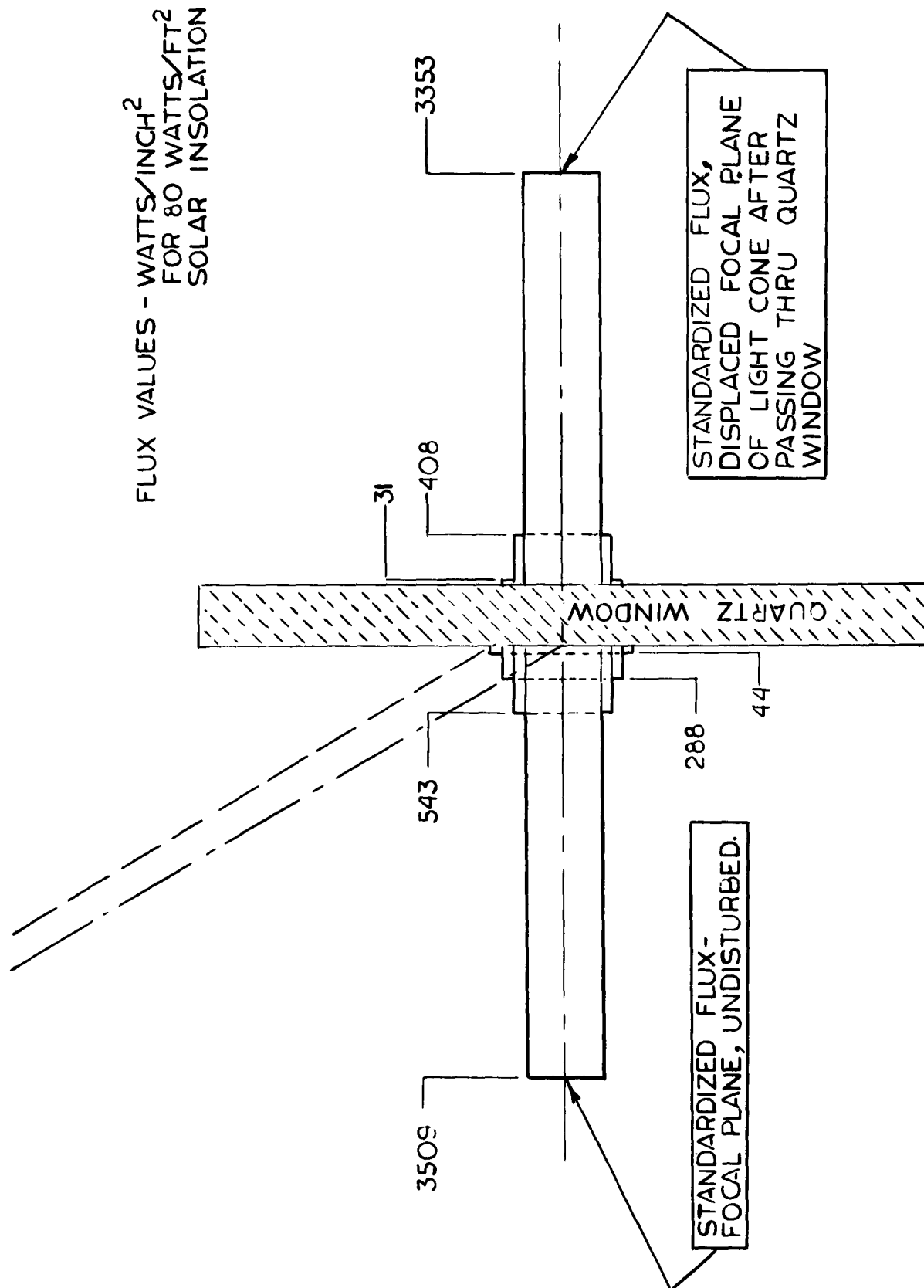
Figure 31. Focal Plane Flux Patterns

FLUX VALUES - WATTS/INCH^2
FOR 80 WATTS/FT^2
SOLAR INSOLATION

3353

31

408

543

288

44

3509

STANDARDIZED FLUX, DISPLACED FOCAL PLANE OF LIGHT CONE AFTER PASSING THRU QUARTZ WINDOW

QUARTZ WINDOW

STANDARDIZED FLUX - FOCAL PLANE, UNDISTURBED.

5.3 Cavity Size and Losses

In sizing the CVG generator for the most efficient use of the available incoming energy, and to determine the various subsystem losses, several analyses have been performed on the reflective and re-radiation losses from the CVG cavity. The calculations are aimed at predicting these values for the parameters of aperture diameter, re-radiation, and reflection. Losses from the cavity must be minimized. The CVG cavity, although hexagonal in shape, has been treated as cylindrical, in order to effect the various analyses.

5.3.1 Absorptivity

Concentrated solar radiation which streams through the aperture is reflected repeatedly before it leaves the cavity opening. Depending upon the surface absorptivity of the cathode shoes which form the cavity, after a very large number of reflections, the percentage of radiation absorbed will approach 100 percent. For a theoretically ideal cavity, the aperture area is infinitesimal when compared to the cavity internal surface area; however, this configuration would possess little practical value. For the CVG cavity, sufficient energy must enter the aperture to drive the thermionic converters, yet the cavity surface area should be as small as possible to keep down insulation losses. Three analyses of the CVG cavity absorptivity have been made.

5.3.1.1 "Aperture Corrections For Artificial Black Bodies" by Andre Gouffe (Translated from the French)

In this reference it has been suggested that uniform redistribution of diffuse flux is accomplished after the second reflection. Also the assumption is made that the material of the cavity shoes has the properties of an isotropic diffuser. From page 5 of the above, the cavity absorptivity is given by:

$$F_a = \frac{a\left[1 + (1 - a)\left(\frac{s}{S} - \frac{\Omega}{\pi}\right)\right]}{a\left(1 - \frac{s}{S}\right) + \frac{s}{S}}$$

where
- a = .430 = Tantalum solar absorptivity (DMIC Memo 141)
- s = Ratio of aperture surface area to
- S = Cavity internal surface area
- π = 3.14159
- Ω = Solid angle defined by the below Figure
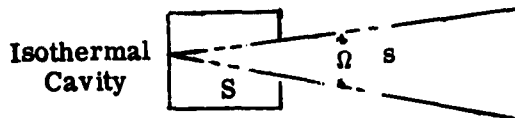
Values of F_a have been computed and are plotted in Figure 32 vs. aperture diameter. For the one inch diameter aperture used, the cavity solar absorptivity calculated by this method is 0.828.
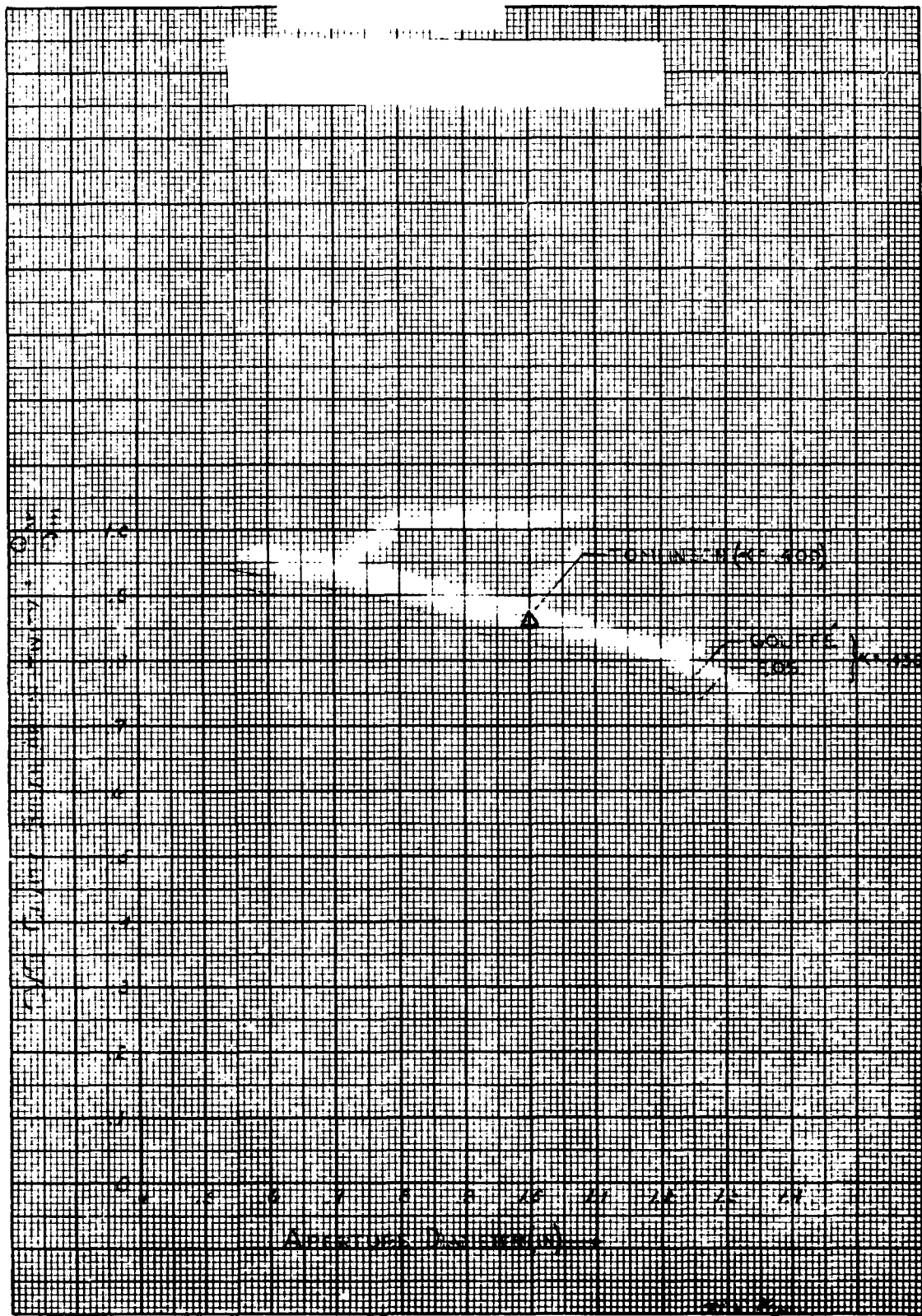
Figure 32. Solar Absorbtivity for Cavity 1. 4 in. Long

5.3.1.2 Computer

To accurately estimate re-reflective losses the incoming energy distribution as it impinged on the surface of the cylindrical generator interior has to be estimated. A graphical analysis was performed and a plot of intensity as a function of depth of cavity, is shown in Figure 33. The generator cavity and front entrance was then divided into 18 nodes. The thermal impedances between each node as well as the shape factors from one node to another were then obtained. Computations were then made which defined the amount of energy absorbed by each node after several reflections. The data was then extrapolated to determine the energy absorbed after an infinite series of reflections. Diffuse energy reflection was assumed. This assumption will produce some discrepancy between measured and calculated values since the energy is both specularly and diffusely reflected. Sufficient instrumentation of the generator cavity has been supplied for solar testing. The 18 nodes are shown in Figure 34. From the analysis the solar energy and heat balance can then be computed assuming a constant energy input to the converter. The results of this energy balance are shown in Table 2.

5.3.1.3 EOS Analysis

This analysis assumes that:

1. The amount of flux entering the cavity per unit area of cavity opening is constant.

2. All radiation reflected by a surface is assumed to be hemispherically diffuse with an intensity varying as the cosine of the angle with the surface normal

The fraction of possible heat absorbed is given by:

$$F_a = \frac{\alpha}{1 - (1 - \alpha)(1 - \theta)}$$

TABLE 2

ENERGY BALANCE FOR CVG CAVITY ONE INCH DIAMETER APERTURE

	2" Diameter Cavity		1.4" Diameter Cavity	
Solar Energy Entering Aperture (watts)	448	250	434	660
Solar Energy Reflected out aperture (watts)	32	34	60	91
Energy Emitted out Aperture (watts)	163	64	126	204
Energy Through Insulation (watts) (Preliminary Estimate)	10	3	5	8
Energy Through Aperture Lip	4	2	4	6

Energy Entering Ceramic Rings	5	3	5	9
Energy Through Converters (Preliminary Estimate)	<u>234</u>	<u>144</u>	<u>234</u>	<u>342</u>
Cathode Temperature ^{O}K	1650	1400	1650	1850
Solar Absorptivity	.4	.4	.4	.4
Emissivity	.1	.1	.1	.1

where θ is defined as the average fraction of light reflected from the surface of the cavity interior and which passing directly out through the cavity opening. θ has been plotted in Figure 35, against values of s/S for three different ratios of cavity length-to-opening radius. Fa is plotted in Figure 32, vs. aperture diameter. For a 1.00 inch diameter opening, Fa is 0.829.

5.3.1.4   Absorptivity Analysis Comparison

The curves of cavity absorptivity are shown in Figure 32. In general, all three methods agree quite closely with the EOS and Gouffe analysis coinciding at Da = 1.00 inch. The absorptivity found by the Tomlinson (.862) is believed to be the most accurate because of the sophistication involved in the analysis.

5.3.2   Cavity Emissivity

One of the largest losses encountered with the CVG cavity is caused by reradiation. Since the cathode shoes are hot, they radiate energy some of which is transmitted directly out the aperture, the remainder being transmitted to other locations within the cavity, partially absorbed, and reflected out the aperture. To obtain the value of the emergent heat flux from the cavity, it is necessary to account for the multiple diffuse reflections which take place within the cavity. Three analyses have been made to obtain the reradiation losses from the aperture.

5.3.2.1   Computer

The computation of the emission through the aperture is done in a manner similar to that of paragraph 5.3.1.2, except that the energy is initially considered as being emitted from each node with an emissivity assumption since it has been calculated that the net radiation interchange between nodes due to temperature difference is negligible when compared with the conduction heat transfer. Equations have been written for each node and the entire matrix solved by computer for three different cathode temperatures. The results for these sets of equations are shown in Table 2 for a 2 inch cavity and 1.4 inch cavity. The 1.4 inch points are also illustrated in Figure 35.

5.3.2.2   Integration Analysis

An integration analysis has been performed to determine the reradiation losses from a cylindrical shaped cavity. A derivation was made to determine the
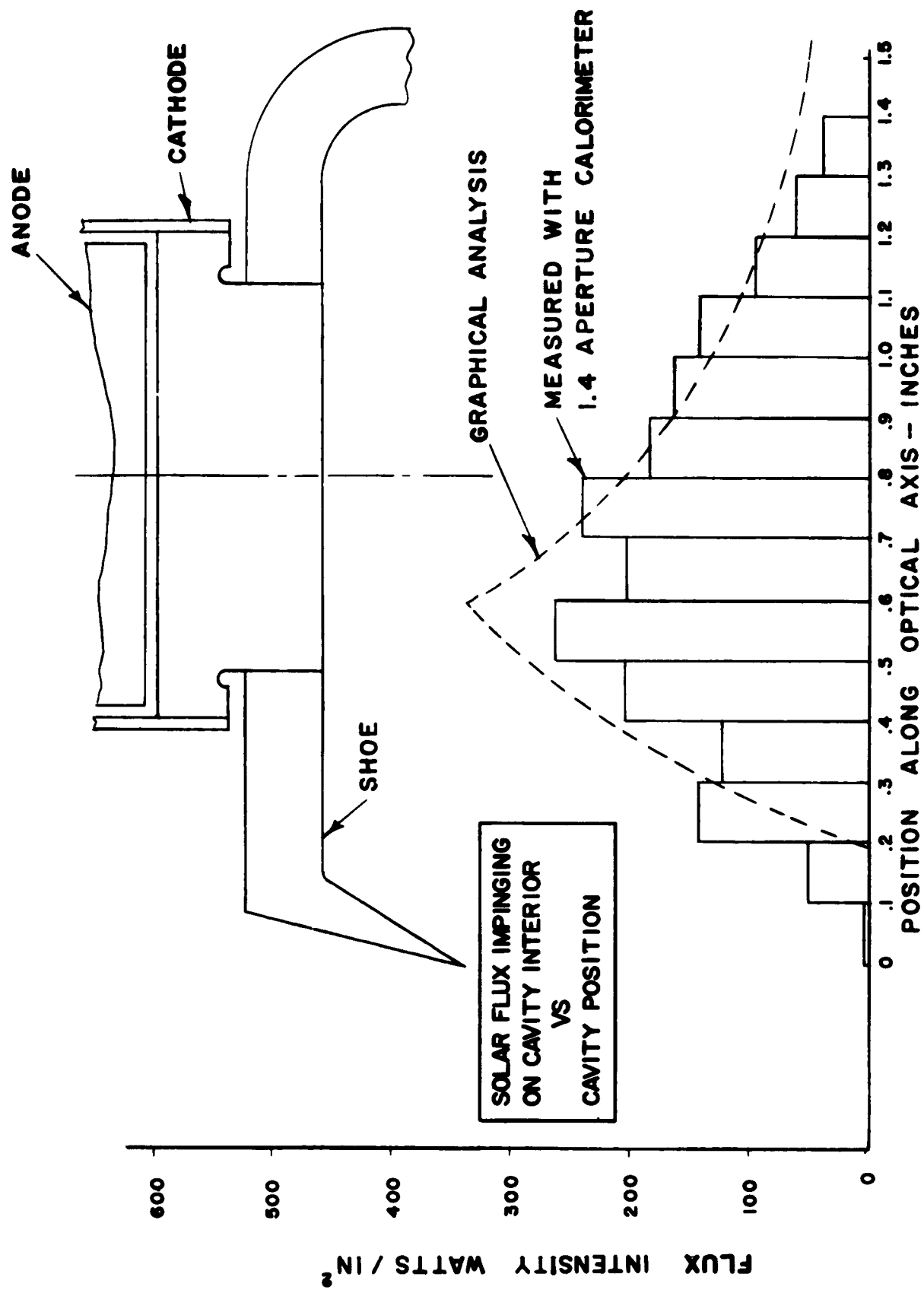
Figure 33. Intensity as a Function of Cavity Depth

CATHODE

ANODE

GRAPHICAL ANALYSIS

MEASURED WITH
1.4 APERTURE CALORIMETER

SHOE

SOLAR FLUX IMPINGING
ON CAVITY INTERIOR
VS
CAVITY POSITION

POSITION ALONG OPTICAL AXIS — INCHES

FLUX INTENSITY WATTS / IN²

47
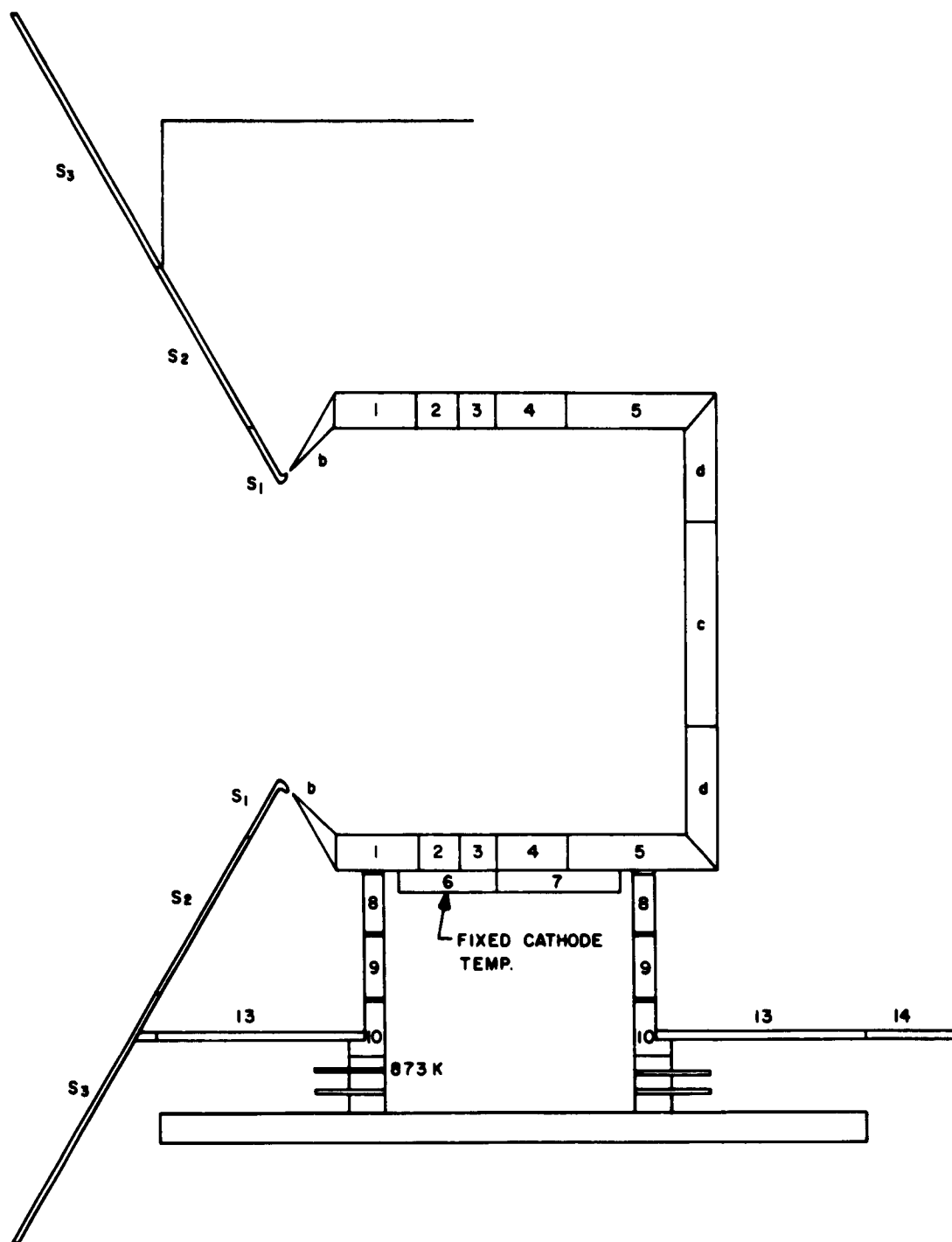
Figure 34. Plot of Nodal Positions for Computer Analysis

48
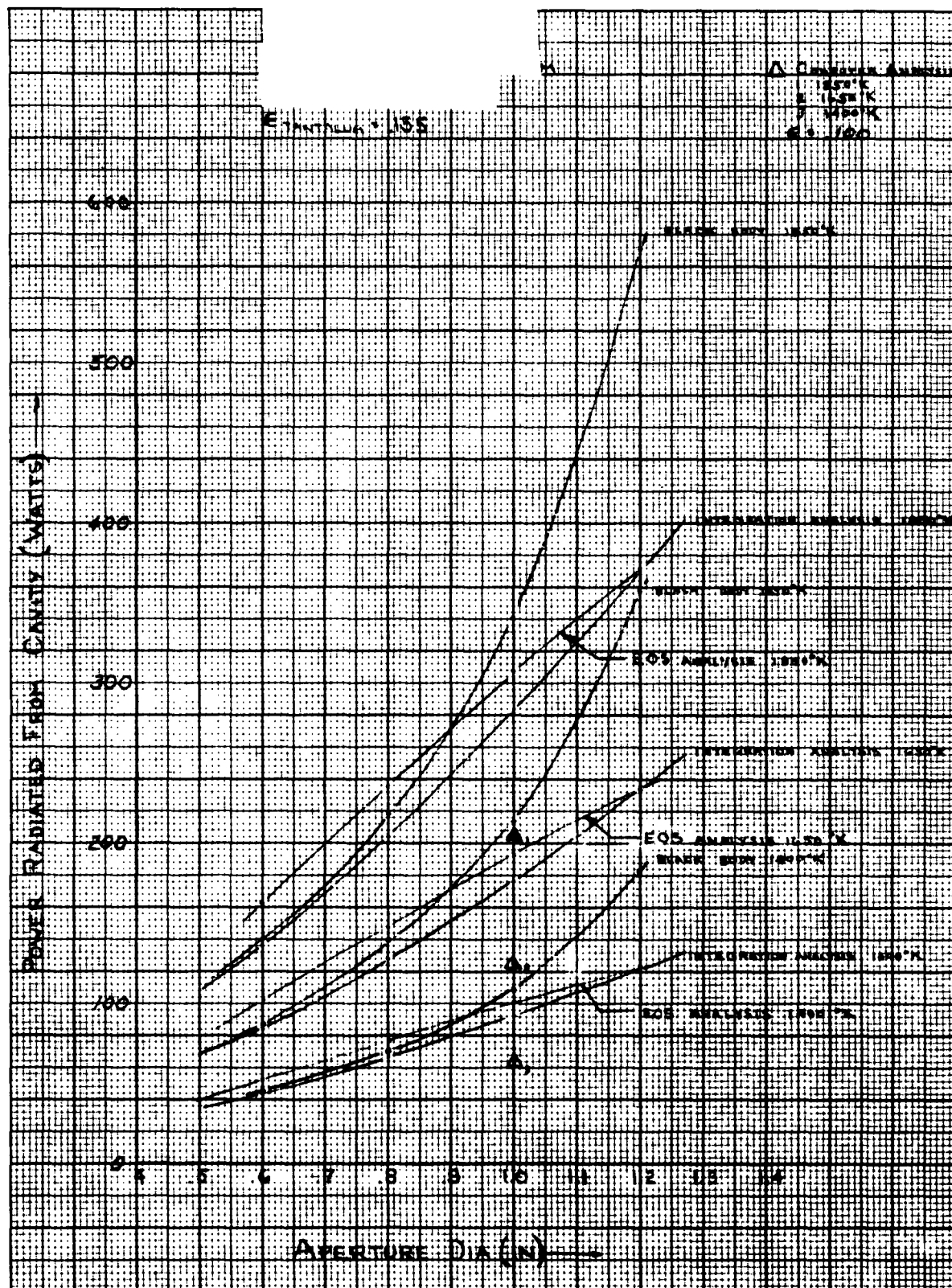
Figure 35. Power Radiated from Cavity

direct radiation loss and the indirect radiation was treated in a manner similar to that described in paragraph 5.3.1.1. This derivation and subsequent results are plotted in Figure 35. Again the assumption of an isothermal cavity has been taken, with the assumption that the radiated energy is uniform after the first reflection.

5.3.2.3 EOS Analysis

This analysis is restricted to an isothermal cylindrical cavity. The total amount of energy lost through the cavity opening by reradiation from the cavity interior surface is:

$$Q_b = \sigma T^4 A_a$$

where A_a = Aperture area
Q_b = Black body radiation from cavity
θ = As defined in Section 5.3.1.3.

These values are plotted in Figure 35.

5.3.3 Total Losses

The radiation characteristics for a black body cavity have been computed and are displayed in Figure 35. These losses are given by the formula:

$$Q = A_a \, \sigma \, E \, T_c^4$$

Where $E = 1.00$

A comparison of the EOS analysis and integration procedure show fairly close agreement; however, only the integration analysis approaches a black body characteristic, or ideal cavity, as aperture diameter becomes smaller and smaller. As seen from Figure 35, a large discrepancy exists in the computer analysis. This is due to tantalum emissivity values of 0.1 being used, instead of the 0.155 value as actually measured for tantalum. Therefore, the integration analysis will be considered as the correct value of reradiation loss and will be utilized in studying the subsystem efficiencies and system losses.

5.4 Converter Des gn

5.4.1 Regression Analysis Description

The most important parameter in the converter design is the electrical power expected as a function of cathode temperature. In order to assess this performance carefully, a regression analysis was performed by T. Marshall on data obtained by E. A. Baum and A. Jensen of the Power Tube Department, V. C. Wilson of the Research Laboratory and N. Razor of Atomics International. Data was available for molybdenum electrodes with the exception of Wilson's data which was available for tungsten. This regression analysis is a technique for determining, by curve plotting, the dependence of a specific variable on a large number of other variables. The only assumption is that the independent variables must be factors multiplying in an equation.

From this analysis a plot of peak power as a function of cathode temperature as well as load lines from 1400 to 2400°K cathode temperature were prepared, as

50

shown in Figure 36. From these load lines and a knowledge of the expected converter geometry, preliminary thermal and electrical estimates of the converter performance were obtained. Included in the computation was the optimization of the area of the envelope to the lead length. This is an important variable in that it defined some of the geometric considerations necessary in the design of the converter. This ratio of envelope area to envelope length is given in Figure 37. In addition, values of optimum anode temperature, cesium reservoir temperature, and seal temperature were obtained.

5.4.2 Envelope Length

With estimates of the converter performance for planar geometry made these estimates had to be put into a realistic configuration. The configuration which has been shown in Figure 2, is consistent with an area to length ratio to provide a maximum efficiency at approximately 1650°K cathode temperature. The length was also determined by the requirement of obtaining sufficient length to provide room for the heat shield insulation that was developed for this generator. It was also to provide some leadway for motion of the foils with respect to the envelope to enable the ceramics to be kept away from the cathode weld area during welding. These parameters are shown in Figure 38. The envelope is part 4, the cathode is part 2 of this assembly drawing. This drawing also shows the heli-arc weld of the envelope to the cathode but does not show the cathode pick up shoe attached to the cathode. In this drawing the cathode and the anode slug (part 3) are separated to provide the inter-electrode space by alumina pin spacers which are assembled under compression. As the thermal energy passes through the anode slug a ΔT is experienced from the surface of the anode to the anode radiating fin. This ΔT is necessary to lower the temperature of the anode radiating fin to keep the seal cool. The thermal energy is then radiated from the anode radiating fin (part 10) to the wall of the tank which simulates free space. Part 7 is a long cesium reservoir tube which extends from the anode fin to provide for a decrease in temperature at the tip of the cesium reservoir tube. A heater (part 14) heats the cesium reservoir tube and provides a fine control of the cesium temperature. This was necessary since an approximation only could be made, at the onset of the program, of the optimum cesium reservoir temperature for the various cathode and anode temperatures expected during operation of the generator. An anode heater is also supplied (part 16) for heating of the anode to increase its temperature and to obtain technical data on the converter performance at higher anode temperatures.

5.4.3 Fin Size

The initial converter fin diameter was 3 inches. This was increased to 3.6 inches following tests of some of the early converters which found the anode running too hot, causing the emission of the tube to be less than anticipated. This was made evident by the fact that any heating of the anode during the operation of the converter with a three inch diameter .060" thick fin, caused degradation of the output. This increased size of the anode is also helpful in cooling the seal.

5.4.4 Ceramic-to-Metal Seal

The ceramic-to-metal seal (part 5) was designed to withstand cesium attack and to operate in the vicinity of 600°C. Considerable difficulty was experienced for the duration of the program, in maintaining this seal and failure of the seal due to difficulty in manufacturing was an early problem. These problems have
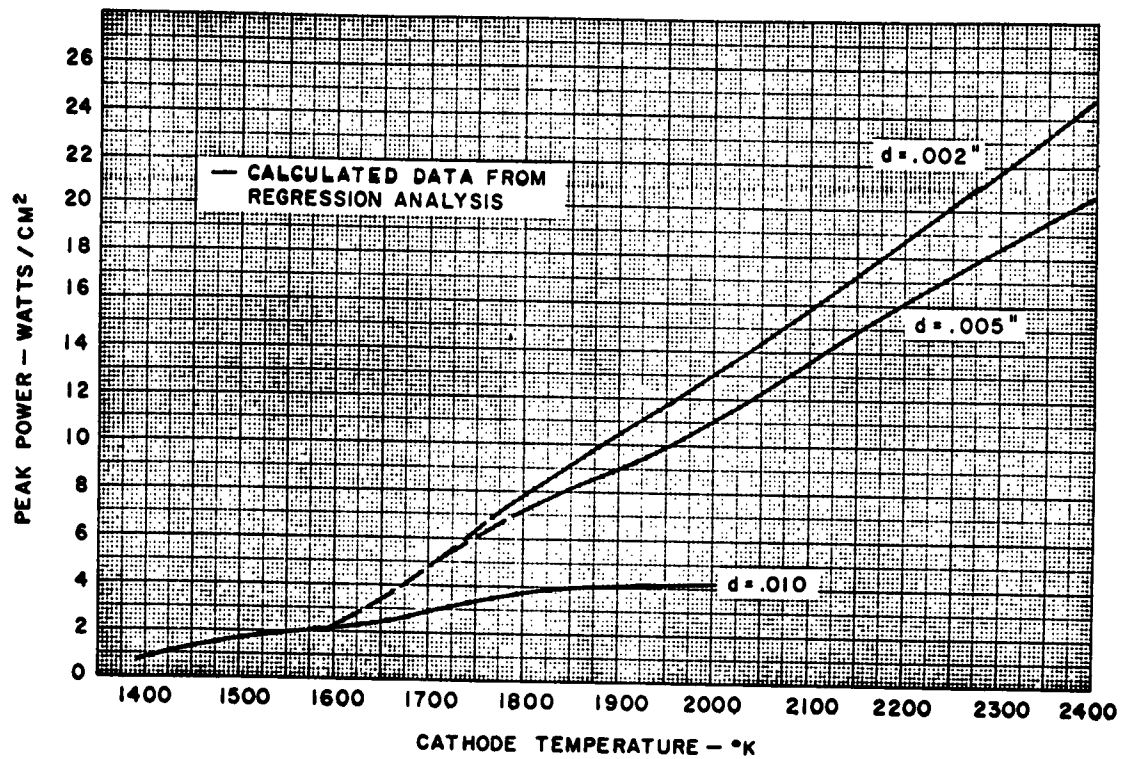
Figure 36. Peak Power as a Function of Cathode Temperature
and Load Lines
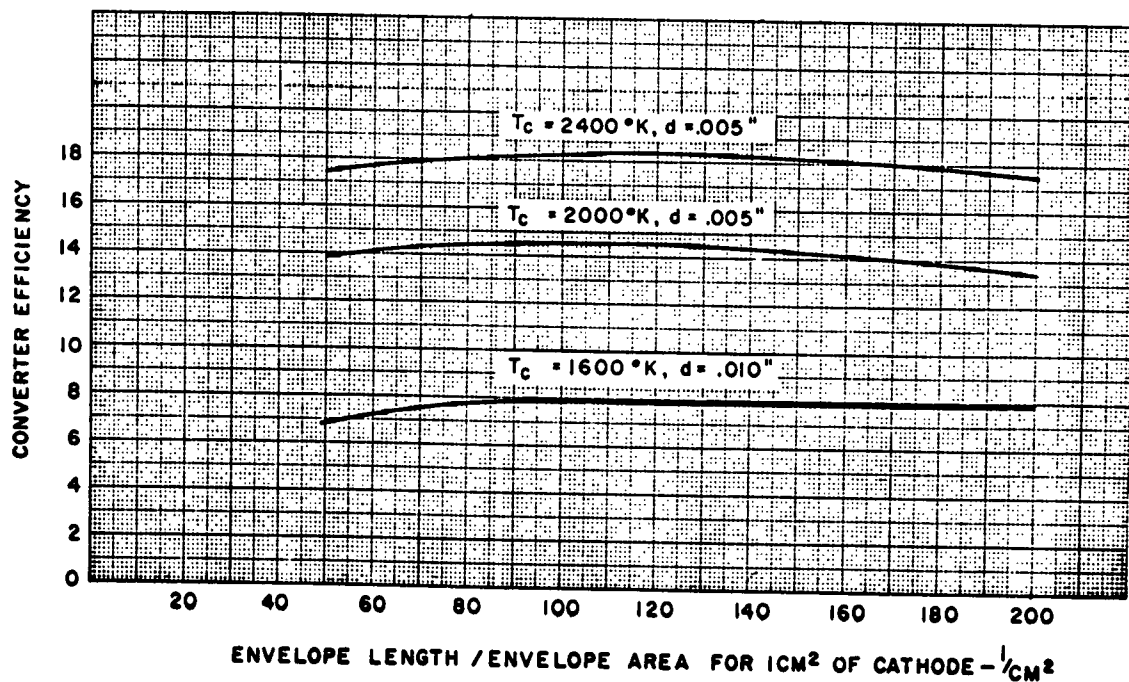
Figure 37. Converter Effeciency vs. Envelope Length-to-Area Ratio

52

Figure 38. Converter Assembly

been reduced by the use of a high-alumina ceramic coupled with a braze particularly developed for cesium at high temperature. During the course of the program, part 6 was increased in thickness in order to reduce the drop between part 6 and part 10, thus causing part 6 to run cooler than originally expected.

5.4.5 Computer Program Description

Since the performance estimates discussed in the appendices were based on an analysis which divided the converter into three sections and computations were by means of the slide rule, it was necessary to compute the characteristic of the converter by means of a more accurate computer program. The computer nodes are shown in Figure 39. Since the anode temperature-optimum was uncertain and the thermal impedance of the anode slug was not completely known, a series of runs assuming different anode temperatures, heat subtractions from the anode and fin sizes from the anode rejection fin was obtained. The results of this 7090 analyses are shown in Table 3. It is possible to compute the thermal energy requirement of the converter and the temperature distribution within the converter by means of this computer program. From the temperatures of the various nodes, over-temperature problems of the seal and cesium reservoir were pin-pointed to allow for slight converter redesign. Measured values of conductivity, emissivity, and resistivity, as a function of temperature, were used to establish the thermal impedances between the various converter nodes.

TABLE 3. RESULTS OF 7090 ANALYSES

Cathode, $^{\circ}K$	1650	1650	1650	1650
Electron Cooling, w/cm^2	16	20	16	16
Anode, $^{\circ}K$	1070	1070	970	1170

NODES	A	B	C	E
CASE NO.				
16	1648	1647	1647	1649
17	1622	1622	1618	1627
18	1577	1575	1567	1588
19	1547	1544	1533	1561
20	1520	1516	1502	1538
21	1482	1477	1459	1506
22	1456	1450	1429	1484
23	1431	1424	1400	1462
24	1398	1390	1362	1434
25	1374	1365	1334	1413
26	1352	1342	1310	1395
27	1323	1312	1277	1370
28	1310	1298	1261	1359
29	1304	1292	1255	1354
31	1557	1554	1544	1570
32	1450	1444	1422	1479
33	1365	1356	1324	1406
34	1286	1273	1234	1339
35	1197	1180	1132	1262
36	1109	1088	1032	1186
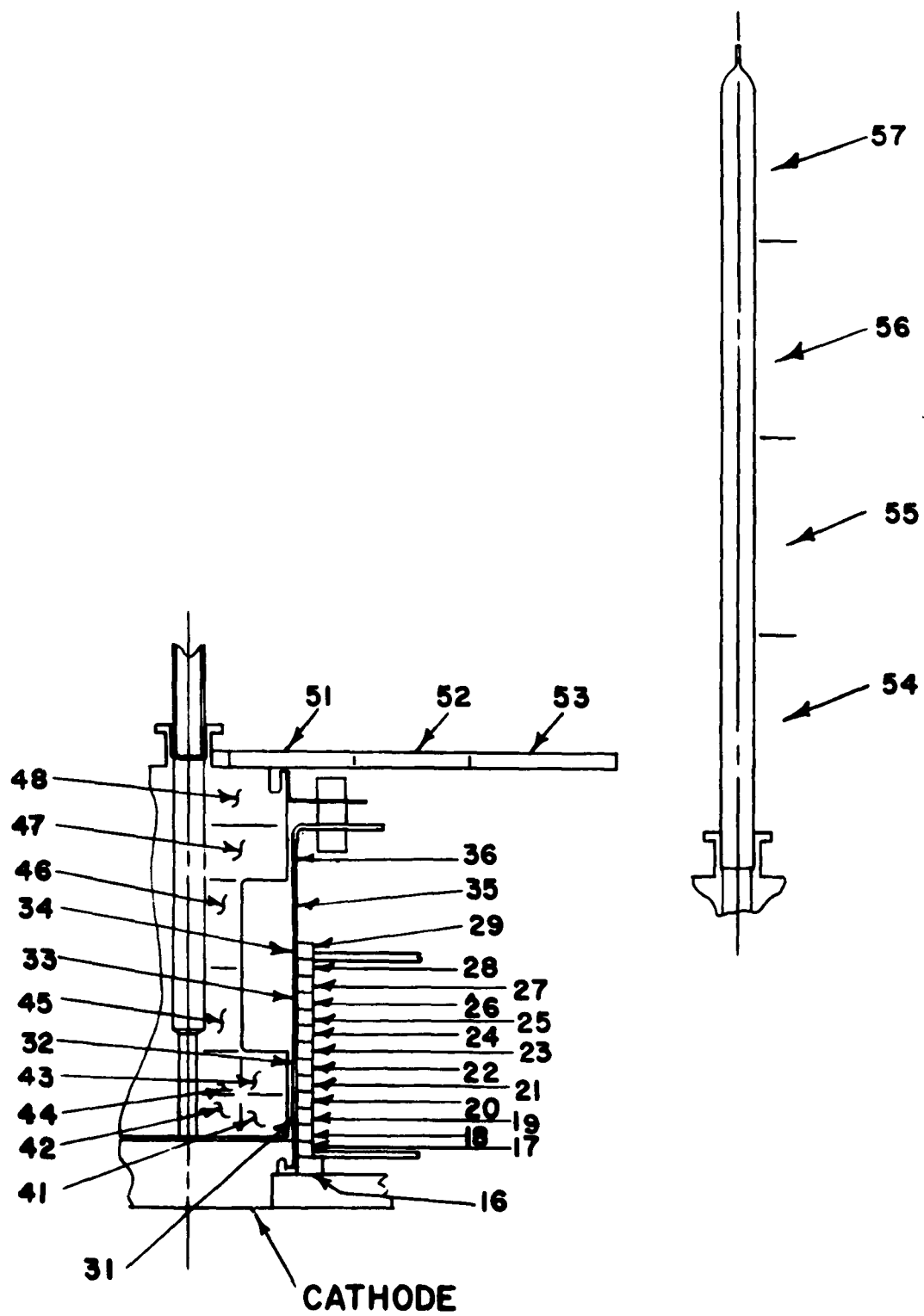
Figure 39. Node Definition, Converter Computer Analysis

TABLE 3. RESULTS OF 7090 ANALYSES (CONT.)

Cathode, ^{O}K
Electron Cooling, w/cm^2
Anode, ^{O}K

1650	1650	1650	1650	
16	20	16	16	
1070	1070	970	1170	

NODES / CASE NO.	A	B	C	E
15	992	966	899	1086
41	1070	1070	970	1170
42	1065	1064	964	1165
43	1065	1064	964	1165
44	1051	1048	950	1152
45	1003	991	900	1106
46	938	915	833	1043
47	901	871	794	1008
48	890	859	783	998
51	852	814	741	962
52	821	775	702	939
53	814	761	683	945
54	776	750	691	861
55	637	622	589	686
56	568	561	548	588
57	570	570	570	570
Q1	29.4	11.0	49.4	107.9
Q2	0.92	1.02	1.22	0.61

Cathode, ^{O}K
Electron Cooling, w/cm^2
Anode, ^{O}K

1850	1850	1850	1850	1850
15	40	15	15	20
1070	1070	970	1170	970
				New choke fin 3.08" dia.

NODES / CASE NO.	M	N	P	R	S
16	1838	1837	1837	1839	1832
17	1808	1803	1803	1812	1793
18	1747	1735	1736	1757	1713
19	1706	1689	1691	1721	1661
20	1670	1648	1651	1688	1616
21	1619	1590	1595	1644	1556
22	1584	1549	1556	1612	1514
23	1552	1510	1519	1583	1473
24	1508	1459	1471	1545	1421
25	1477	1422	1436	1517	1385
26	1450	1388	1406	1493	1350
27	1413	1343	1364	1460	1309
28	1396	1323	1345	1445	1287
29	1389	1314	1338	1439	1279
31	1719	1705	1706	1732	1664

TABLE 3. RESULTS OF 7090 ANALYSES (CONT.)

Cathode, ^{O}K	1850	1850	1850	1850	1850
Electron Cooling, w/cm^2	15	40	15	15	20
Anode, ^{O}K	1070	1070	970	1170	970
					New choke dia. 3.08" dia.

NODES	M	N	P	R	S
CASE NO.					
32	1575	1540	1546	1604	1529
33	1465	1408	1423	1507	1375
34	1365	1286	1312	1418	1262
35	1253	1146	1185	1318	1130
36	1142	1010	106?	1219	990
15	995	829	898	1088	845
41	1070	1070	970	1170	970
42	1064	1058	964	1164	964
43	1064	1058	964	1164	963
44	1049	1028	948	1149	948
45	995	920	891	1097	896
46	921	776	813	1026	826
47	879	694	768	985	784
48	867	670	756	974	769
51	821	587	706	931	715
52	782	496	658	900	662
53	768	436	631	898	635
54	756	590	668	840	719
55	625	527	575	673	634
56	563	522	542	582	581
57	570	570	570	570	570
Q1(watts)	7.6	258.5	91.0	70.5	82
Q2(watts)					2.9
Energy through choke(watts)					89
Energy through envelope(watts)					16
Total energy required					105
Loss from seal					1
Energy into cesium tube					1

5.4.6 Converter Materials

Materials were selected on the basis of their resistance to cesium, their compatibility with ceramics, and their thermal and electrical properties (Figure 38). The cathode and anode were molybdenum selected primarily because of their expected emission at the low temperature of 1650°K. An envelope of tantalum was selected due to its ductility and its thermal expansion matching that of the alumina seal as well as its high vapor pressure. The high-alumina seal was selected for its capability to withstand cesium attack at 600°C and a molybdenum fin was selected for its high thermal conductivity, strength at elevated temperatures, and the fact that it could be brazed to the molybdenum anode.

5.4.7 Converter-to-Generator Interface

The converter-to-generator interface is well illustrated by Figure 40. In this figure, the pick-up shoe (part 13) which forms one-third of the solar cavity can be seen heli-arc welded to the cathode of the converter. This is the last operation to be performed on the converter prior to final test. The thermocouple holes for the immersion couples which are inserted through the insulation after assembly of the generator are shown at the top of this figure. Three thermocouple holes are shown, one for measurement of the temperature at the rear of the shoe, one for measurement of the temperature at the front edge of the shoe, and a third, an immersion couple placed at the center of the cathode. This hole is drilled prior to assembly and re-drilled after assembly since the heli-arc weld tends to seal the hole during the final weld. In the final generator, only one converter was completely instrumented with the three couples, the other converters only having couples inserted into the central cathode hole. The insulation sections described in section 5.5.1 are shown assembled around the exterior of the generator and the mechanical attachment between the converter and the insulation sections is performed by a screw (part 12) which goes into the stud of part 2 and is insulated from the converter fin by parts 10 and 11 which are alumina separators. Beneath the seal are a series of spiral tantalum heat shield foils (part 4) which hold the ceramic rings in place.

In the upper right of this illustration the anode power terminal and the cathode power terminal are shown. Not shown, are the copper spider wires which come from the envelope to the cathode power terminal. This power terminal is also insulated from the anode fin by alumina separators. The thermocouple positioning is more clearly shown in Figure 41 which shows the converter segment assembled into the generator, and the positioning of the thermocouples.

The anode fin is flame-spray coated with zirconium carbide whose emissivity is plotted in Figure 42.

5.5 Generator Description

5.5.1 Insulation

5.5.1.1 Manufacturing

For the converter and back generator insulation sections, tantalum foils shown in Figure 43 were cut to the proper size (see Figure 44), drilled to accommodate support wires and thermocouple holes, and then dye-pressed with .010 inch high conical dimples as shown in Figure 45. The corner sections, see Figure 46 and 47, presented a difficult manufacturing problem due to their dovetailed shape. To solve this, alternating layers of tantalum and steel were glued together to form a block. This block was then machined to the required shape. The assembly was then drilled as necessary and broken apart by ultrasonic cleaning, as shown in Figure 48. The steel spacers were then discarded and the tantalum shields were subsequently dimpled. This same procedure was followed for the generator front-aperture sections where the conical shaped aperture hole was bored while this section was in block form. To all sections, inside .020 inch thick tantalum plates were added, and .030 inch thick outside plates. These outside plates, when all bolted together form the exterior surface of the generator. Each insulating section is held together by .010 inch diameter tantalum support wires, with the exception of the aperture section. Here the assembly is rigidized by tack welding the insulation itself, since the aperture would not afford sufficient room for support wires. Vacuum firing of all generator insulation was carried out at 1200°C for one hour under a vacuum of 1×10^{-6} Torr. Drawings and photographs of a completed section are shown in Figures 49, 50, and 51.

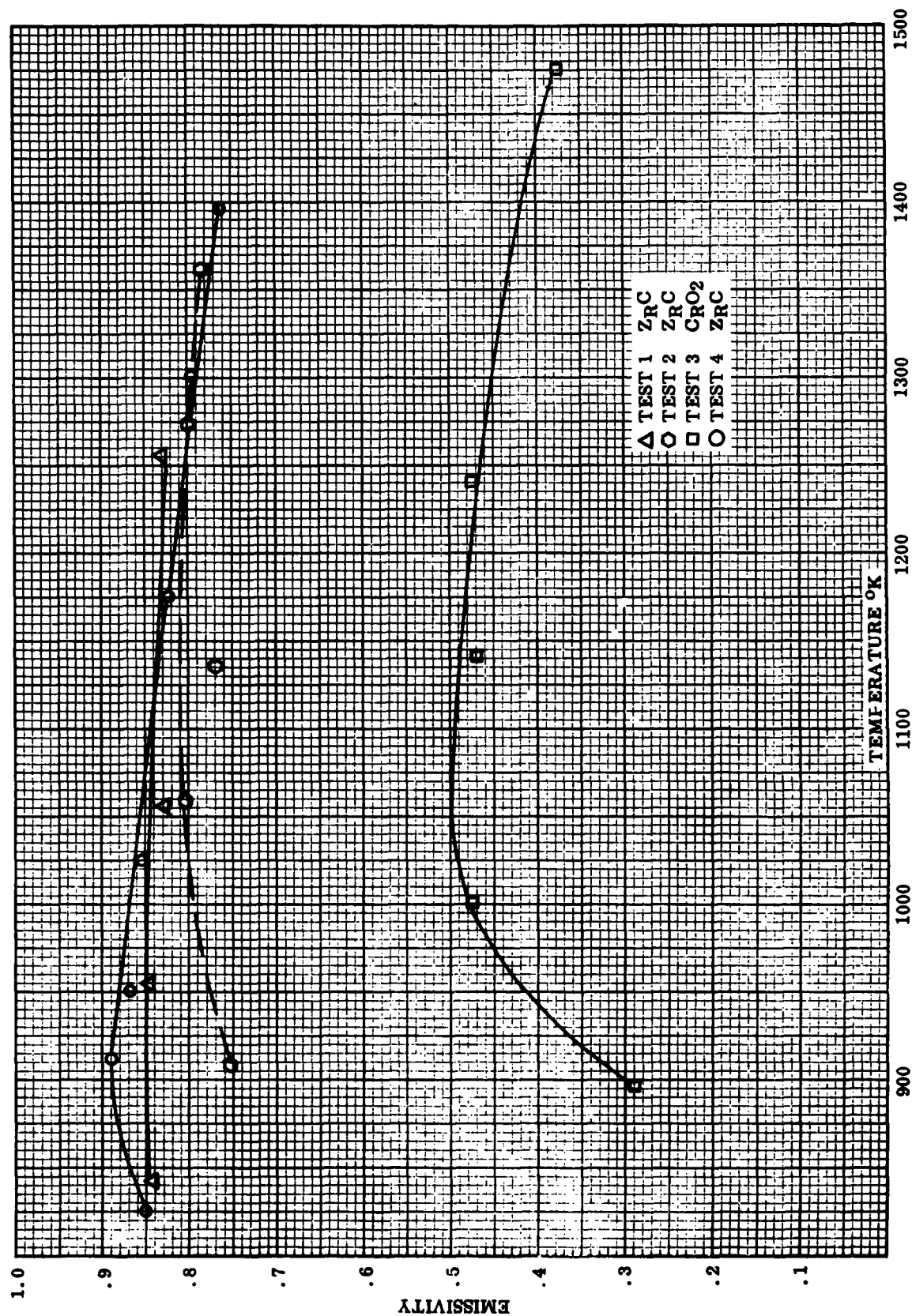**Figure 40. Converter Segment Assembly**

Figure 41. Generator Assembly

Figure 42. Emissivity of Zirconium Carbide and Chronic Oxide
Coatings on Molybdenum

61

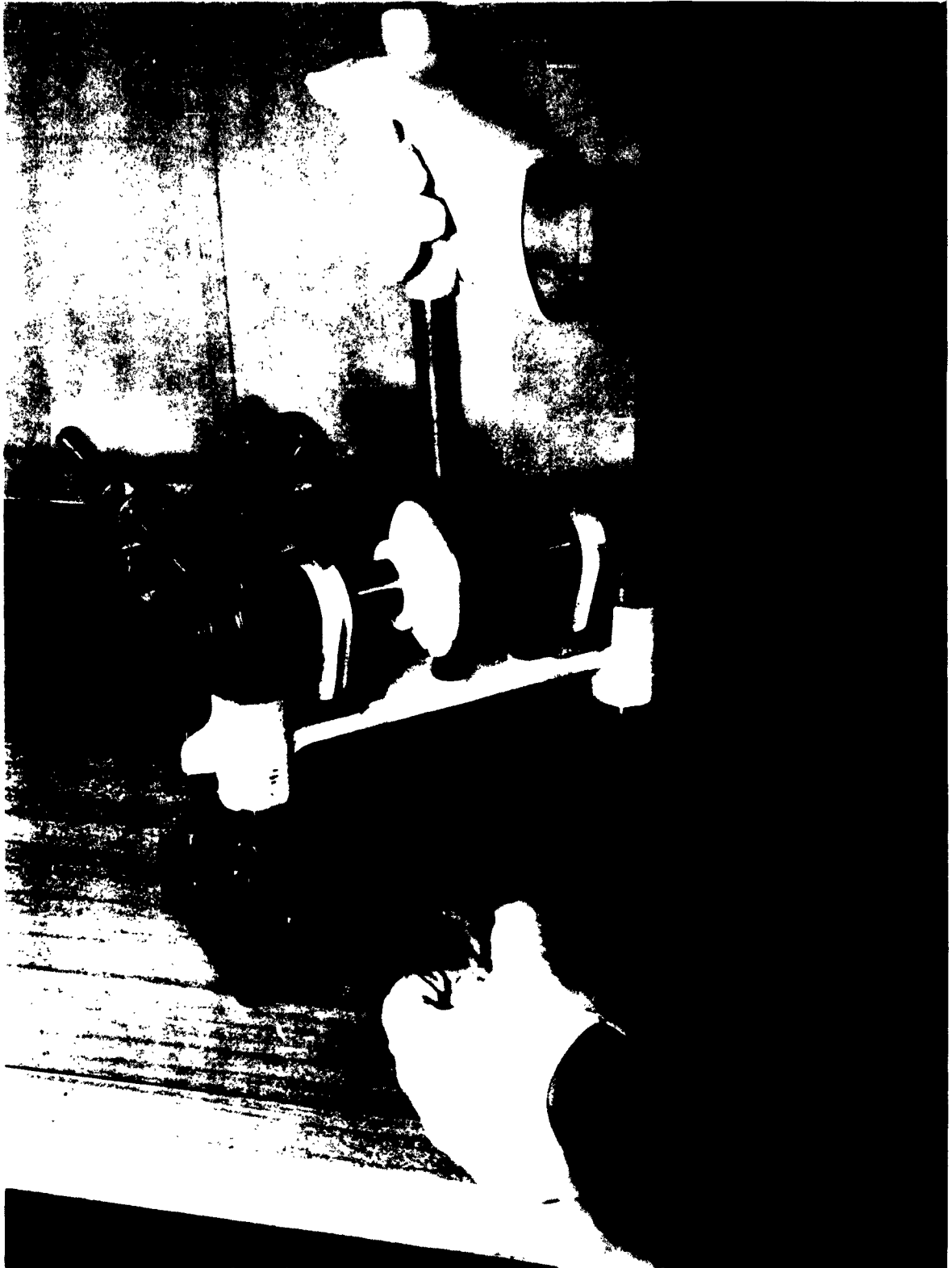**Figure 43. Foil Insulation**
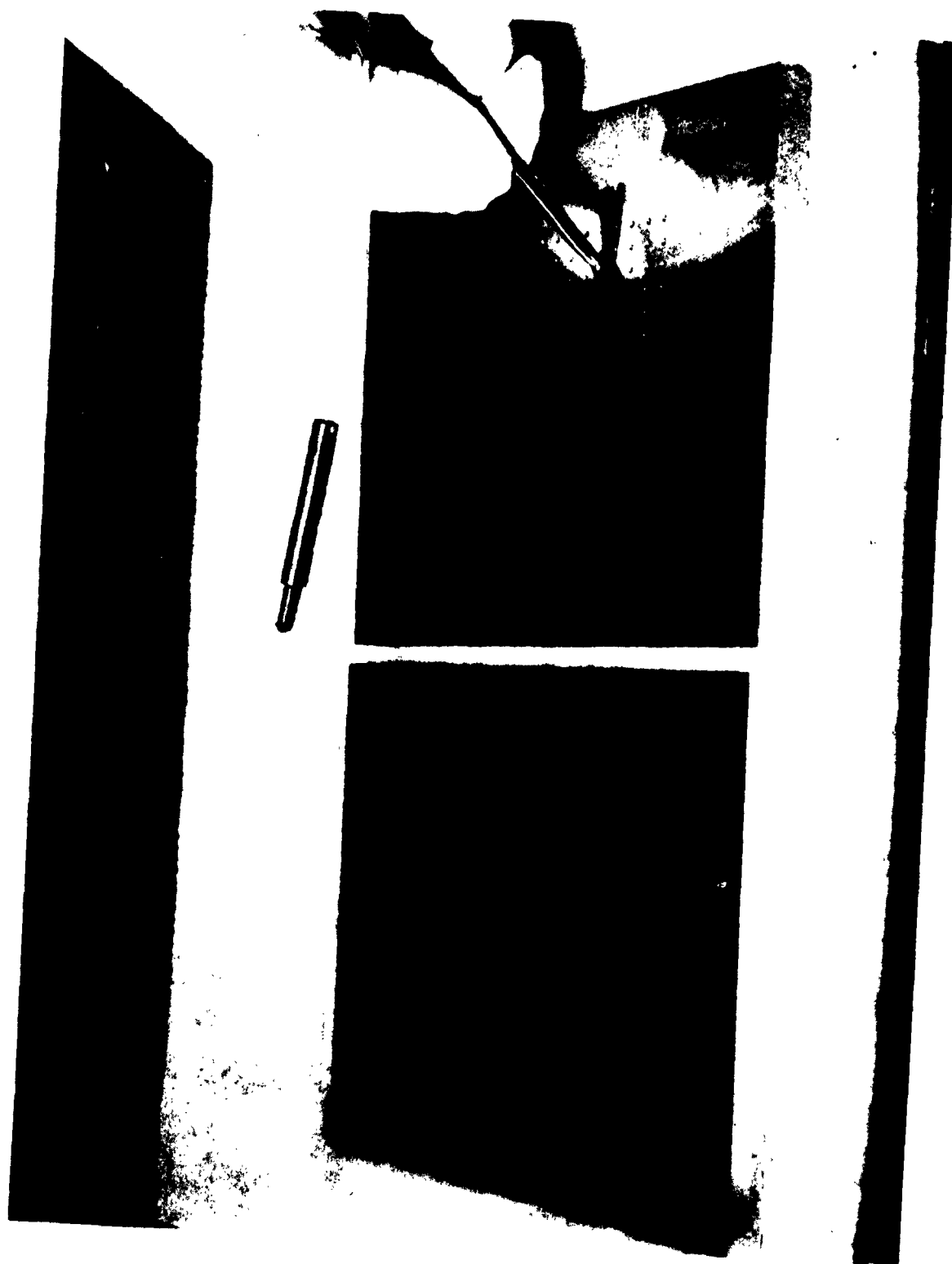
Figure 44. Cutting of Foil Insulation
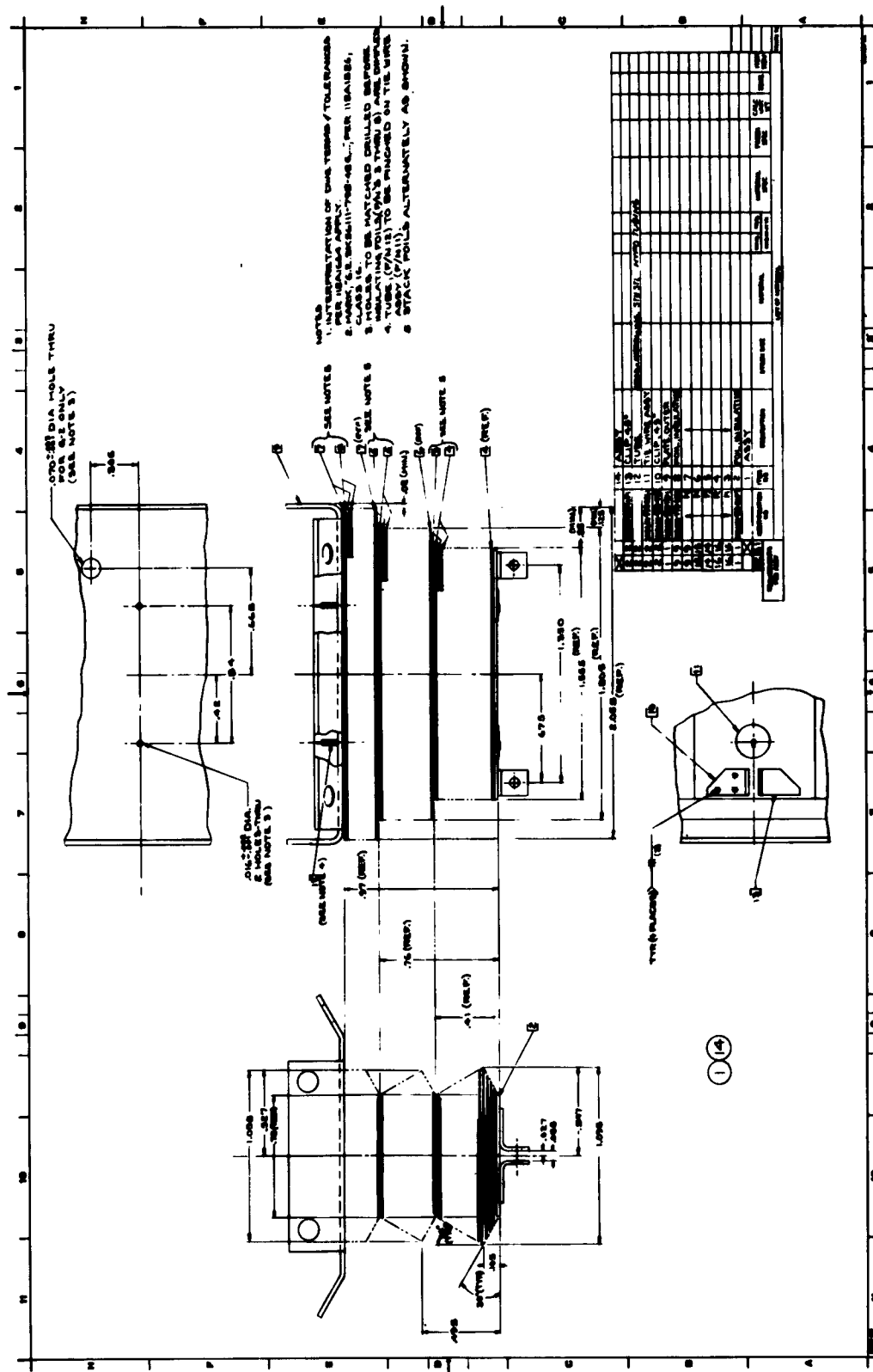
Figure 45. Foil Insulation Dumpling Tools

Figure 46. Corner Segment Assembly

Figure 47. CVG Cover Insulation Section

66

Figure 48. Ultrasonic Cleaning of Insulation Sections

Figure 49. Segment Assembly

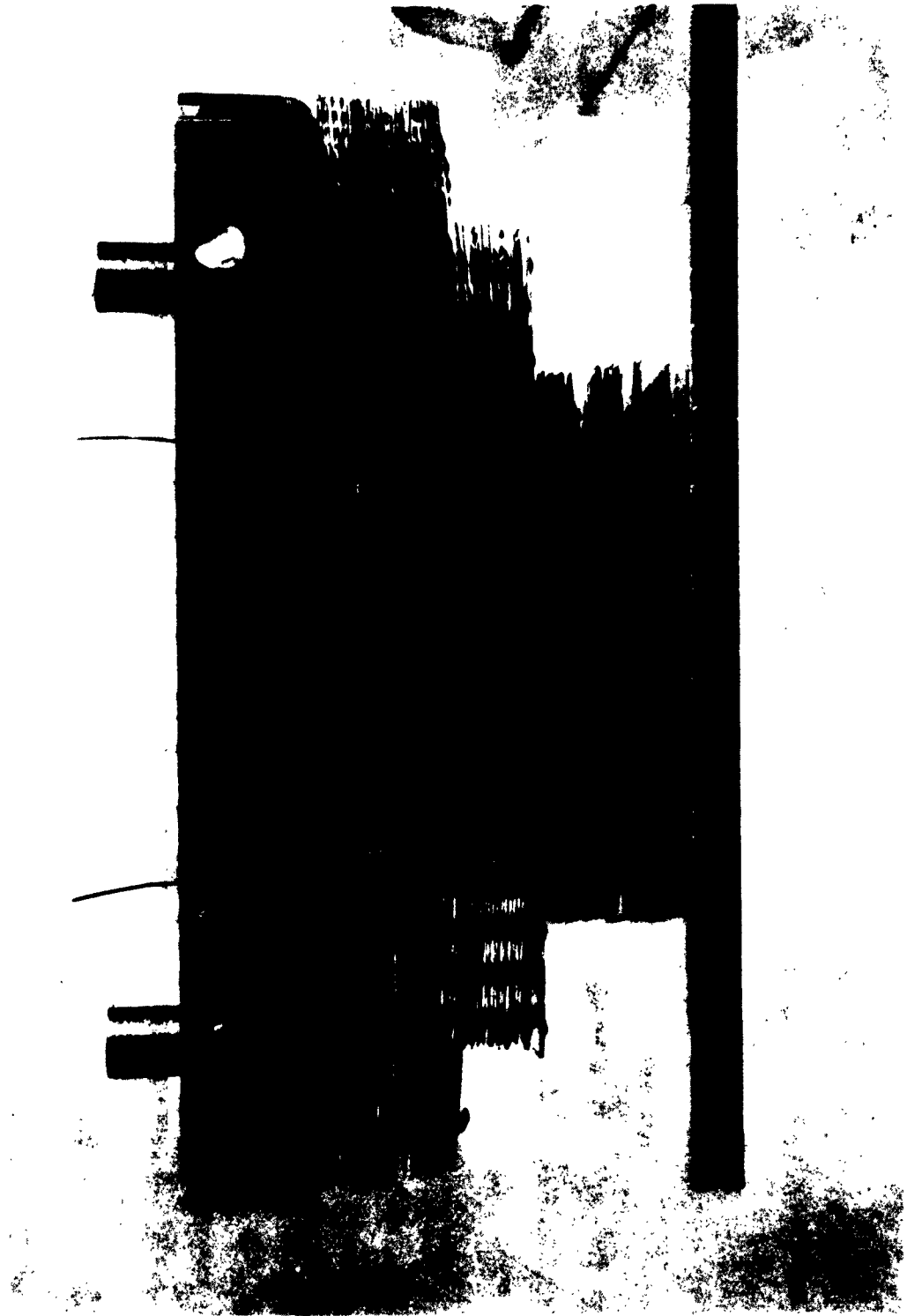Figure 50. Generator Insulation Prior to Assembly with Converter

Figure 51. Side View of Generator Insulation Section

5.5.1.2 Theoretical Performance

Because of the vacuum environment the heat transfer loads through the generator insulation are limited to radiation and conduction. The conductive heat loss through the dimples was found to be negligible since the contact area of each dimple is slight and the loading pressure on each insulation stack is very small or undetermined. The staggered arrangement of the dimples also provides a tortuous heat conduction path. The heat losses per square inch of insulation foil are shown in Figure 52. This loss is based upon emissivity values of tantalum discussed in paragraph 5.5.1.4.

5.5.1.3 Material Selection

Insulation of the generator is composed of 58 layers of two-mil-thick polished tantalum foil. Since it is recognized that the predominant mode of heat transfer is by radiation, tantalum is advantageous because of its low total hemispherical emissivity. Its high melting point affords a wide range of temperature operation, yet it can also be readily pressed, formed, and machined into a variety of shapes at room temperature.

5.5.1.4 Emissivity Measurements

Because emissivity values of any material will change with variations in surface finish, it was thought necessary to obtain the emissivity of the tantalum foil used as radiation shields in the generator.

The principles involved were basic. All the values of the Stefan-Boltzman Equation were measured, with the exception of Fe. Fe turns out in this case to be ϵ and simplifies the calculations. The resulting curve is shown in Figure 53.

It appears that, in the immediate vicinity of the cathode shoes, the emissivity may be as high as 0.16, with decreasing values as we approach the outer skin of the generator.

Data for molybdenum is shown in Figure 54.

5.5.2 Entrance Cone Selection

The front entrance section is composed of a 60° smoothed polished tantalum cone. Tantalum was selected as the cone material since it can be readily spun into a conical shape and also to avoid thermal growth mismatches with the remaining generator structure. The 60° cone angle is consistent with the collector rim angle. The aperture cone also acts as a protective radiation fin for the front portion of the generator since it can dissipate heat which may be caused by large or sudden collector misorientation or tracking errors, where the focal spot could shift from the front aperture hole.

5.5.3 Fastening Techniques

The generator sections are bolted together at the outside plates by stainless steel bolts. The inside plates of the corner sections are held to the rear end aperture sections by tantalum rivets in protruding tabs. These tabs are visible in Figure 55. Converter sections are retained by their outside plates, only to facilitate easy removal. Each converter is retained in its insulation section by two

tantalum posts. Sufficient tolerance has been provided here to allow small adjustments of the converters with respect to each other in forming the cylindrical generator cavity. The aperture cone is fitted with a fine sliding adjustment to permit proper positioning of the focal plane with respect to the generator cavity. Many of these details are evident in the top view of the partially assembled generator shown in Figure 56.
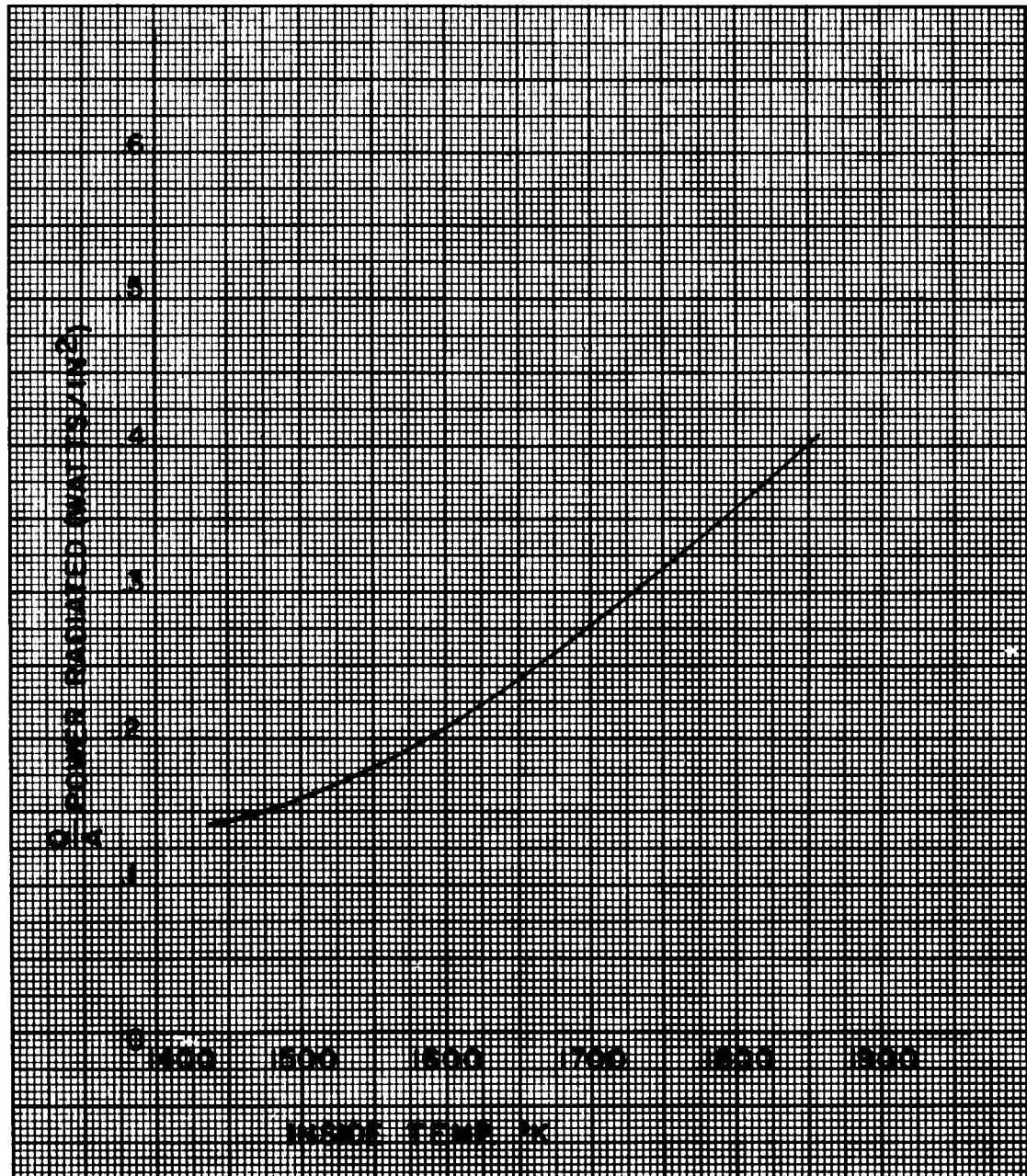

Figure 52. Heat Loss Per Square Inch with 58 Foils
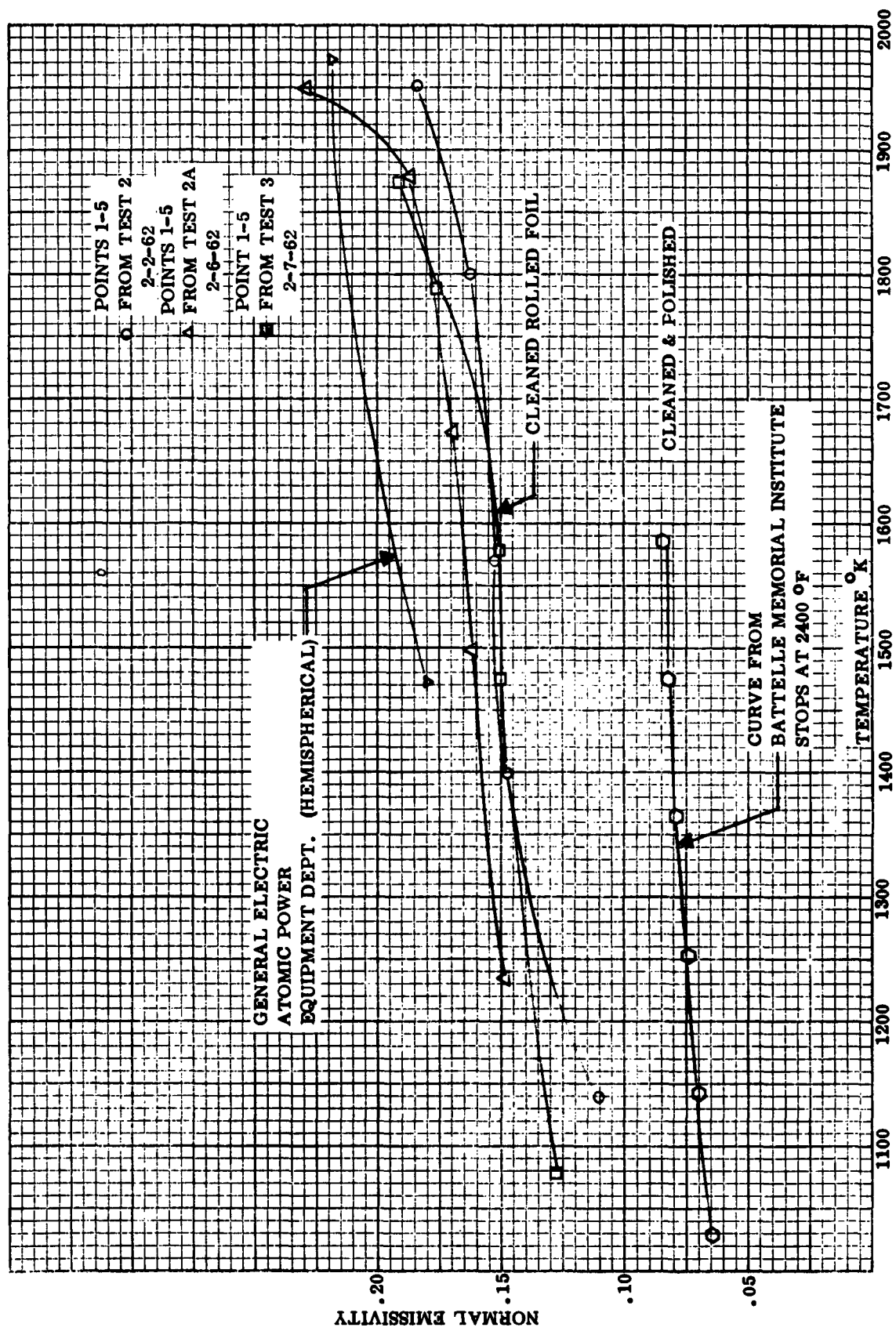
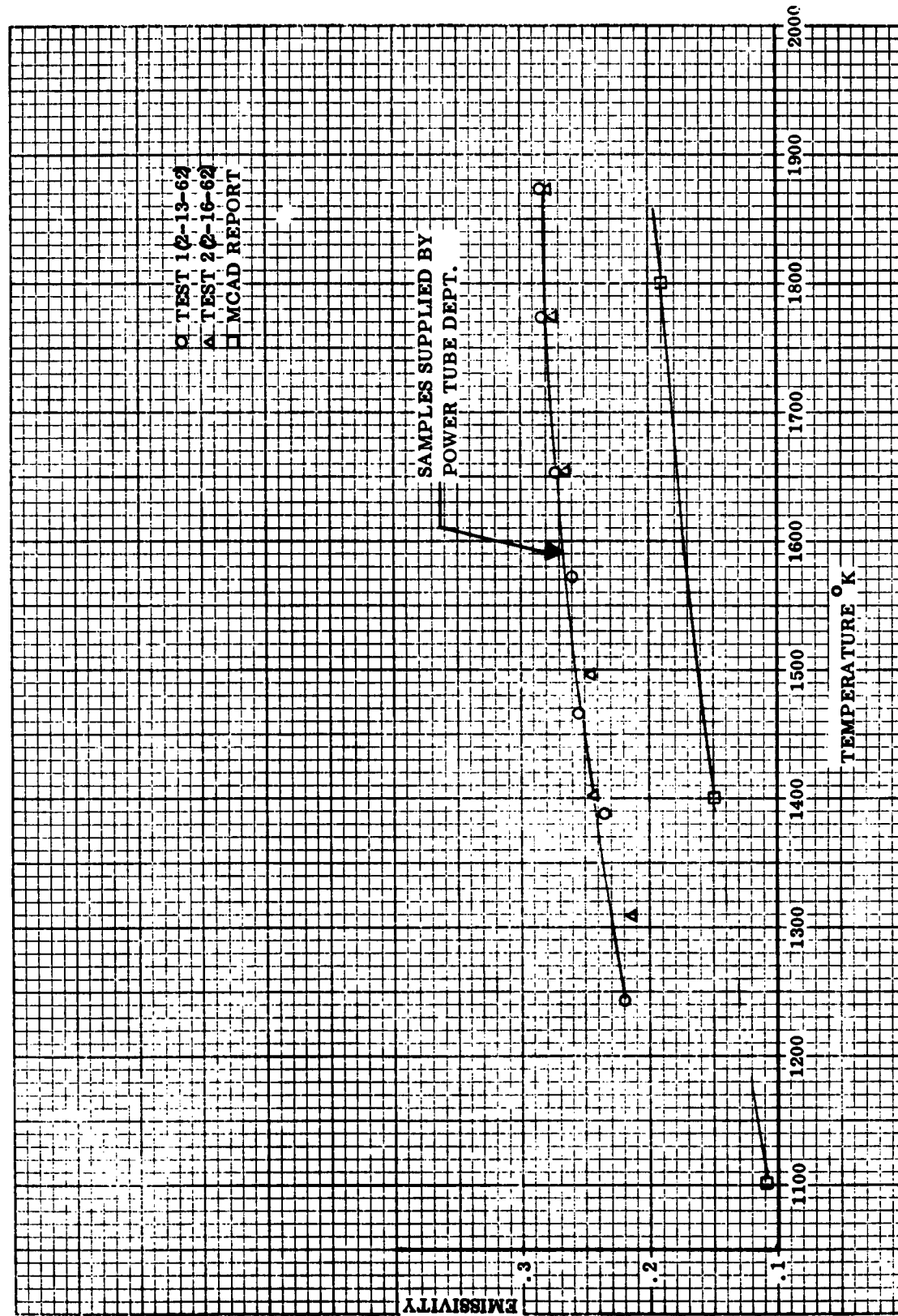Figure 53. Tantalum Emissivity vs. Temperature

73

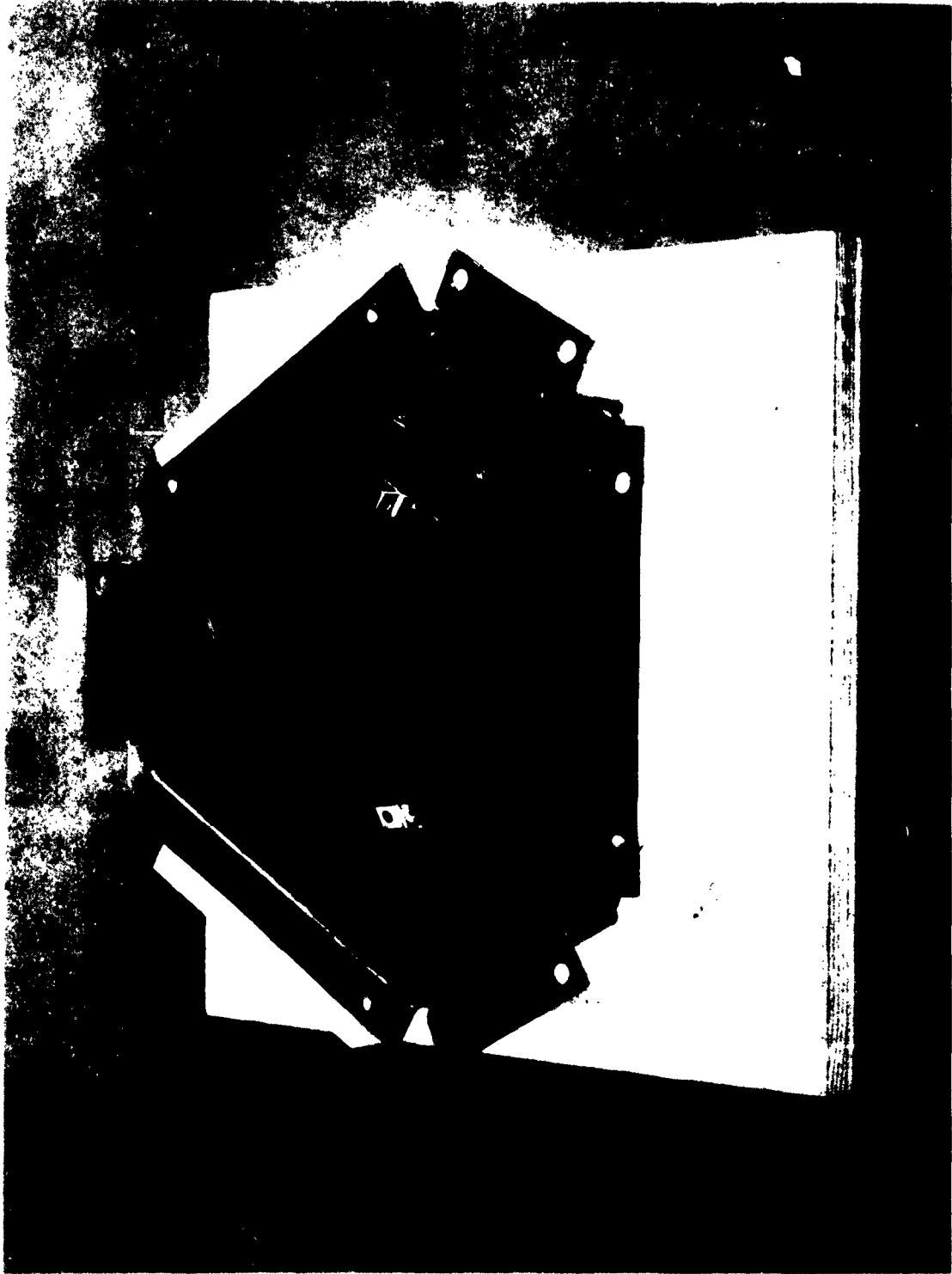Figure 54. Molybdenum Emissivity vs. Temperature

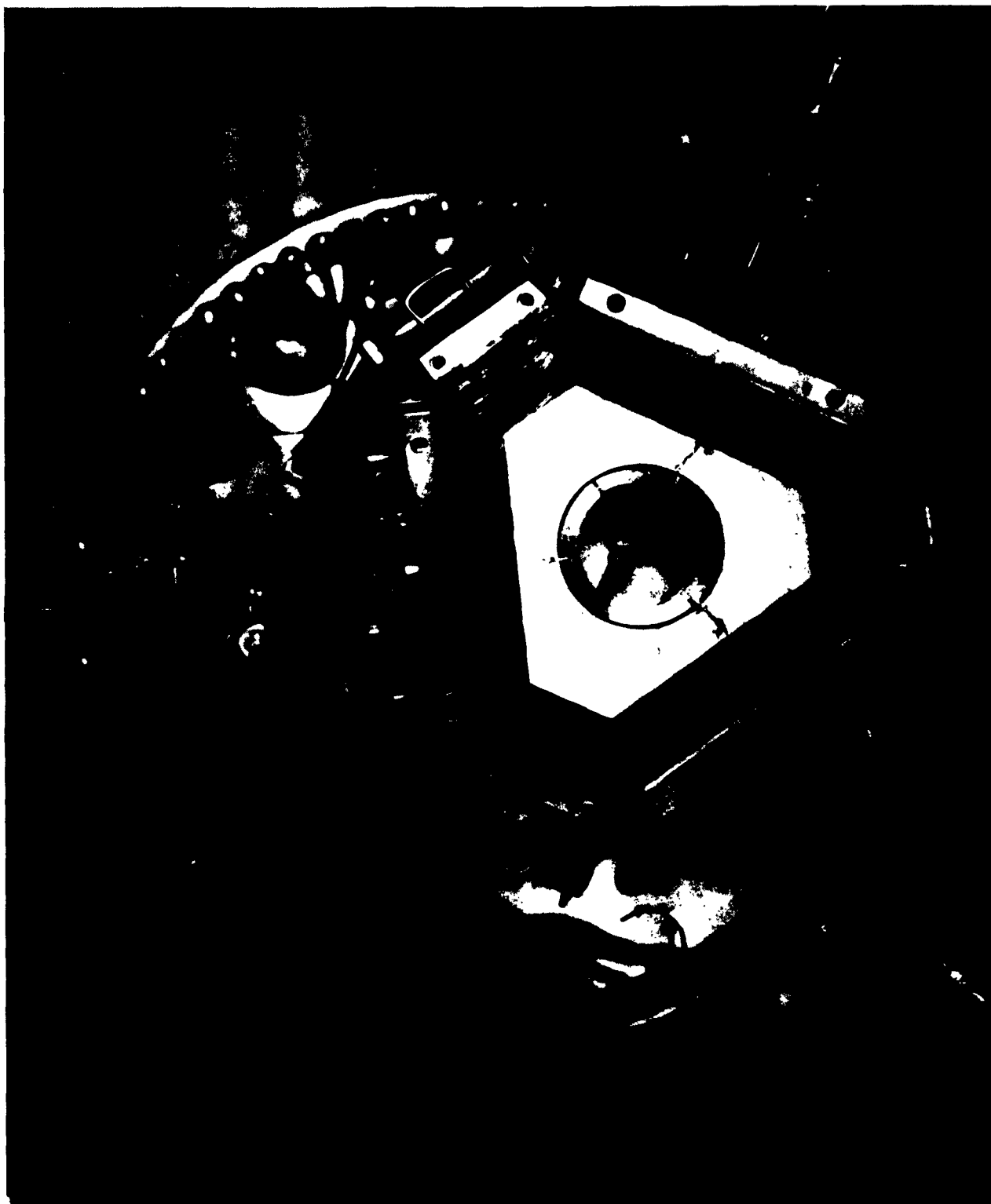Figure 55. CVG End Section Showing Rivet Tabs Protruding Upward

Figure 56. Partially Assembled Generator Showing Cavity

5.5.4 Electrical Insulation Materials

To permit series, parallel, and independent operation of the converters; it is necessary to electrically isolate the cathode shoes from each other and from the generator insulation. High strength is not a large requirement here, so a high purity-coarse grain thoria was selected because of its high melting point, excellent electrical resistance at elevated temperatures, and low vapor pressure. Previous compatibility testing of tantalum and thoria showed favorable results at the expected temperatures. The high temperature tungsten-rhenium thermocouples used in the generator cavity, are insulated by beryllia tubing, because of its availability in the small sizes needed.

5.5.5 Method of Assembly

The generator itself is mounted on the vacuum base plate with a tripod stand, as shown in Figure 3. Small support brackets anchor the generator corner section to the tripod. These corner sections are then bolted to the rear section on the outside plates and internally by means of the previously mentioned tantalum rivets. The converter sections then slide into place and are fastened with stainless steel bolts. At this point, the radiation leakage insulation shims are then added. On top of this assembly is placed the aperture section onto which the aperture cone fits. Thermocouple instrumentation, heater leads, and converter tower leads are then installed to the generator. These wires fasten directly to the feed-throughs at the base plate.

5.5.6 Edge effects of Stepped Foils

Manufacturing tolerances and flexibility of the generator sections caused rather large cracks at the generator corners. After vacuum firing these parts, most of the insulation foils tended to warp, which also contributed to the edge cracks. Small tantalum foil shims were added to the corners during generator buildup to reduce radiation losses.

5.5.7 Instrumentation Techniques

The instrumentation layouts for the entire CVG final system are shown in Figures 57 and 58. Six W/W26% Re thermocouples were used for measuring the various cavity temperatures. These are all read on G.E. two-channel, type HL, continuous recorders. The cathode temperature of each thermionic converter is monitored, and for one converter the shoe side and shoe rear also, to determine the cavity temperature distribution. One thermocouple has also been installed at the aperture cone-inside lip for purposes of measuring the heat loss from the cone and for warning of collector misorientation. All remaining thermocouples are chromel-alumel. Cesium reservoir temperatures for each converter were continuously monitored by GE recorders, since the generator power output is very sensitive to cesium bath temperatures. All remaining chromel-alumel thermocouples are displayed on a 24-channel Daystrom-Weston recorder. All converter power leads, voltage monitoring leads, heater wires, and thermocouples, are insulated by either alsimag fishspine beads or aluminum tubing, from the generator exterior to the vacuum base plate (Figure 59).

Instrumentation for the dummy generator testing is listed in Table 4. Here 4 W/W25% Re thermocouples continuously measured the inside section plate temperatures; the remaining T/C's, being chromel alumel, were wired to the Daystrom recorder.
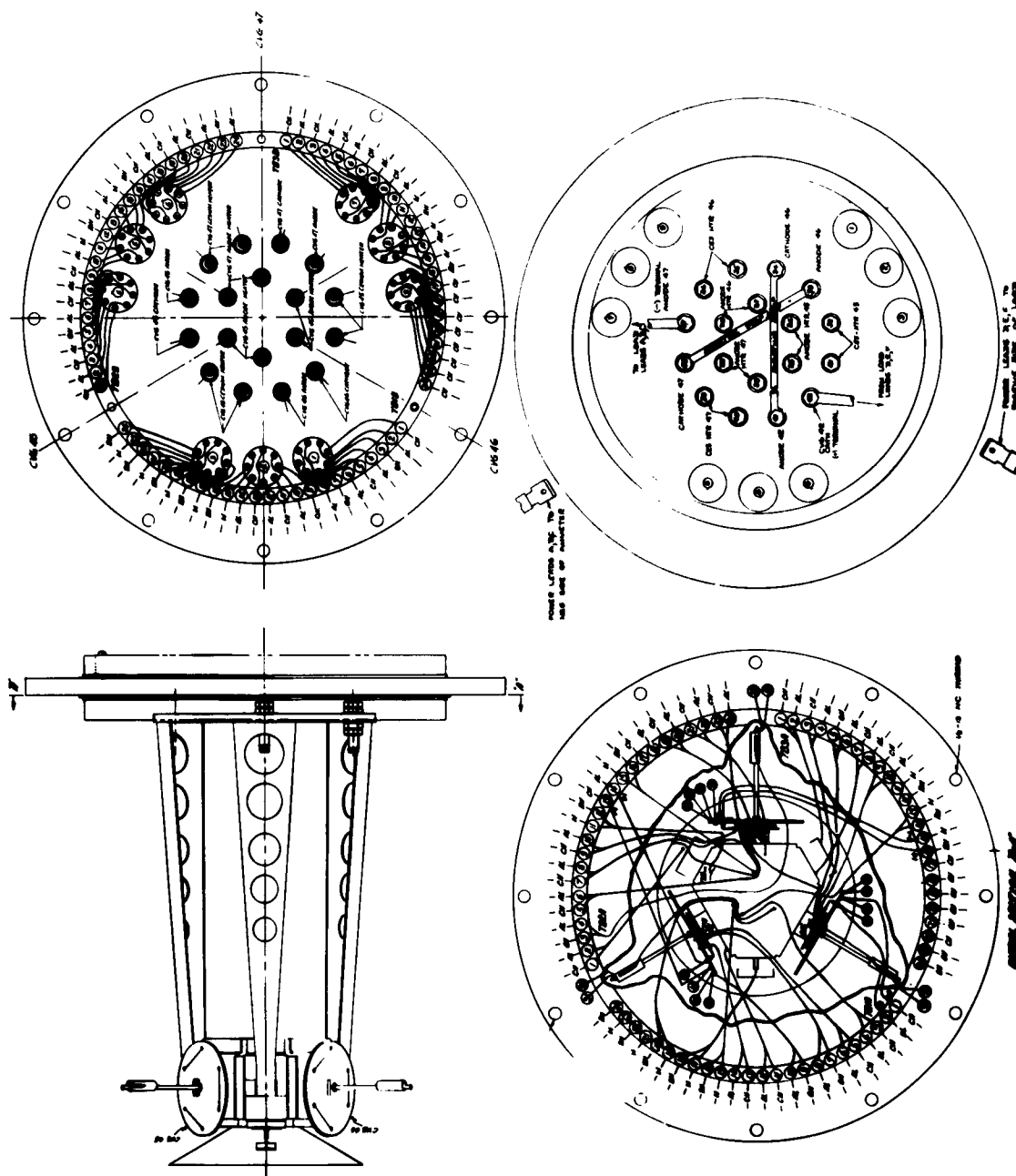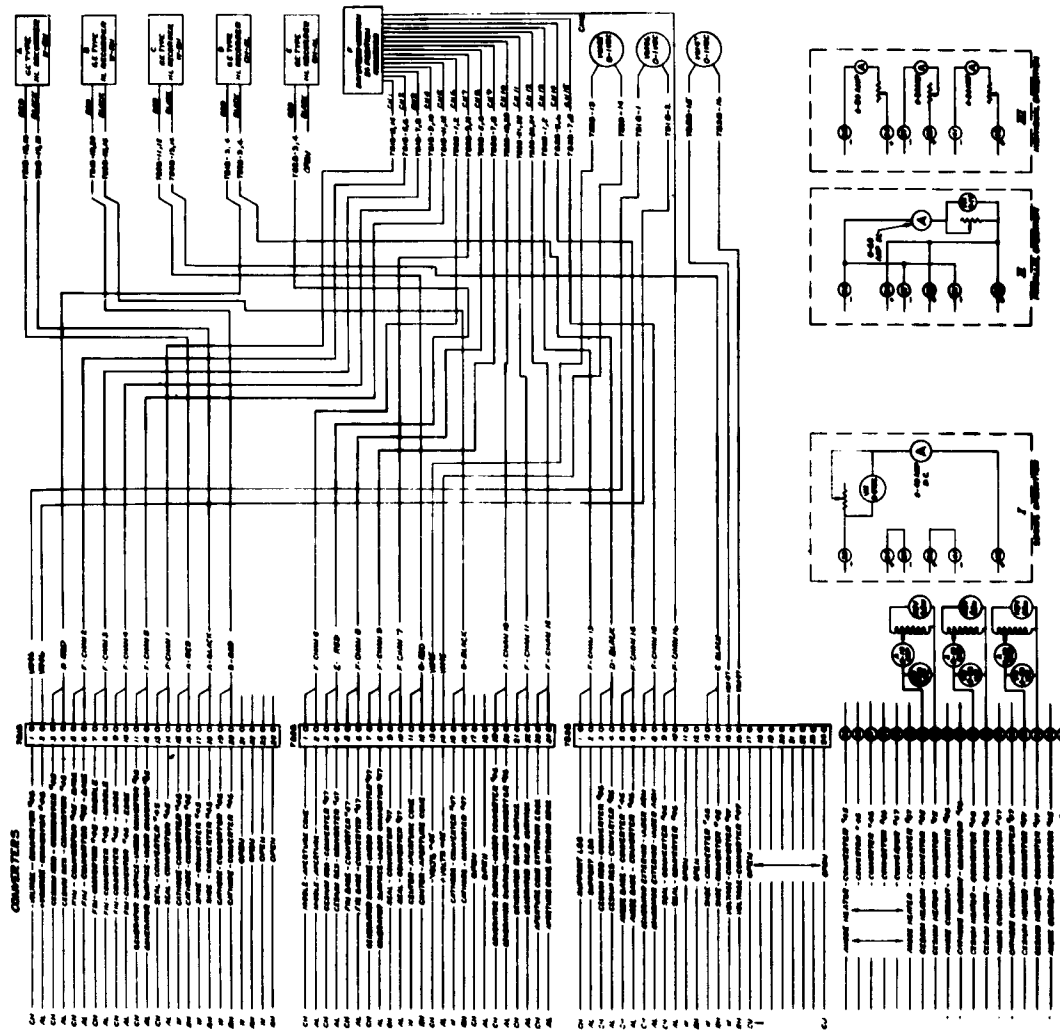
Figure 57. CVG Wiring Diagram
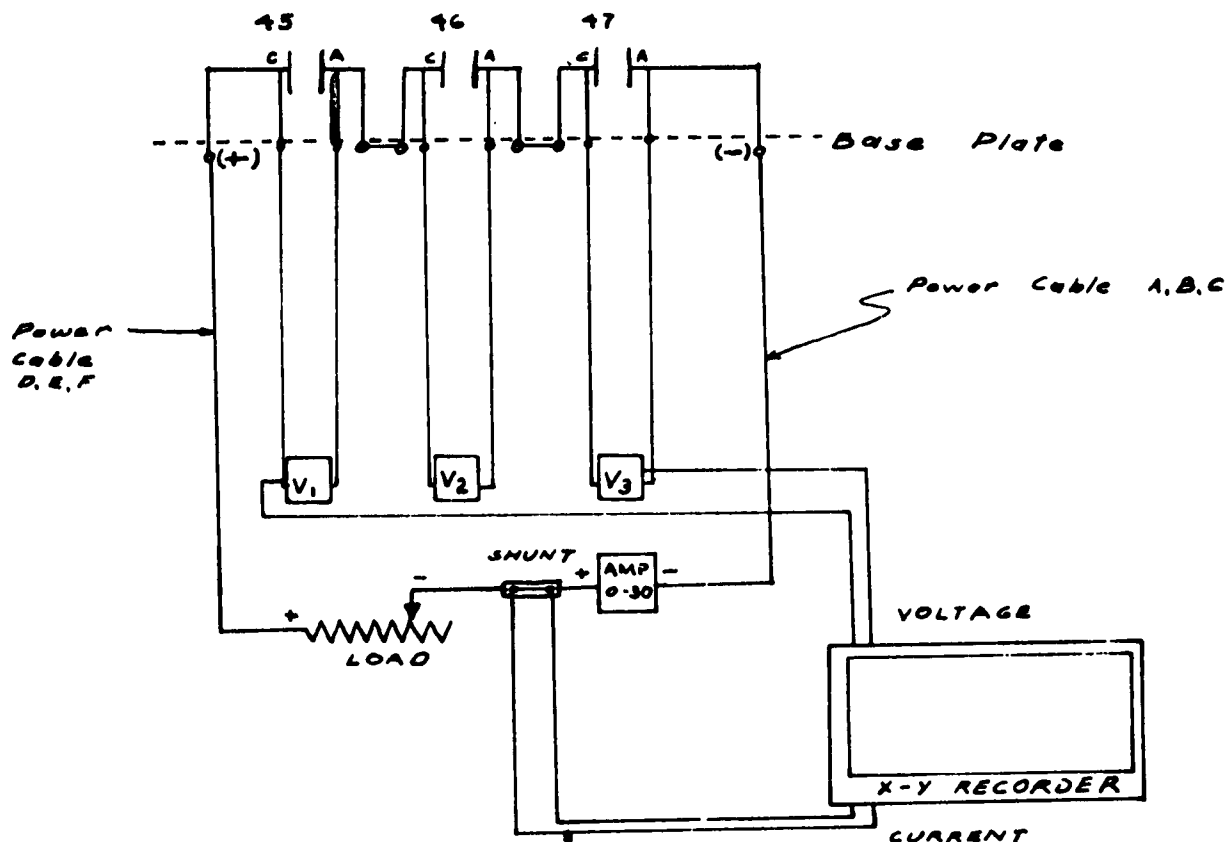
Figure 58. CVG System Schematic

Figure 59. CVG Performance Test Wiring Diagram

5.6 Heater Design

An electric heating unit may be used to pretest the CVG converters prior to their final system testing with the parabolic collector. The heater may be inserted into the cavity to permit the measurement of certain parameters that are incapable of being measured with the collector configuration. Since power input to the cavity is all electrical, it may be more readily measured than with the collector configuration. This allows for a good measurement of efficiency of the generator, converters, and insulation shields. In addition, the heater test will allso the uncovering of any malfunctions which may then be corrected prior to the final system test in Phoenix, Arizona.

Two types of heating units have been considered: an electron bombardment unit, and a resistance type heater. Each is designed to operate in a vacuum of at least 10^{-5} mm Hg, and supplies sufficient power to the converter cathodes to bring them to the three design points of $1450^\circ K$, $1650^\circ K$, and $1850^\circ K$. The units have been designed to produce the least lead loss possible, thereby giving a better measurement of generator efficiency. This requires the use of very small lead wires, which must still be capable of carrying considerable current without overheating. The maximum temperature attained must be well below the melting point of the wire as well as being low enough to avoid excessive vaporization of the ceramic insulation.

80

The heater analysis indicates temperatures of approximately 2500°K required to supply the necessary cathode power for the 1850°K design point (See section 5.4.5). This temperature area limits the materials available and the analysis has considered tantalum and tungsten as the electrical and thermal conductors with thoria as the electrical insulator.

Aside from power required by the cathodes, the heater must supply energy lost through the dummy aperture or heater section, the loss through the thoria lead insulators, and lead losses which are a function of wire size for the various heaters.

TABLE 4. DUMMY GENERATOR INSTRUMENTATION

TERMINAL BOARD NO.	RECORDER CHANNEL	PIN NO.	THERMOCOUPLE TYPE	THERMOCOUPLE LOCATION
1	DW#1	7	C	outside of Converter Sec.
1	DW#1	8	A	outside of Converter Sec.
1	DW#2	9	C	outside of Corner Sec.
1	DW#2	10	A	outside of Corner Sec.
1	DW#3	11	C	outside of Converter Sec.
1	DW#3	12	A	outside of Converter Sec.
1	GE #A-Black	21	W	Cavity Side - Tantalum Wire Method
1	GE #A-Black	22	Re	Cavity Side - Tantalum Wire Method
1	GE #B-Red	23	W	Cavity Side
1	GE #B-Red	24	Re	Cavity Side
2	DW#4	9	C	Aperture - outside tip
2	DW#4	10	A	Aperture - outside tip
2	DW#5	17	C	Aperture - Center of Cone
2	DW#5	18	A	Aperture - Center of Cone
2	DW#6	19	C	Aperture - inside tip
2	DW#6	20	A	Aperture - inside tip
2	DW#7	21	C	outside of Generator Back
2	DW#7	22	A	outside of Generator Back
2	DW#8	23	C	outside of Corner Sec.
2	DW#8	24	A	outside of Corner Sec.
2	DW#15	1	C	Base Plate
2	DW#15	2	A	Base Plate
3	DW#9	7	C	outside of Corner Sec.

TABLE 4. DUMMY GENERATOR INSTRUMENTATION (Cont'd)

TERMINAL BOARD NO.	RECORDER CHANNEL	PIN NO.	THERMOCOUPLE TYPE	THERMOCOUPLE LOCATION
3	DW#9	8	A	outside of Corner Sec.
3	DW#10	9	C	outside of Converter Sec.
3	DW#10	10	A	outside of Converter Sec.
3	GE #B-Black	11	W	Cavity Interior - Rear Section
3	GE #B-Black	12	Re	Cavity Interior - Rear Section
3	GE #B-Red	13	W	Cavity Interior - Rear Section
3	GE #B-Red	14	Re	Cavity Interior - Rear Section

Meter Nomenclature:

DW - Daystron Weston 24 Channel Recorder
GE - General Electric 2 Pen Recorder

Thermocouple Nomenclature:

C - Chromel
A - Alumel
W - Tungsten
Re - 75% Tungsten
     26% Rhenium

5.6.1 Resistive Heater

The resistive heater employs a tungsten filament wrapped in a helical fashion on a thoria core (see Figure 60). An attempt may be made to eliminate the thoria core with a cautious look at the filament maintaining its shape. The filament is 15 turns of 20 mil tungsten wire on a 0.65 inch diameter core 1.2 inches in length. The core size has oeen dictated by the cavity size and wire dimensions have been taken to give desired power while not having to exceed our 2600^0K thoria limitation. In this heater the tantalum can has been eliminated so that the cathode of the converters are directly heated by the filament. This, of course, means more power to the filament than with the bombardment heater and therefore, incorporates higher lead losses. The middle thermal resistance, however, the can, has been eliminated so that the heating is direct and Figure 61 shows the required filament temperature for desired power and cathode temperature. It is believed that not only will the filament radiate, but the thoria core as well. Therefore, Figure 10 considers partial radiation from the core and an average emissivity of tungsten and thoria has been used. Wire size and number of turns are a function of the power desired and the maximum number of turns, it is felt, could be put on a 1.2 inch length core.

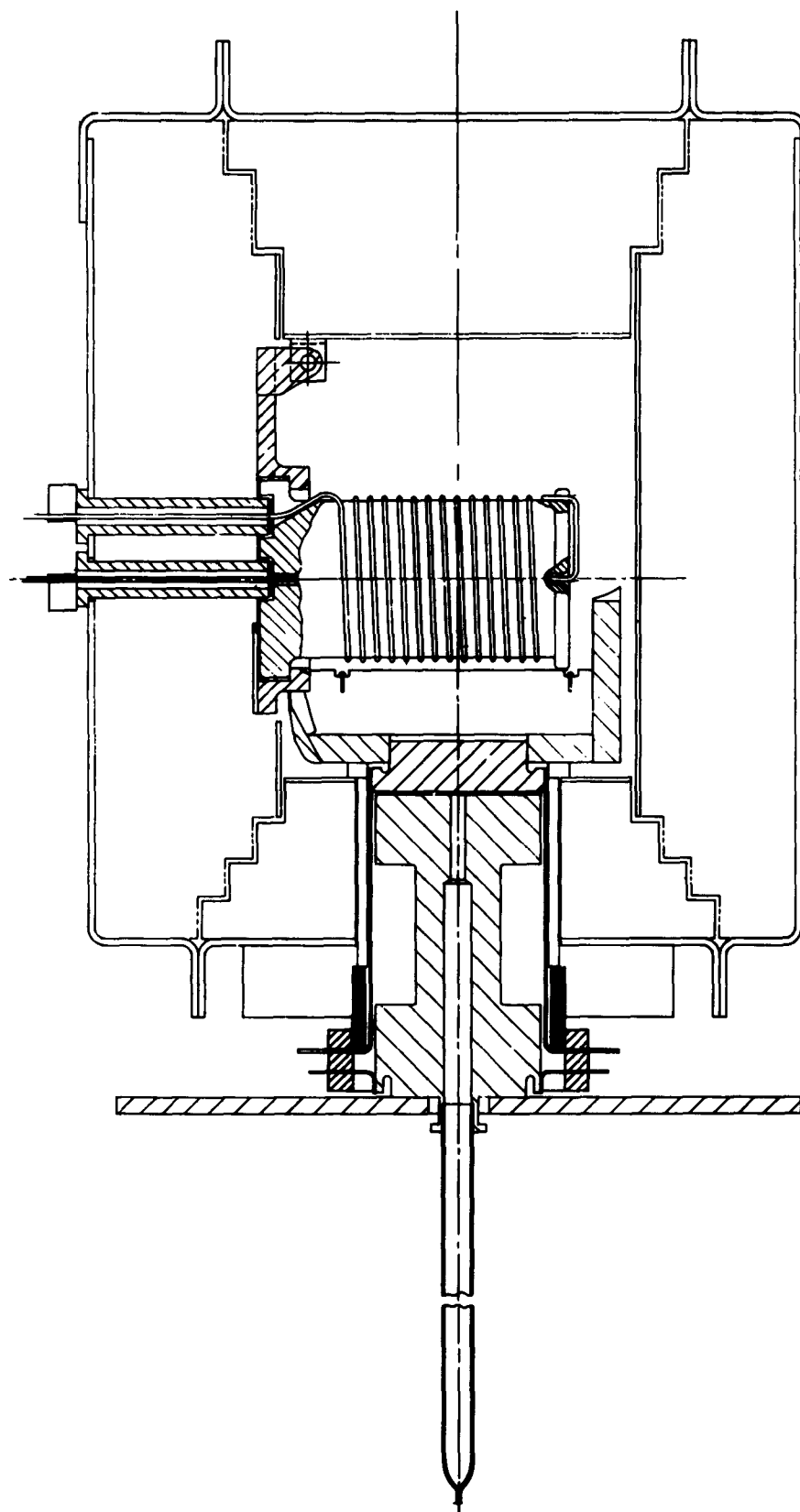The tungsten and tantalum filament bombardment units operate in both space charge and saturation regions.
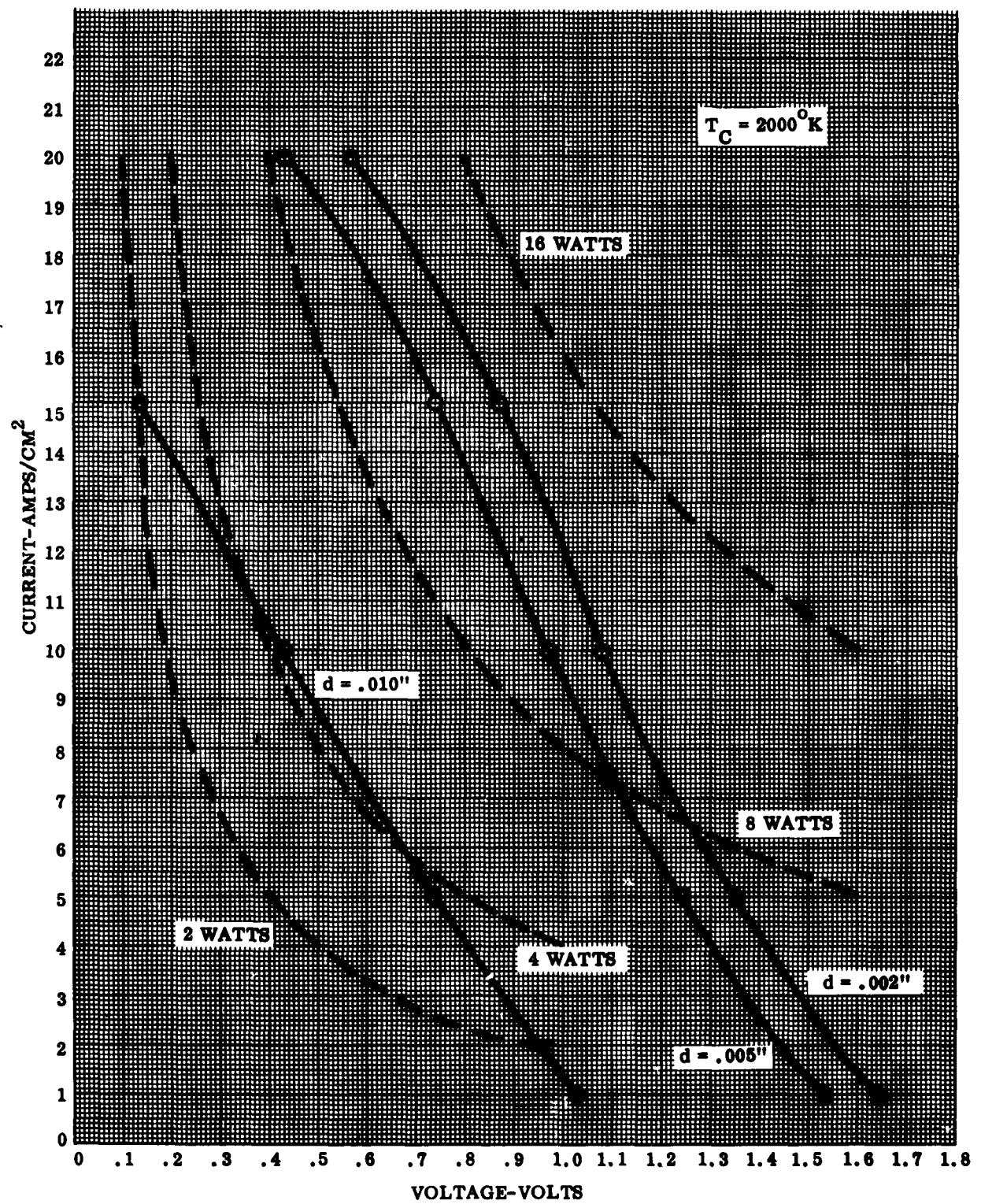
Figure 60. Resistive Heater

Figure 61. Calculated Current vs. Voltage

5.6.2 Electron Bombardment Heater

The electron bombardment heater employs a filament made of either tantalum or tungsten wrapped in a helical fashion on a thoria core and enclosed by a hollow tantalum can (see Figure 62). A low voltage high current supply is connected to the filament for heating purposes and a high voltage DC supply between the filament and tantalum can for acceleration of electrons emitted from the filament by thermionic emission.

The generator design limits the can OD to one inch. Using a 0.100 inch can thickness and a 0.150 inch gap between the filament and can, permits use of a 0.50 inch diameter core on which to wind the filament. In depth, again, generator design limits the cavity depth and allows a core length of 0.85 inches. The tantalum can is threaded, thereby increasing its emissivity as shown in Figure 63.

The electron bombardment unit, operating on the thermionic emission principle, has a power output which is a function of the high DC potential, the emitting surface area, the Richardson-Dushman equation, and the Langmuir-Child space charge law. The surface area is a function of the number of turns of wire, the core diameter which has been set at 0.5 inches, and the wire diameter. The useful surface area for thermionic emission has been considered as 0.5 of the total wire surface area, since approximately one-half of the wire surface faces the tantalum can and is in the path of the accelerating potential while the remainder of the wire surface area is against the thoria core.

It has been found from the numerous analyses performed that the most desirable performance will be obtained by use of four turns of 10 mil tantalum wire wrapped in a helical fashion on the 0.5 inch thoria core, 5 turns of 20 mil tungsten wire wrapped in a helical manner around the thoria core, or 4 turns of 10 mil 1% thoriated tungsten.

6.0 CONVERTER LABORATORY TESTING

6.1 Converter 29 Life Test

6.1.1 Objective

The fundamental purpose of this test was to obtain maximum operating time with a predetermined power output level. This was to have continued until tube failure occurred or the power output had degraded sufficiently to show the end of tube usefulness. At the time of this test, 28 June to 20 July, many other important facts were needed to complete the design of the converter. These items were, therefore, included in the life test program.

A more complete thermal picture was necessary to correctly size the tube parameters. For instance, after completion of the test it was found that the 3.2 inch anode fin was running much too hot and that it had to be made larger.

To facilitate laboratory testing of the thermionic converter, the converter was placed into the generator body. The second and third converters were replaced by insulation sections. These sections were made up solely of tantalum radiation shields. Sufficient thermal data on these radiation shields had not been recorded up until this time; therefore, this test proved to be a good opportunity to obtain this data. The overall test setup is shown in Figure 64. The heater, cavity and radiation shields are shown in Figure 65.
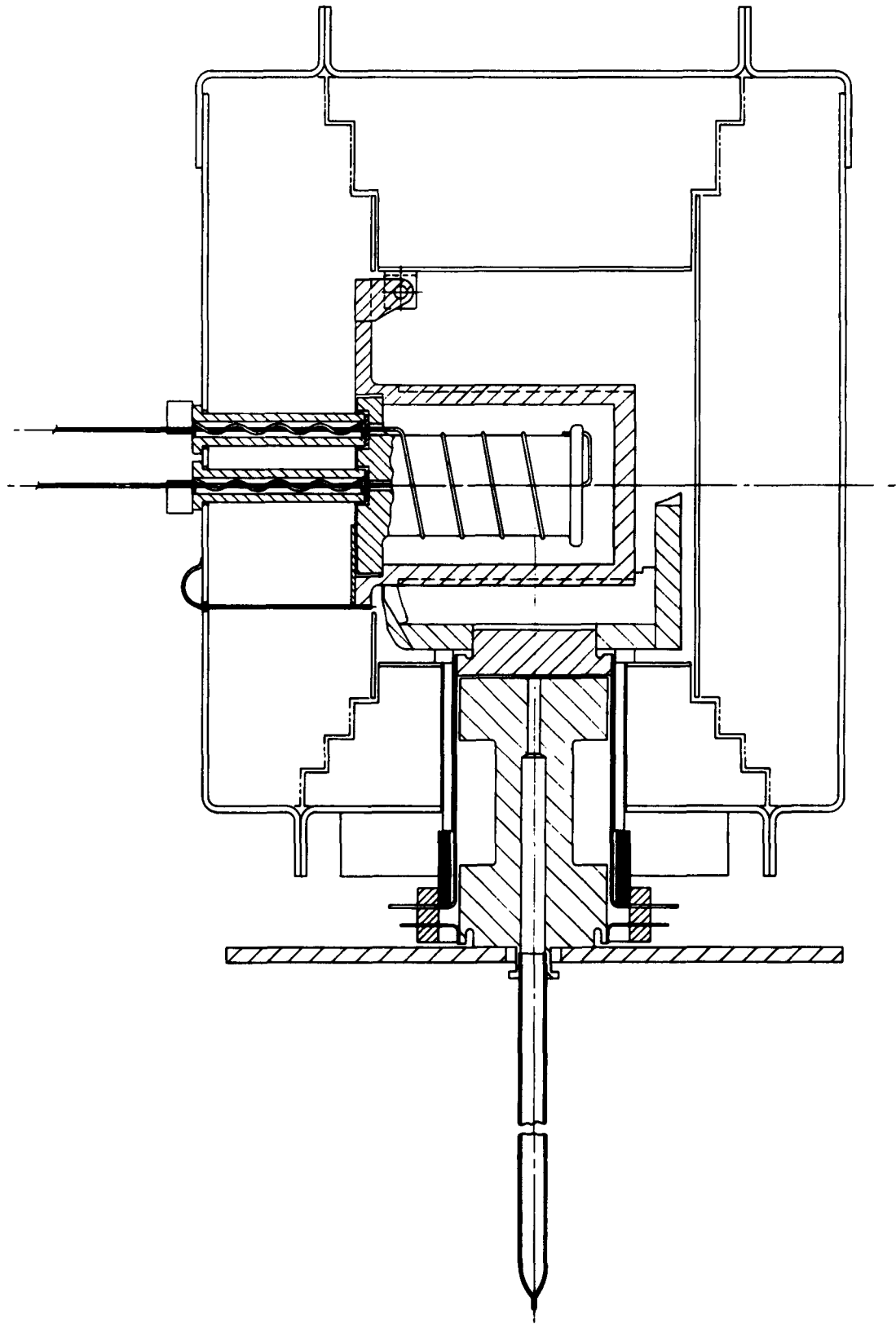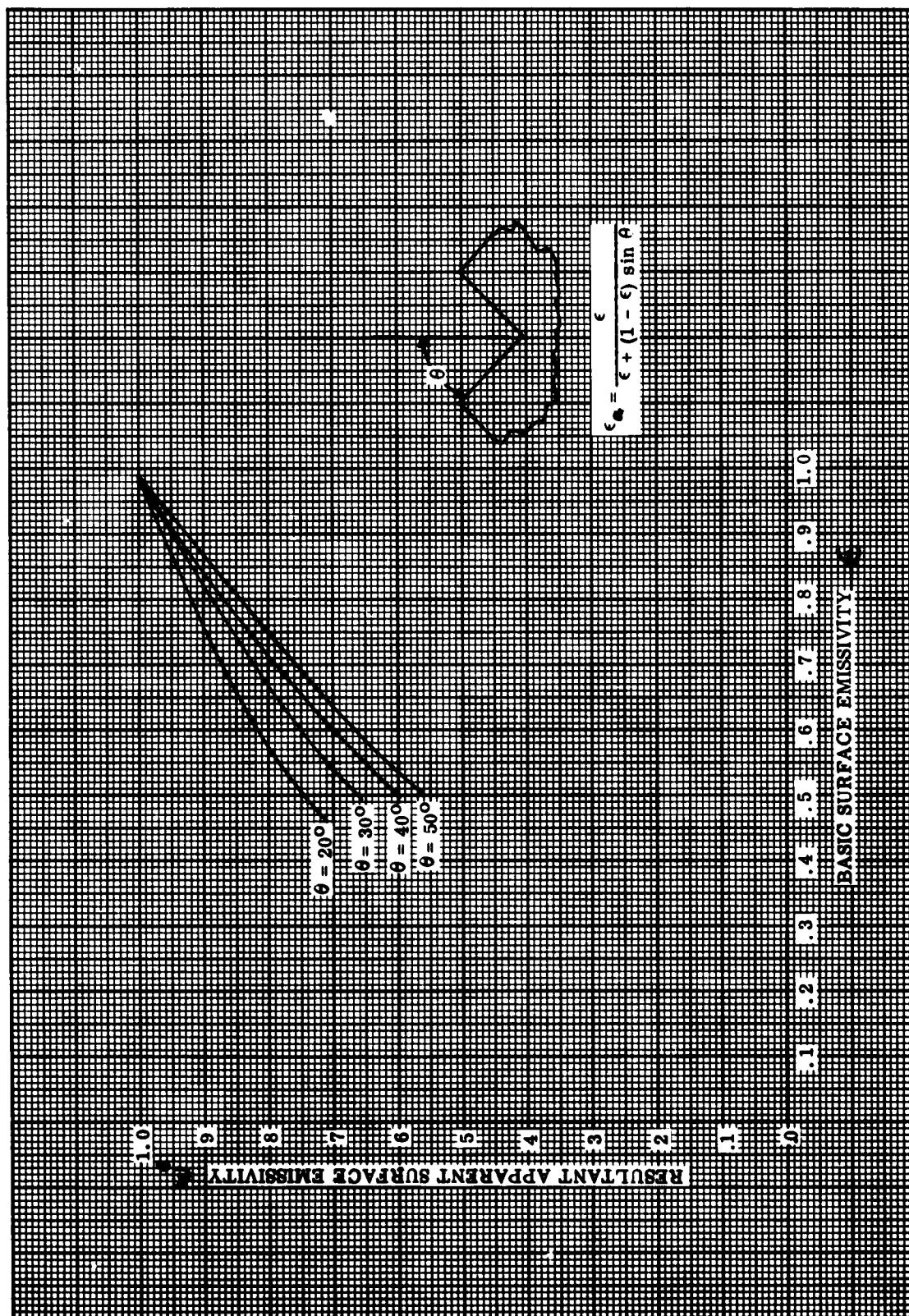
Figure 62.   Electron Bombardment Heater

Figure 63. Emissivity Increase from Grooving
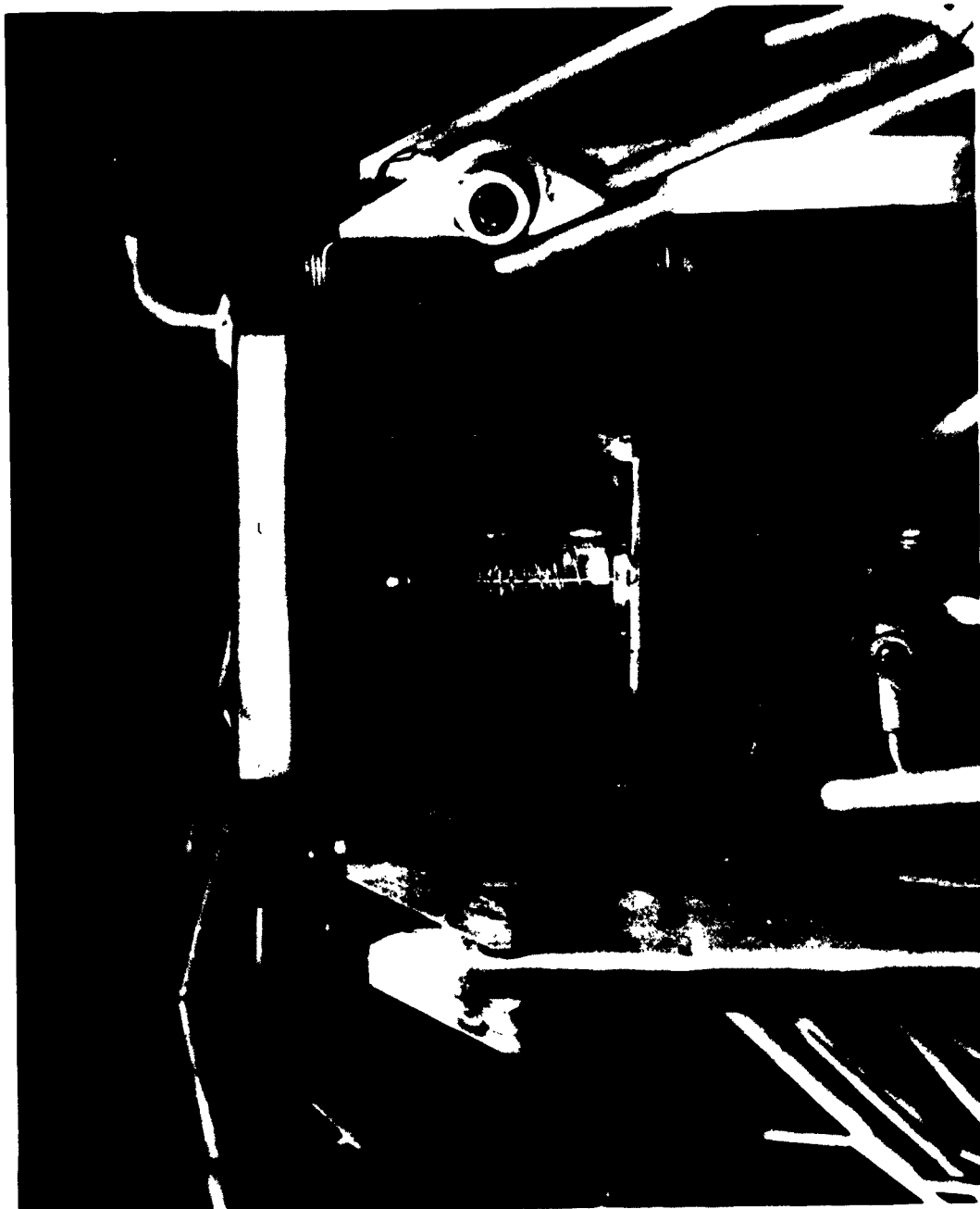
87

Figure 64. Converter 29 Life Test Setup

Figure 65. Cavity Showing Heater, Cathode Shoe, and Radiation Shields

6.1.2 Conclusions

A pressing schedule and a need to run several other important tests, caused us to cut short the life test of Converter 29. The major limiting item that caused the halting of this test turned out to be completely independent of tube or generator performance. Therefore, since there was no converter failure, or for that matter no real drop in performance of converter or insulation, no conclusions can be drawn on these points. After 153 hours of vigorous testing, including thermal cycling, the converter power output was on a par with that of its initial testing. Even though the life test was not completed, much of the re-design data was obtained.

One of the chief areas of concern was the thermal impedance of the screw on junction of the cathode shoe to the cathode. These suspicions were later confirmed by the data and from Figures 66 and 67. A clear picture of the Δ T developed across this junction can be seen. Ultimately this Δ T was greatly decreased by electron beam welding of the joint.

These same two figures show how well the seal and anode temperatures followed each other. There had been some concern over the method of attaching the fin to the anode. Brazing of the fin to the anode proved to be superior to the previous method of tapping the anode and bolting the fin on.

6.1.3 Test Procedure

The principal method used was to allow the system to a thermal steady state while maintaining a constant load. Then from this point, we varied the cesium reservoir temperature and recorded the changes in power output. Also by using this same procedure, we varied the anode temperature and recorded the power output changes. This was done at various levels of electron cooling and at various cathode temperatures.

The effects of cesium reservoir temperature changes on the power output is illustrated in Figure 68. Anode temperature effects are more difficult to show because of the many variables involved. However, a plot of the power output vs. anode temperature at a constant cathode temperature of 1380°C and an optimum cesium temperature of 320°C. (Figure 69)

6.1.4 Insulation Data

Since this was a life test of the insulation itself, as well as of the converter, we obtained a good feel for some of its characteristics. For example, we could see that after 153 hours the insulation was holding up very well. The power output of the converter and the energy into the cavity are plotted against time in Figure 70. This readily shows that the energy losses through the converter and through the generator insulation had remained constant throughout the test.

6.2 Test Data, Converter Performance, and Final Engineering Model Design

In the initial testing period at the Power Tube Department, several EI curves were plotted, each at the same cathode temperature but each with a different cesium reservoir temperature. This was to enable them to optimize the cesium reservoir temperature at a cathode temperature of 1380°C or 1650°K. These curves along with a comparable curve obtained from testing at MSD are shown in Figure 71.
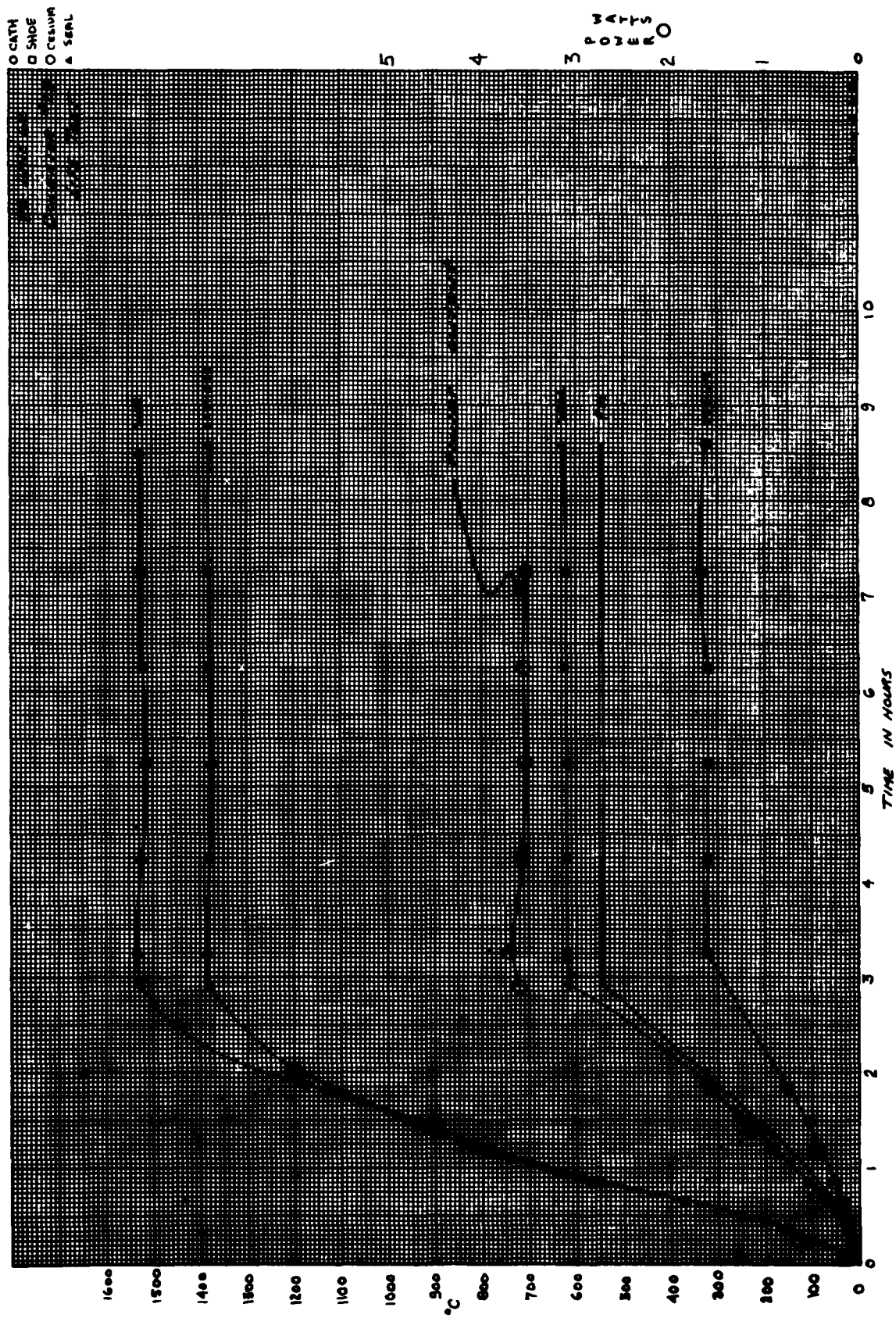
90

Figure 66. Converter 29 Temperature and Output vs. Time
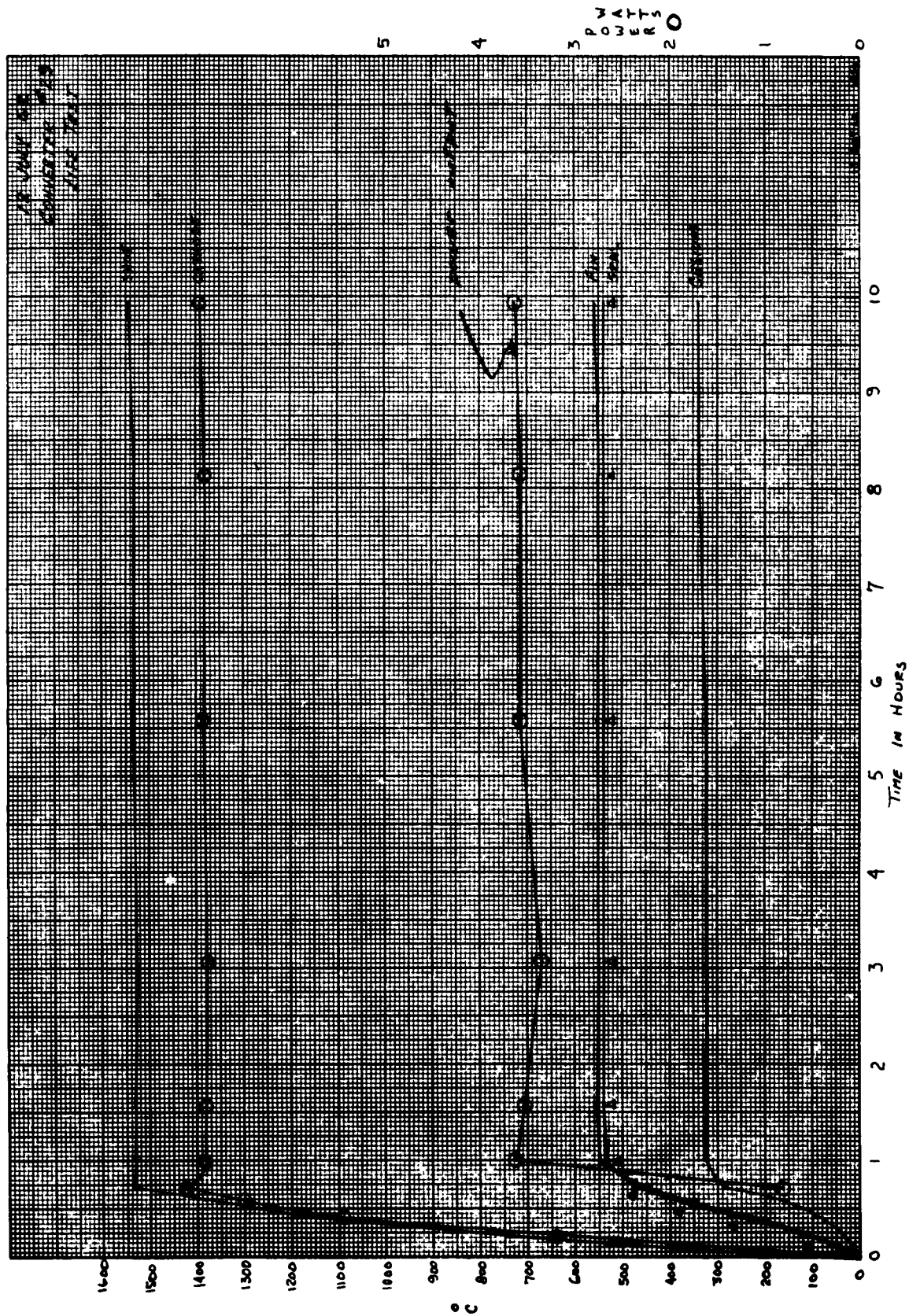
Figure 67. Converter 29 Temperature and Output vs. Time
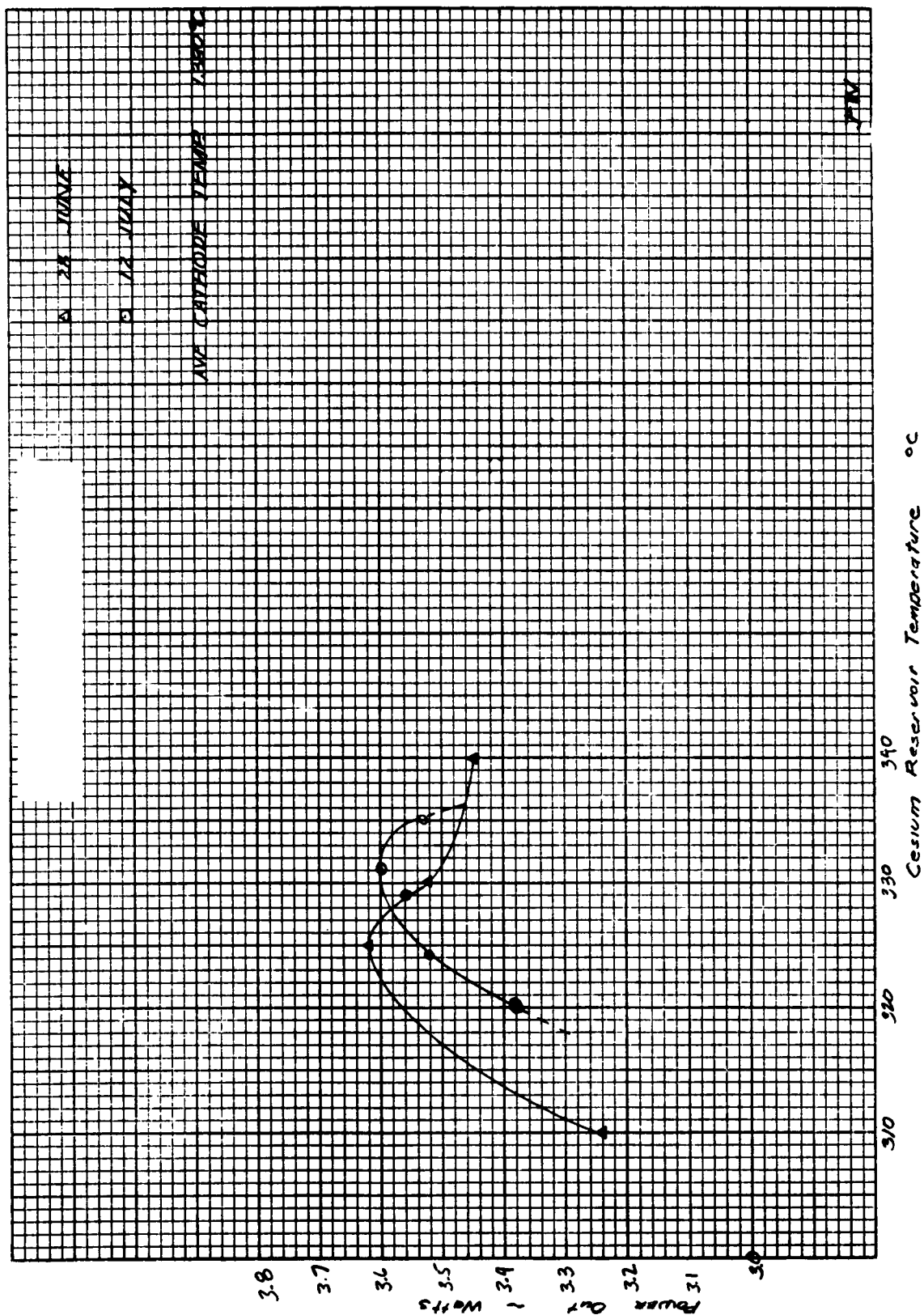
92

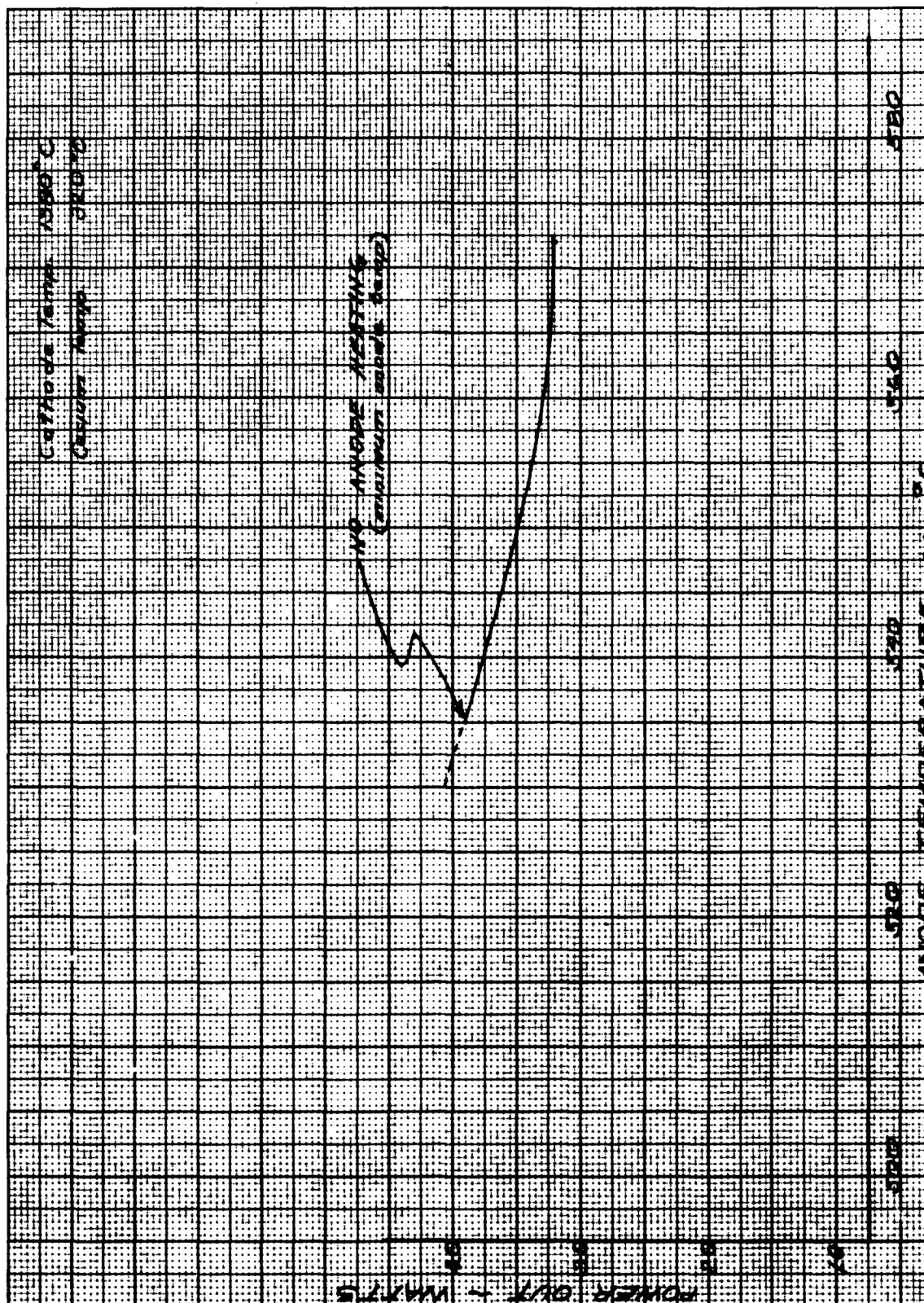Figure 68. Converter 29 Power Output vs. Cesium Temperature

93

Figure 69. Converter 29 Power Output vs. Anode Temperature

94

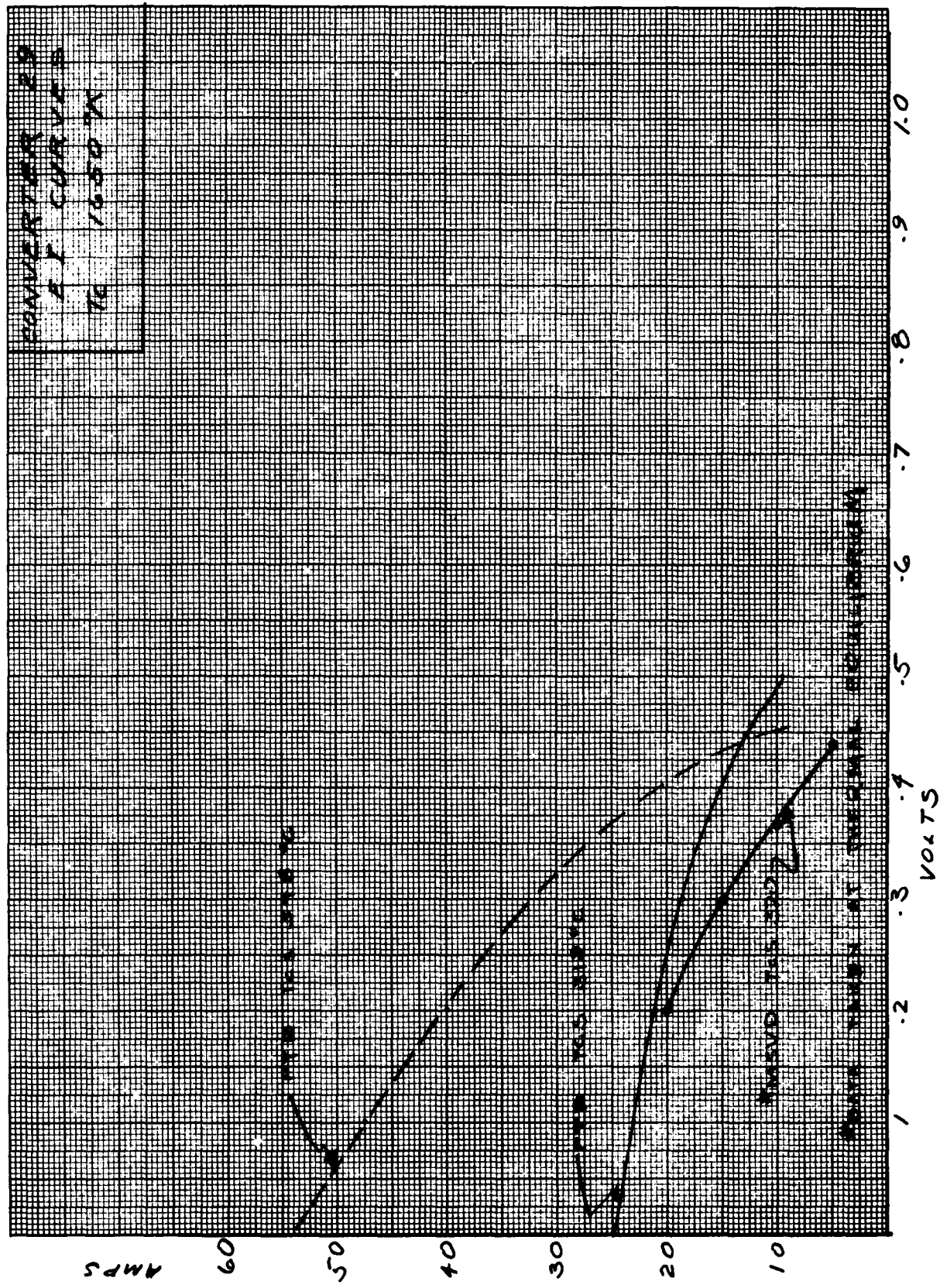Figure 70. Converter 29 Output and Heater Power vs. Time

Figure 71. Converter 29 E-I Characteristics

Upon arrival in Philadelphia Tube No. 29 went through a complete testing program. This included a life test, complete power runs at 1650°K, 1750°K, 1850°K, and finally 1950°K. The curves derived from this testing may be seen in Figure 72.

The discrepancies in the power data obtained at Power Tube Department and MSD may be due to shelf life or to impurities in the materials used in the cathode and anode. These impurities may after a short testing period contaminate the cathode affecting the power output of the tube. This would explain the variances in the power obtained from the Power Tube Department and MSD.

During the life test of converter 29, special emphasis was placed on instrumentation of the cathode and cathode shoe area. The reason for this was the concern over the thermal impedance of the screw-on junction of the cathode shoe to the cathode. These suspicions were later confirmed by the data obtained. In the engineering model converter this ΔT was greatly decreased by electron beam welding of the joint. Subsequently all converters have had this welded joint, greatly decreasing the energy required to obtain a cathode temperature of 1650°K. The ΔT developed across the screw-on joint can be seen in Figure 73, along with the much reduced ΔT after welding of a similar joint.

The effect of anode temperature on power output of the tube has been thoroughly calculated and presented several times before. However, actual performance data thus far is not available, because the anode fin has been incapable of reducing anode temperature below that of the optimum point. Figure 69 shows a curve of power output vs. the anode temperature at a cathode temperature of 1380°C and a cesium reservoir temperature of 320°C. The peak power point is at the lowest anode temperature obtainable; however, it is clear that this peak is at a low point of the curve and would increase with a decrease in anode temperature. This indicates that the 3.2 inch diameter fin was not adequate to sufficiently reduce the anode temperature. During the design of the final engineering model converter a 3.6 inch diameter fin was recommended to help overcome this problem.

6.3   Test Data on Engineering Model Converters

After the re-design period, the Power Tube Department manufactured several engineering model converters. These converters had the radiation shields in place and the cathode shoe welded to the cathode and the 3.6 inch diameter fin brazed to the anode. A typical example of the engineering model was converter No. 45. This converter received a thorough testing at the Power Tube Department and MSD in Philadelphia. The following is a comparison obtained from these two tests. Since the Power Tube Department has been taking data points in both the static and dynamic states care must be exercised to differentiate between the two on comparing with MSD data, which was taken only statically at thermal equilibrium. Dynamic testing results in a much steeper load line due to the fact that the anode temperature operates at an average temperature which is lower than would be experienced in a static test at high values of electron cooling (high currents). Power Tube Department tested CVG No. 45 without the shoe and received a peak power of 8.2 watts. The cathode temperature at this point was 1433°C, anode temperature 455°C, and cesium reservoir temperature 350°C. The current at this point was 30.5 amps, and a voltage .27. After welding of the cathode shoe, they again ran the tube and obtained 8.3 watts at 33 amps and .25 volts. This was at a cathode temperature of 1468°C, anode temperature 540°C, and cesium reservoir temperature 350°C. Both of these points, however, were taken dynamically. Since both of these points are above the design point cathode temperature of 1380°C, they cannot be readily compared with the data obtained at MSD. The maximum power obtained at the design cathode temperatures at the Power Tube Department, was 6.2 watts, at 27 amps and .23 volts. This compares more favorably with the 5.27 watts obtained at MSD at the same design point. Figure 74 is a comparison of PTD EI curve of converter No. 45 with EI curve at MSD.
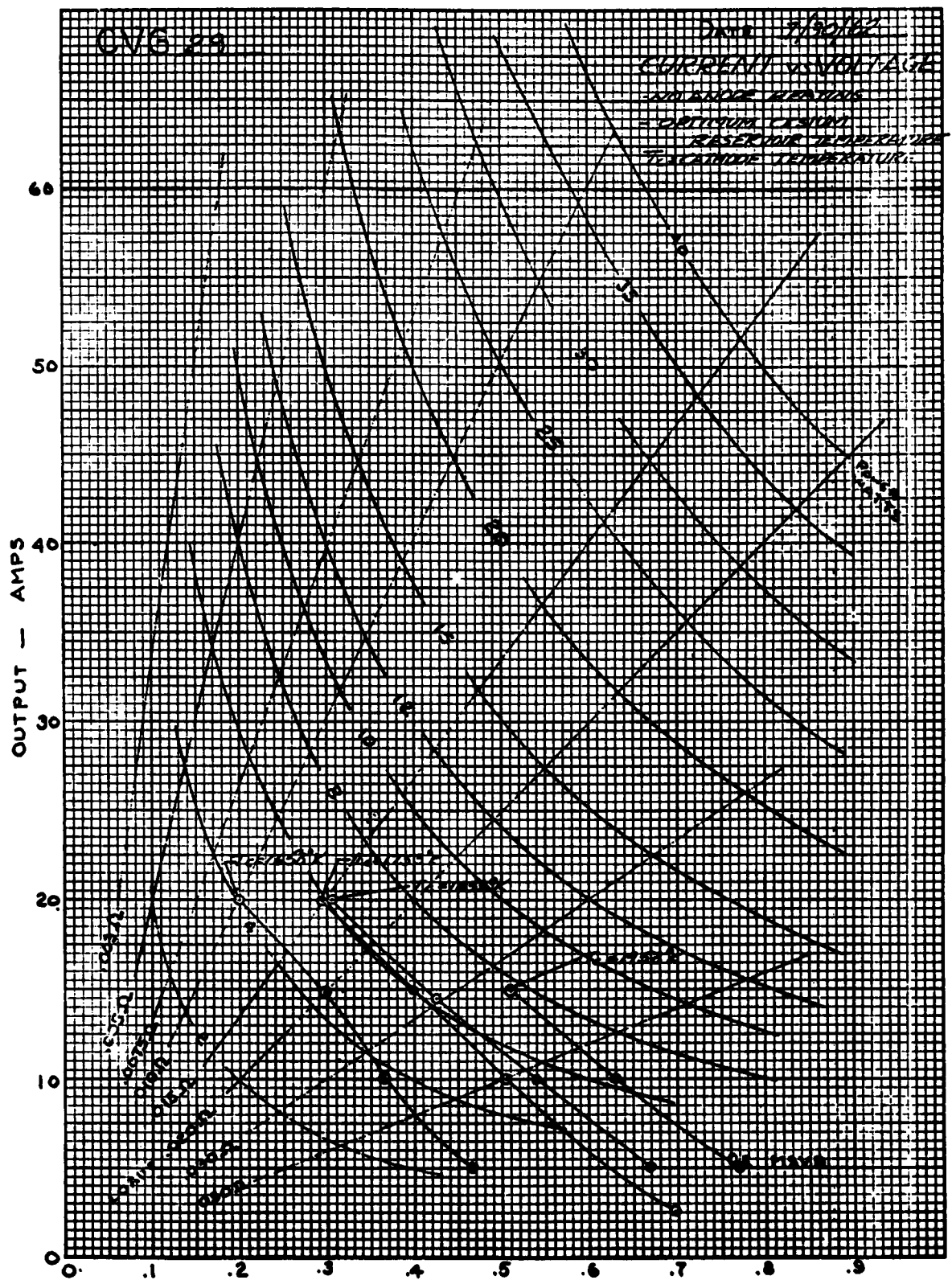
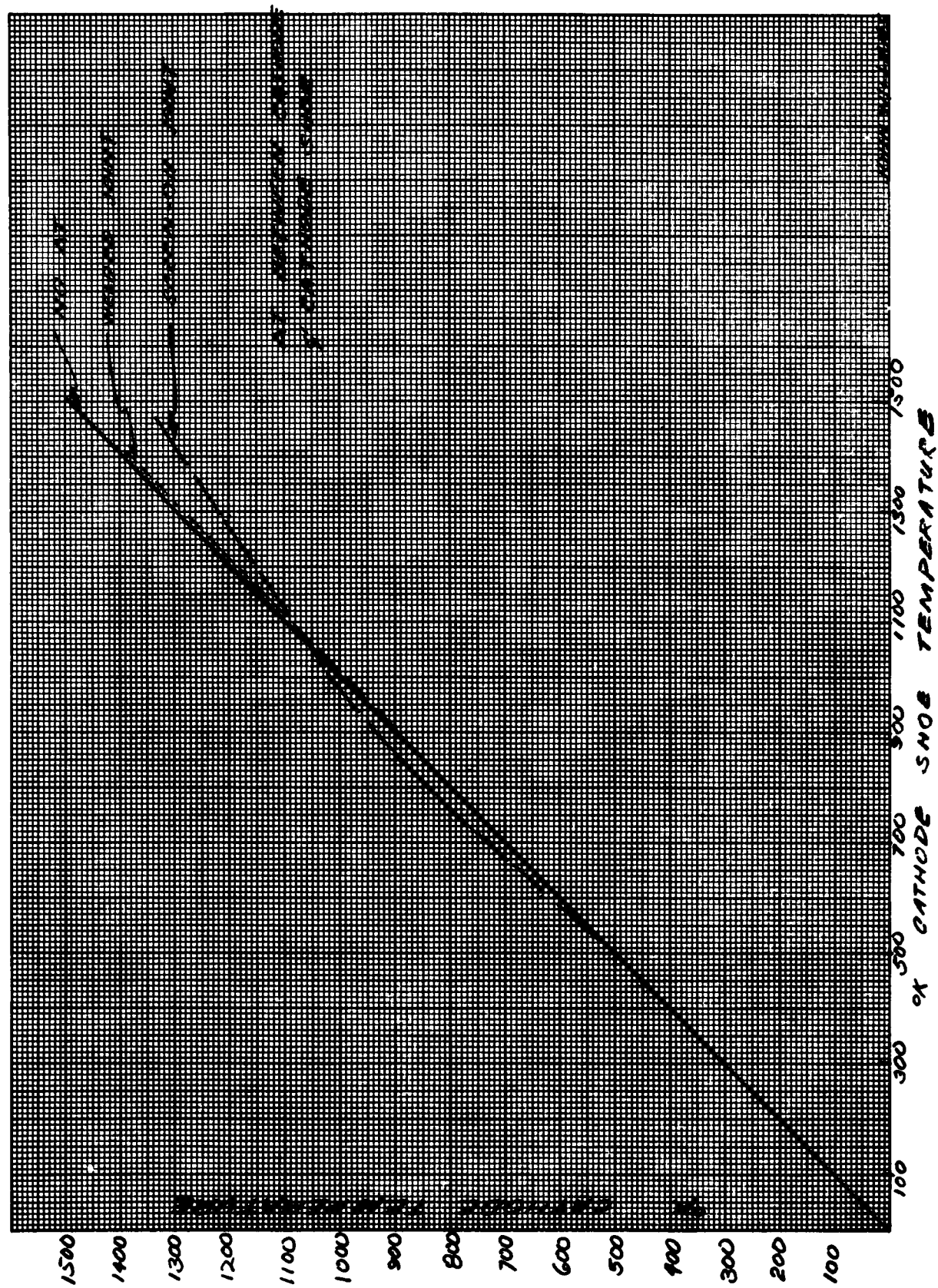Figure 72. Converter 29 E-I Characteristics
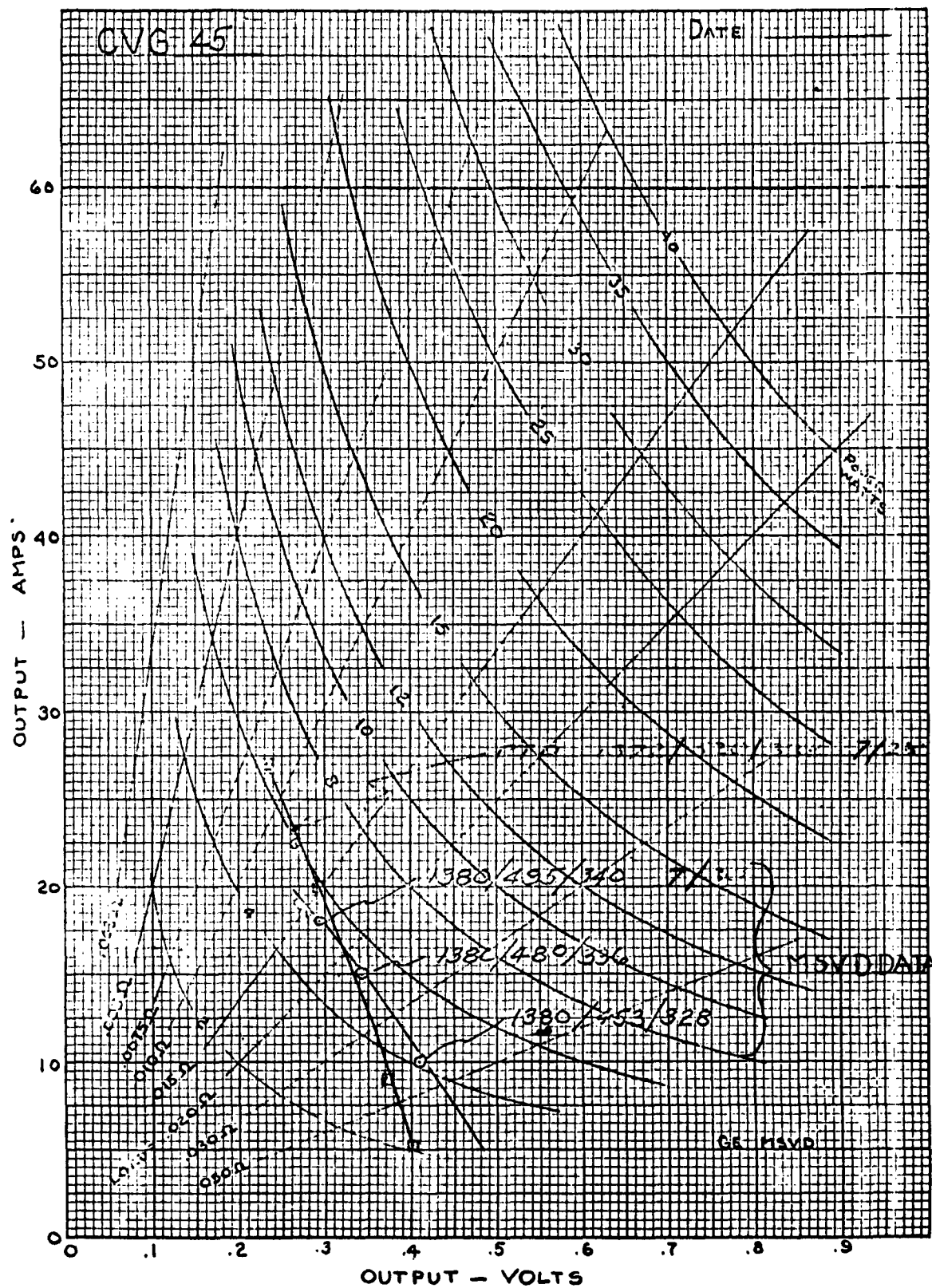
Figure 73. ΔT Between Cathode and Cathode Shoe

Figure 74. Converter 45 E-I Characteristics

7.0 EXPECTED PERFORMANCE

In order to obtain a measure of the insulation effectiveness, the generator was assembled with dummy or blank insulation sections in place of the three converters. The aperture section was replaced by a resistance heater section in which the heater lead material and diameter was optimized to minimize the thermal loss and to prevent overtemperature on the heater leads. The tests resulted in the following plots:

Figure 75: Heater power versus interior temperature (Ti)
Figure 76: Heater power versus exterior temperature (T*)
Figure 77: Exterior temperature (T*) versus interior temperature (Ti)

The exterior temperature is defined as:

$$T^* = \sqrt[4]{\frac{\sum_o^n A_n T_n^4}{\sum_o^n A_n}}$$

This exterior temperature, or mean effective outside temperature, is not considered as an adequate measure of the insulation heat loss for the final generation system because of the interaction of the converter anode radiating fins, temperature variations in each section and the complex exterior geometry, particularly at the aperture cone section.

Subsequent Tests 4 and 5 are also shown in Figures 75 & 76, and illustrate the effects of thermal degradation with time. Test 4 was performed after approximately 150 hours, many of which were spent at temperatures well above the design point temperature of $1650^\circ K$. Test 4 was run with the radiation shims removed and Test 5 with the shims in place and a definite improvement in insulation capability can be noted. The theoretical heat loss through the generator is shown in Figure 75. It is evident that the actual losses are greater than computed by a factor of 2. Losses through alumina insulators and insulation cracks contribute to this higher value. In addition, vacuum fusing of the tantalum heat shields was quite severe and certainly contributed to a large conductive heat loss through the insulation. The insulation loss of 106 watts at $1650^\circ K$ is obtained from Figure 75. This value is used in predicting final generator losses and here it is assumed that the inside of the insulation is at the same temperature as the converter cathodes.

To measure the converter thermal requirements, the interior temperatures of the generator were measured and the losses, as measured without the converter, were then subtracted from the generator losses. The insulation losses are actually greater through the insulation with a converter installed, since the heater must go to a higher temperature resulting in greater losses through the insulation as well as through the heater section. As examples of these measurements, current versus voltage data and thermal data were taken on Converters No. 45, 42, 46, 43, and 47 during laboratory testing. (Figures 78 through 84) The data given for Converters 43, 46, and 47 has been used to predict the final system performance with these converters in series and in parallel. When all three converters are installed, the converter shoes form a cavity which will tend to give an additional shielding effect to the generator insulation, thereby reducing the insulation loss.
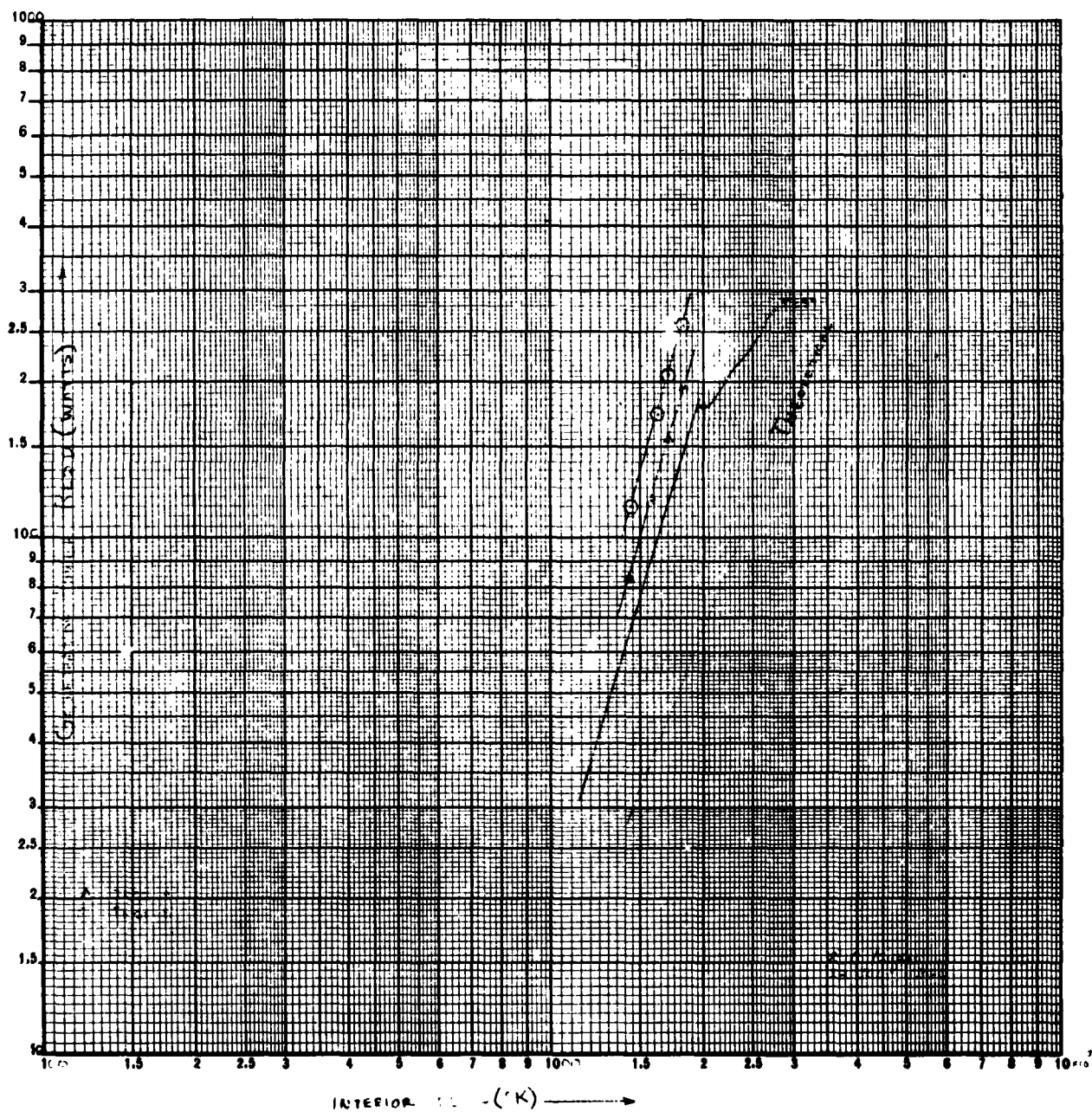
101

Figure 75. Heater Power vs. Interior Temperature (Ti)
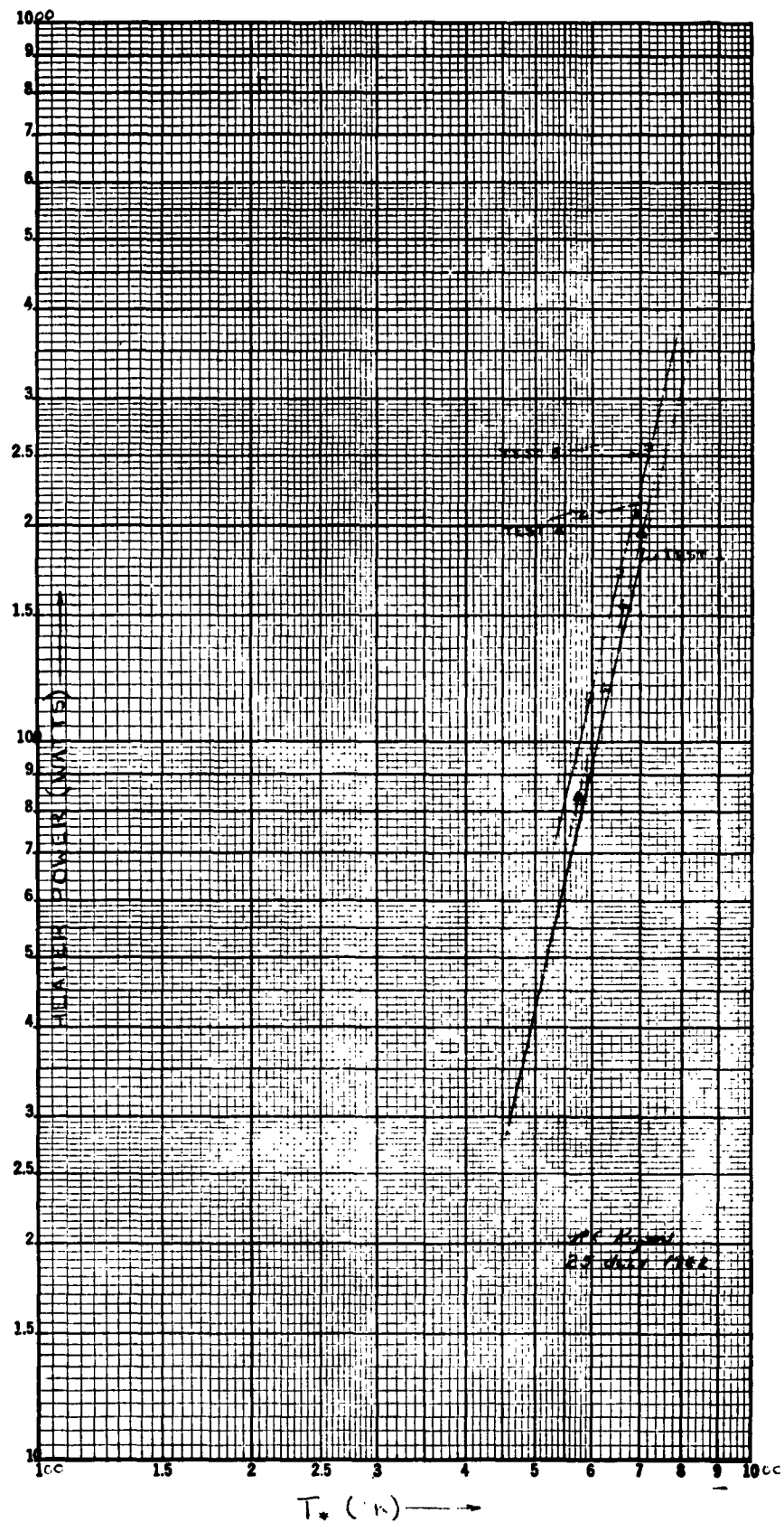
102

Figure 76. Heater Power vs. Exterior Temperature (T*)
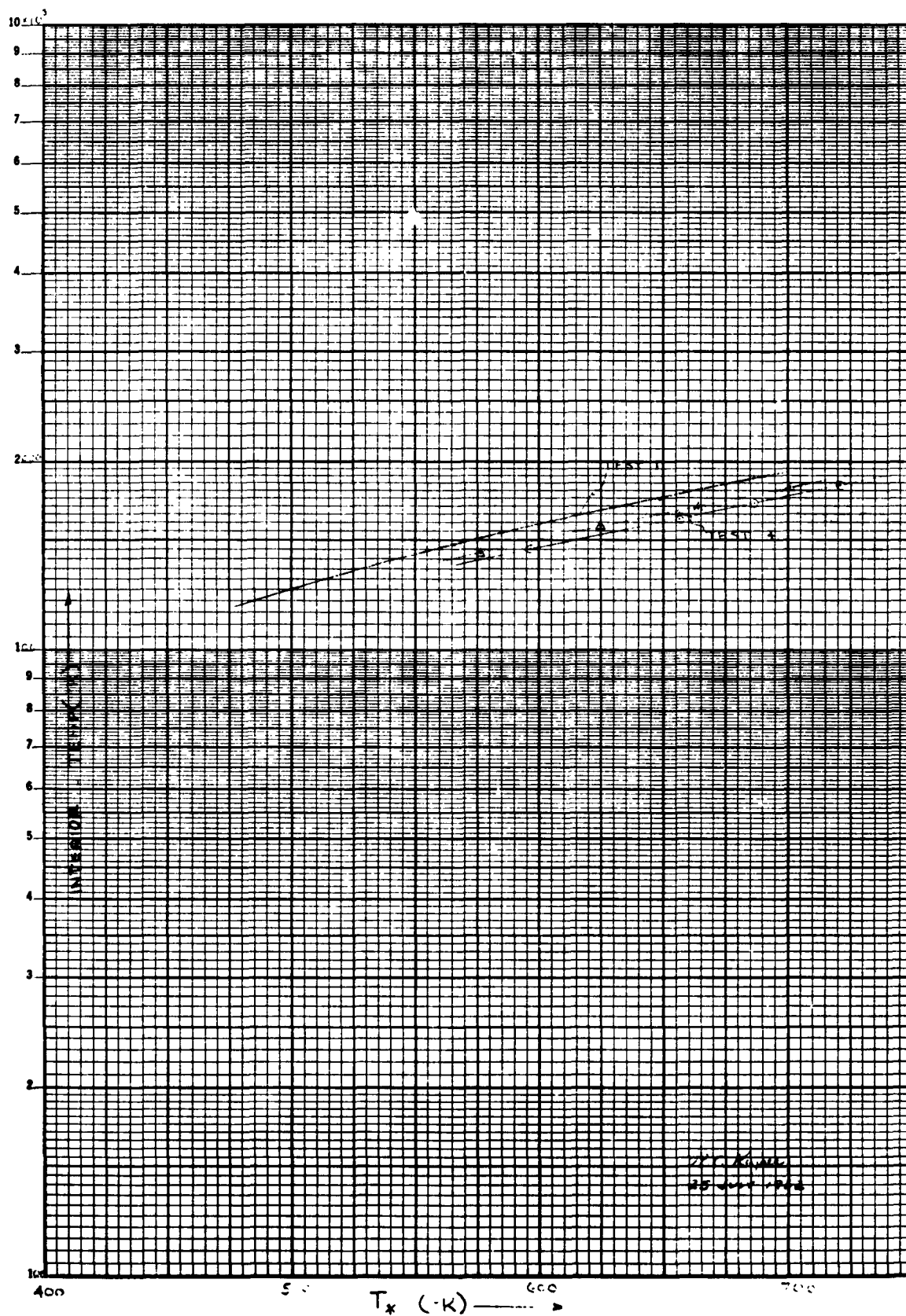
Figure 77. Exterior Temperature vs. Interior Temperature

104
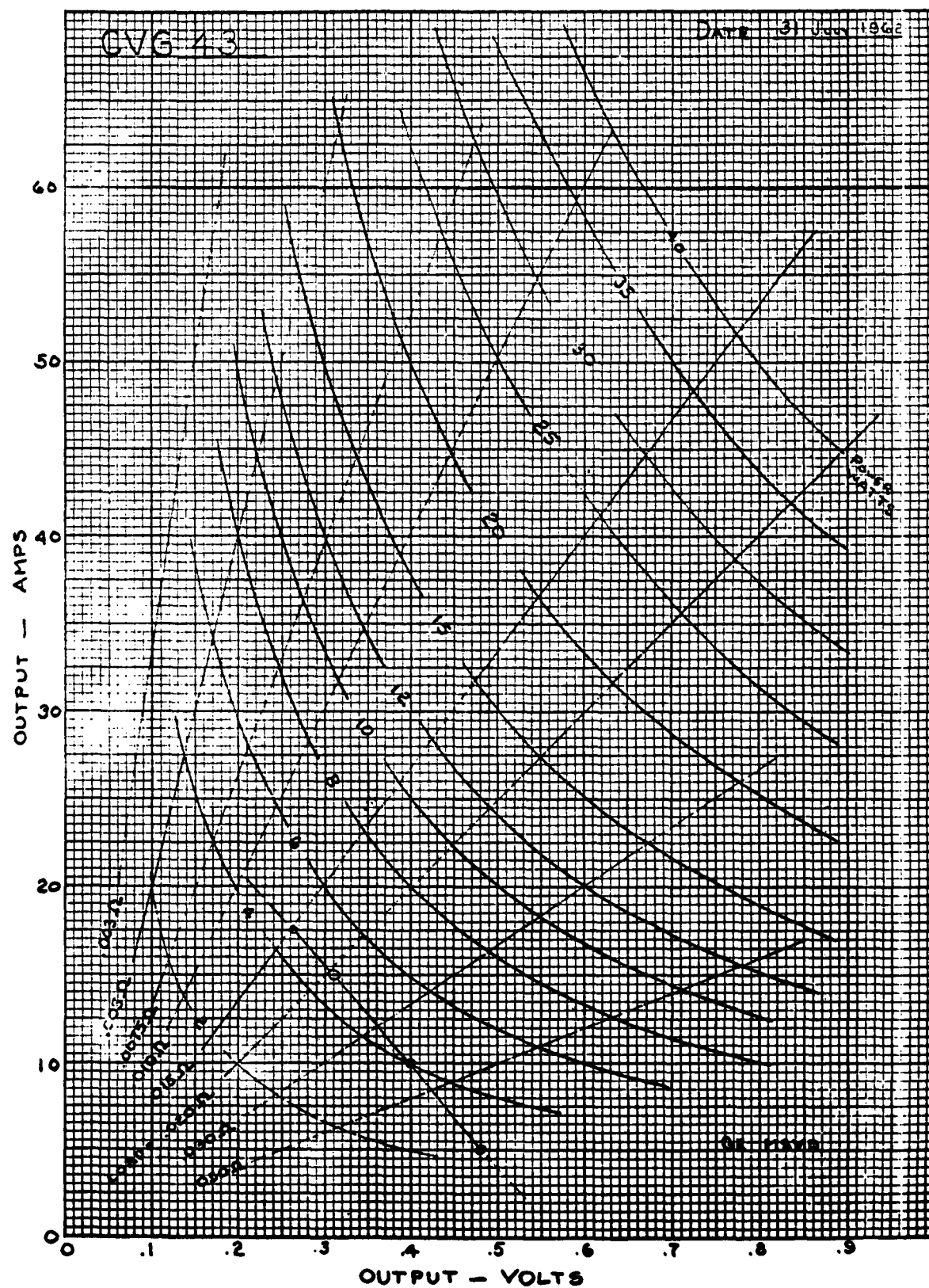
Figure 78. Converter 43 E-I Characteristics

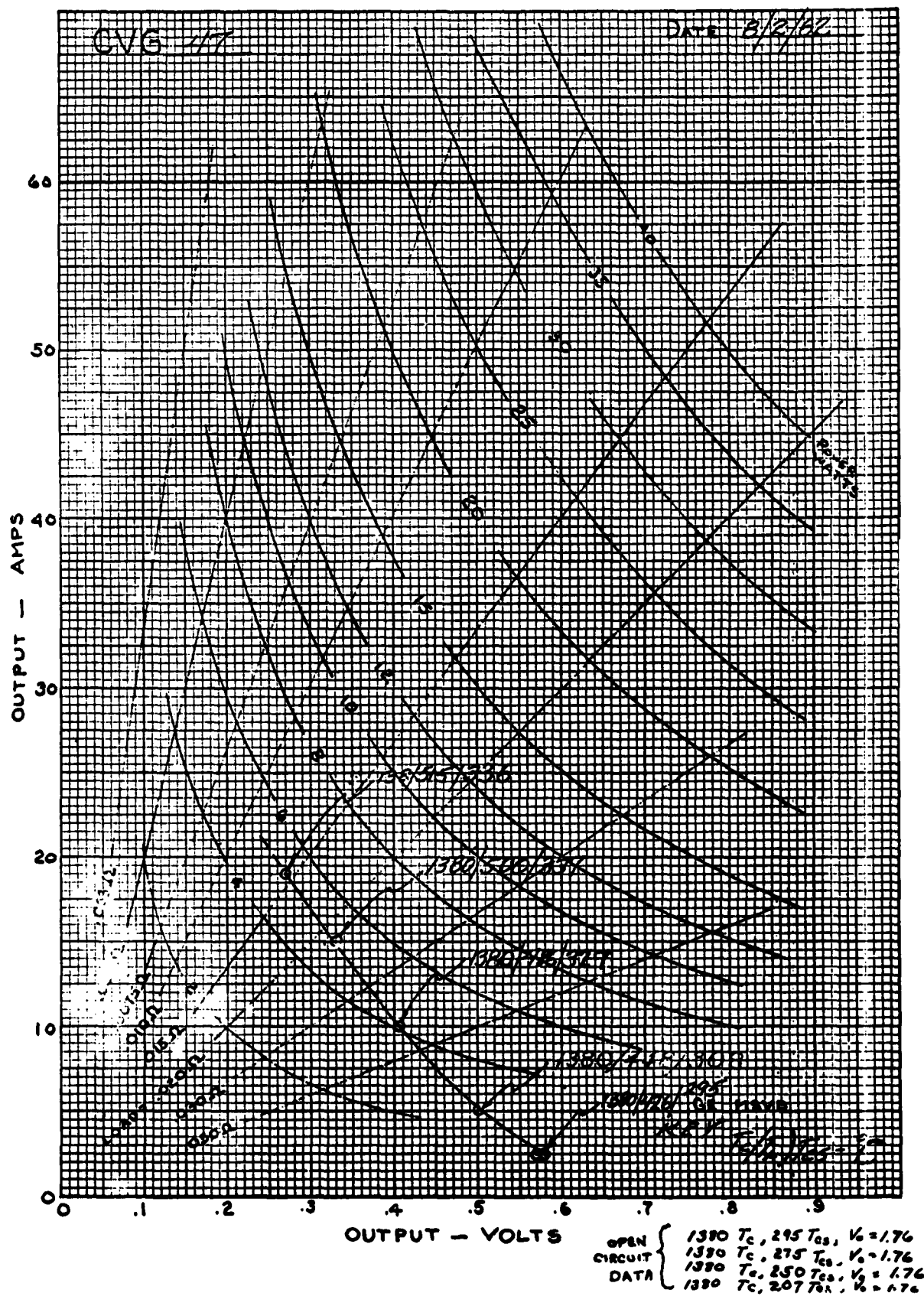Figure 79.   Converter 46 E-I Characteristics
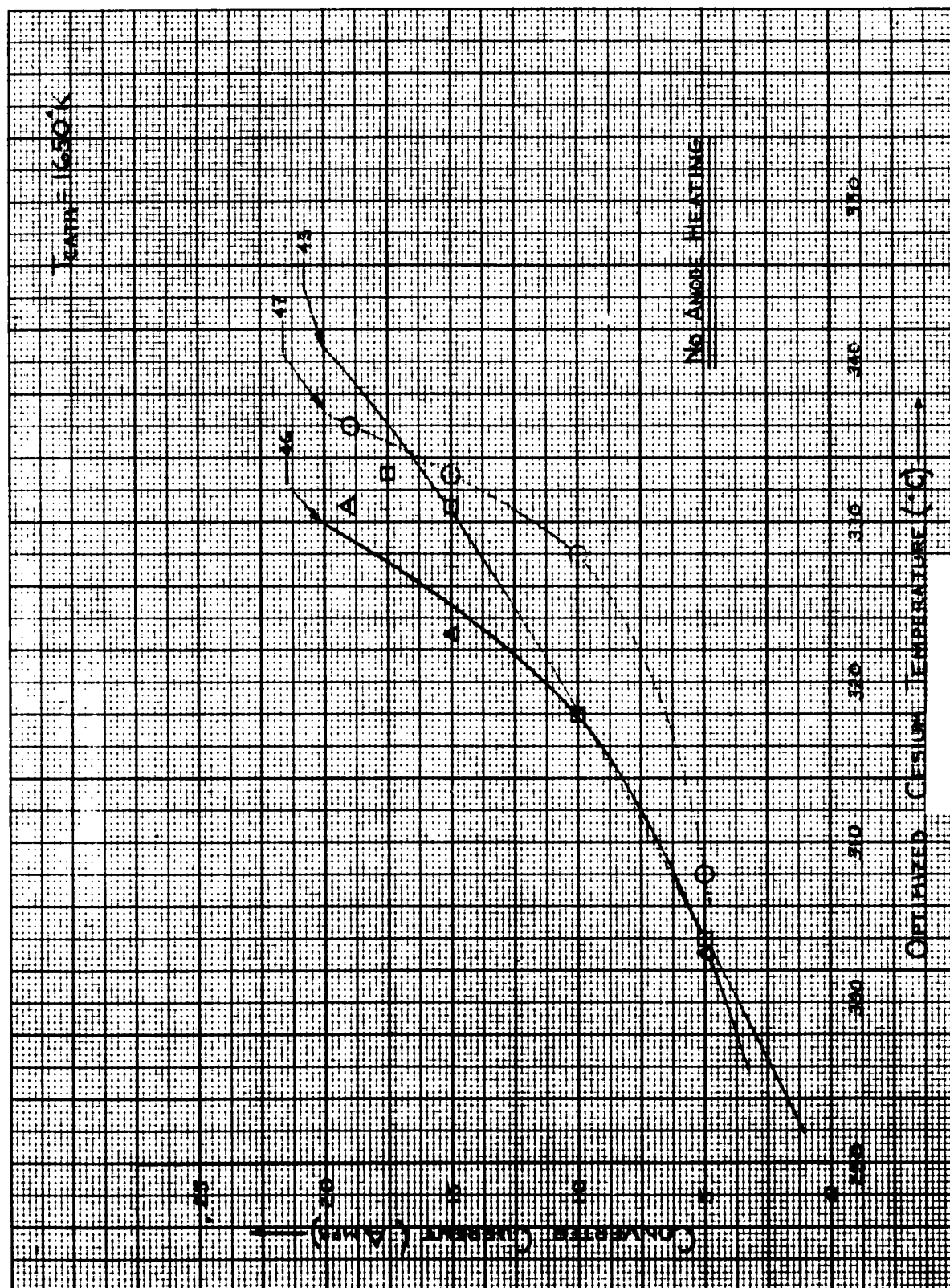
Figure 80.   Converter 47 E-I Characteristics

Figure 81. Converter Current vs. Optimum Cesium Temperature
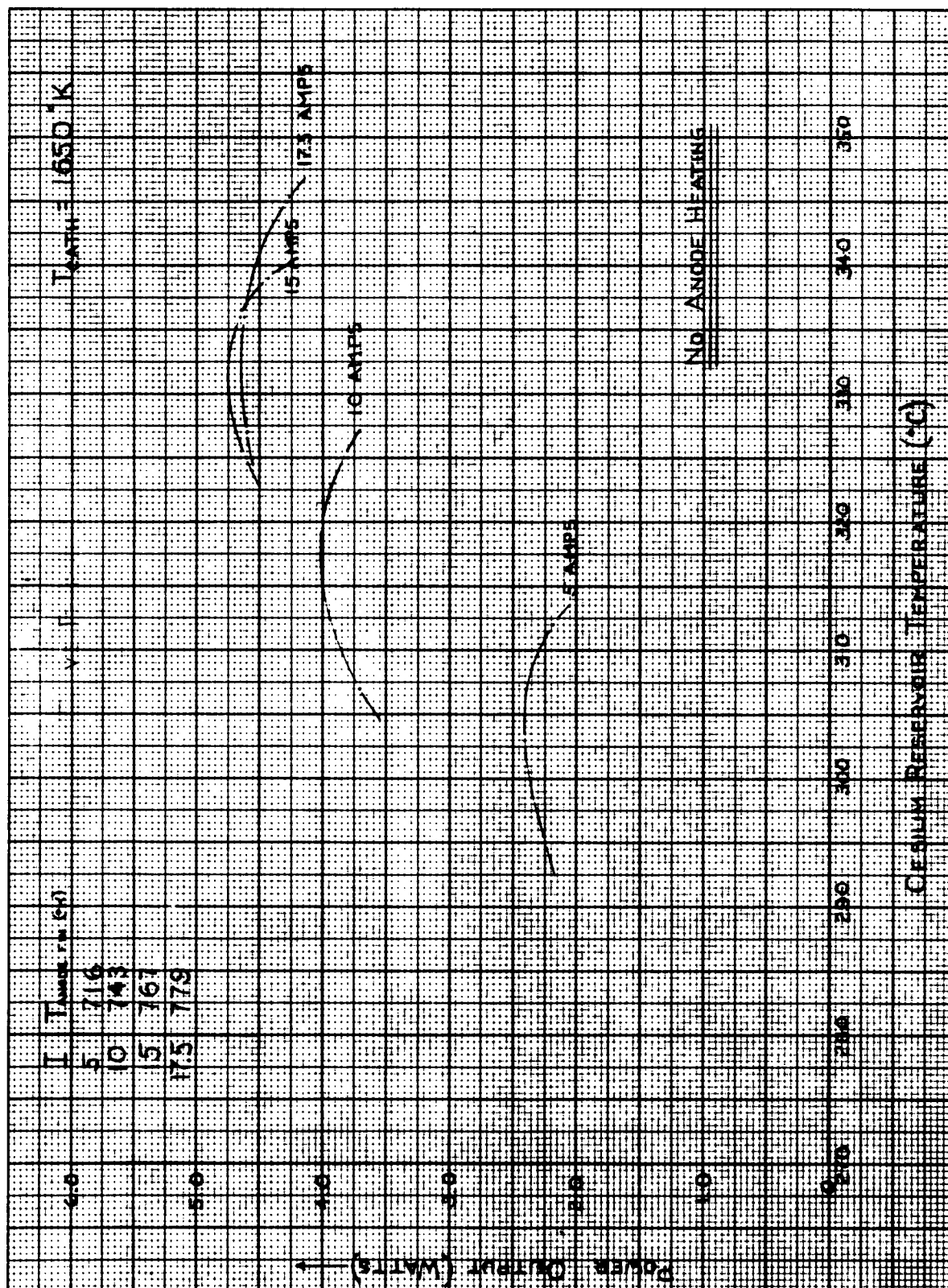
108

Figure 82. Converter 43 Power vs. Optimum Cesium Temperature
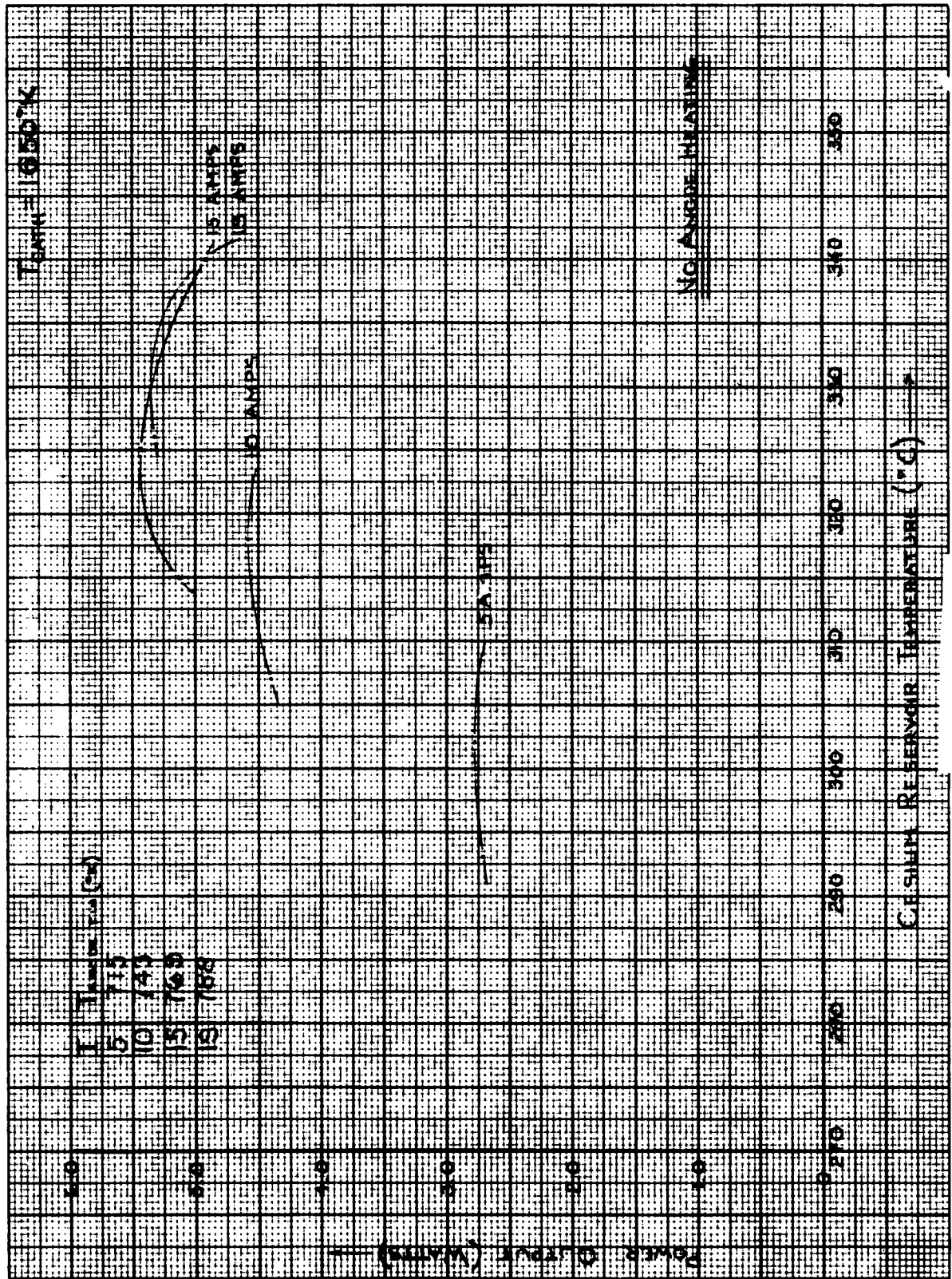
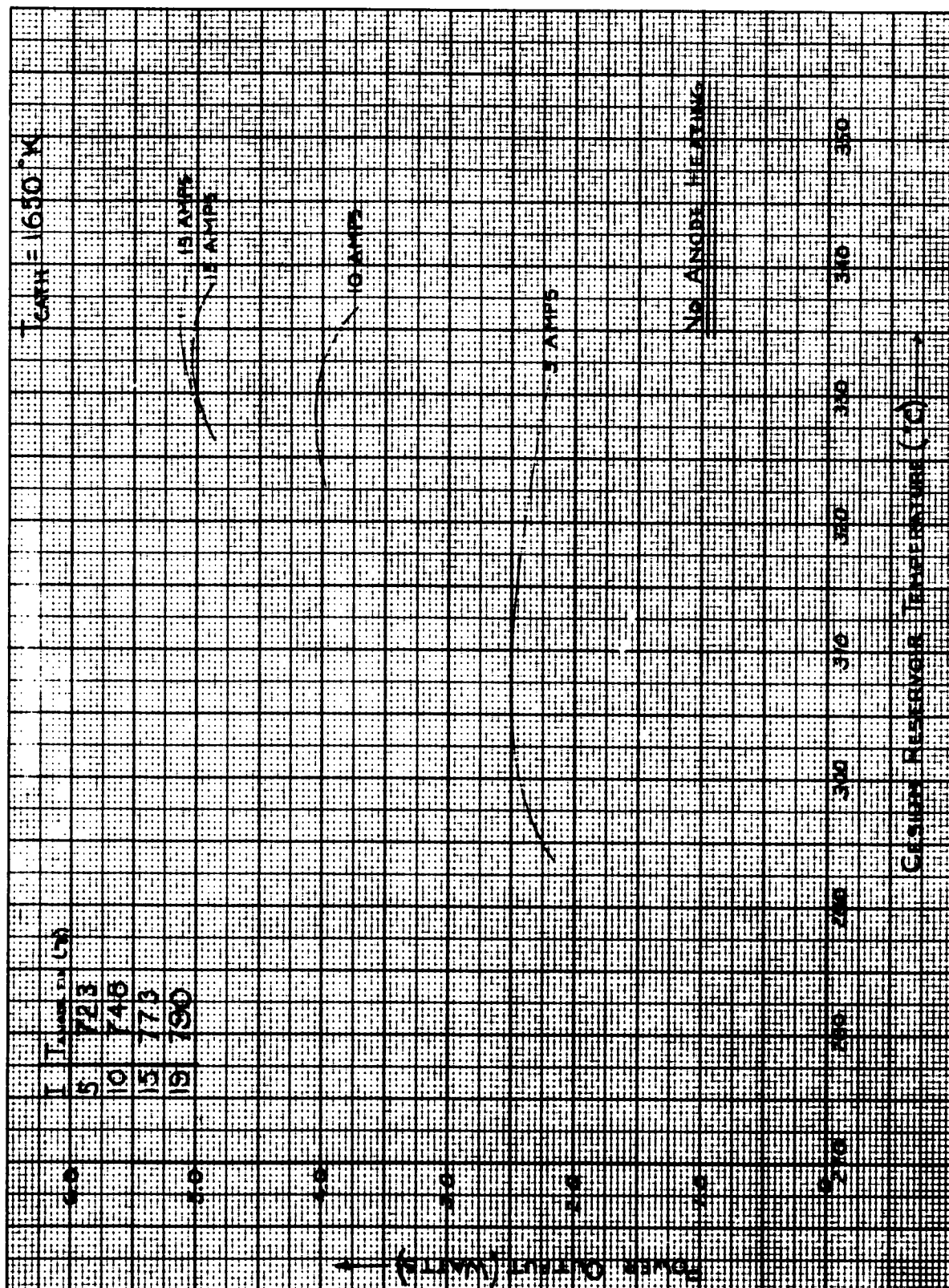Figure 83. Converter 46 Power vs. Optimum Cesium Temperature

110

Figure 84. Converter 47 Power vs. Optimum Cesium Temperature

Since complete performance data was taken on Converters No. 43, 46, and 47, E-I curves have been predicted with these converters operating in series and in parallel (Figures 85 through 88). During laboratory testing of each of the converters, the thermal throughputs were established by the procedure outlined in the previous paragraph. Also, the thermal throughputs were calculated based upon the anode fin root temperatures. These are smaller than those measured because of side losses from the converters.

The individual converter efficiencies have been calculated based upon the anode fin heat rejection. Also, for series operation, the converter efficiencies have been established based upon measured data. By combining the insulation losses, converter throughputs and re-radiation losses with an adjustment for cavity absorbtivity, the power required to run the generator as a power producing unit has been found. Dividing this quantity into the total converter power output, yields the overall generator efficiency. For series operation of the generator, this efficiency is plotted versus output current and for parallel operation the efficiency is predicted versus output voltage. The above procedure is available from the collection subsystem to drive the generator to its prescribed temperatures. Comparing these powers with that determined from calorimetric testing of the generator, shows that sufficient energy is available to run the generator over a wide range of cathode temperatures and current outputs.

8.0 SYSTEM TESTING

8.1 Dummy Generator Tests

Testing of the CVG dummy generator was carried out to establish safe procedures for testing the final generator and also to evaluate the capability of the generator, vacuum, and collection system as an integral unit. A total of 22 data points were taken, of which 4 points were taken at steady state. Of particular interest was the capability of the quartz plate vacuum interface to withstand the vacuum pressure along with thermal stress.

8.1.1 Energy Balance with T*, Calorimeter, Re-radiation, Aperture Fin Loss

Because of the cavity shape without the converters installed, the re-radiation and re-reflections for the dummy generator tests were not evaluated. Of particular interest were the radiation losses from the aperture cone. This has not been accounted for in predicting final system performance. For two of the equilibrium points taken, the cone temperature profiles have been established and the heat losses calculated as shown in Figures 89 and 90.

Heat Loss thru Aperture Cone

ϵ Tantalum = .155

Area Section 1 = 2π (1.18) (.25) = 1.85 in^2 = 11.92 cm^2
Area Section 2 = 2π (1.70) (.50) = 5.34 in^2 = 34.40 cm^2
Area Section 3 = 2π (2.50) (.56) = 8.80 in^2 = 56.70 cm^2

σ = 5.669 x 10^{-5} ergs/sec cm^2 $°K^4$ = 5.669 x 10^{-12} watts/cm^2 $°K^4$

$Q = \sigma \epsilon AT^4$; $\sigma \epsilon$ = .879 x 10^{-12} watts/cm^2 $°K^4$
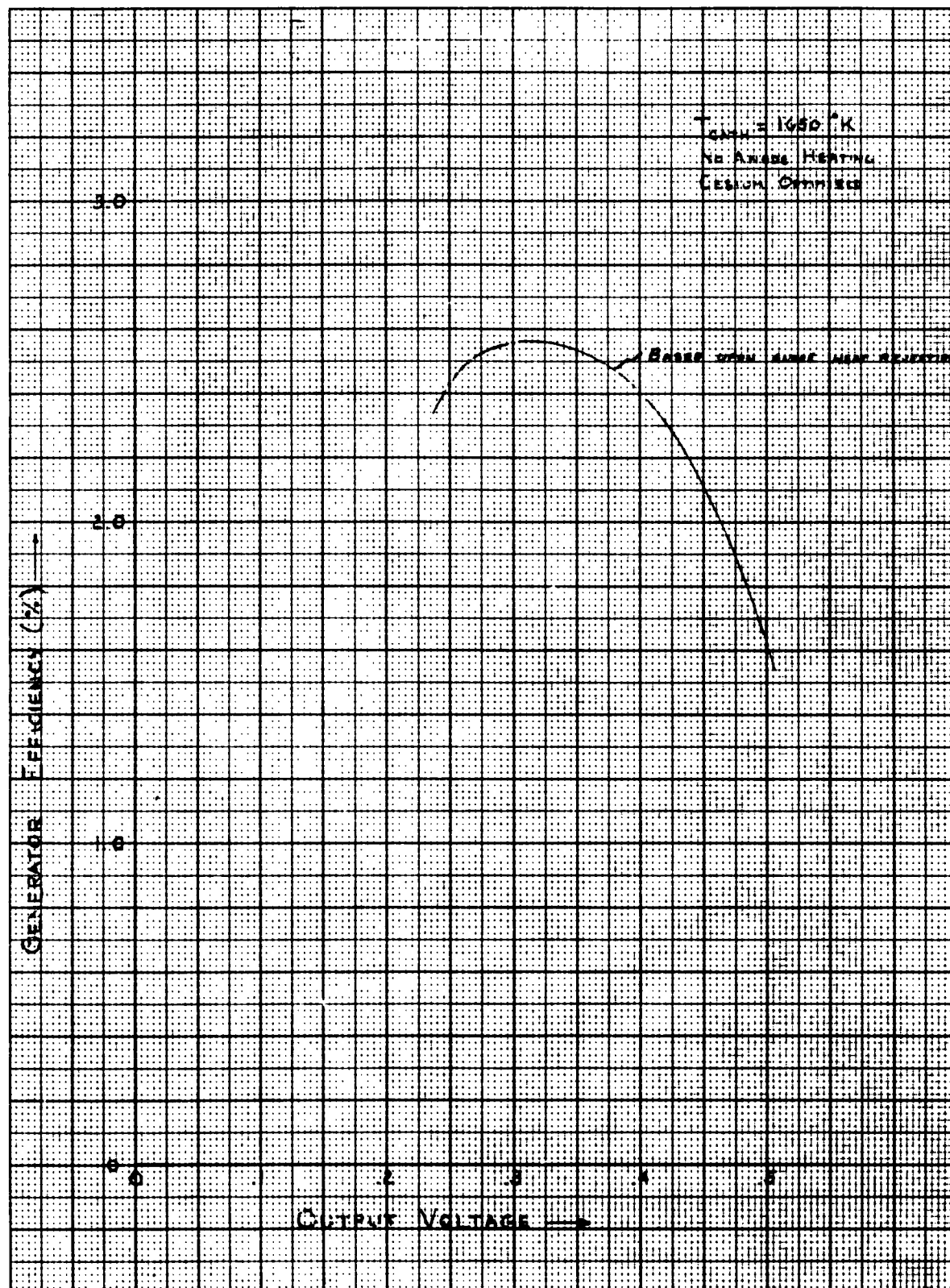
Figure 85. Predicted Efficiency with 43, 46, and 47 In Parallel
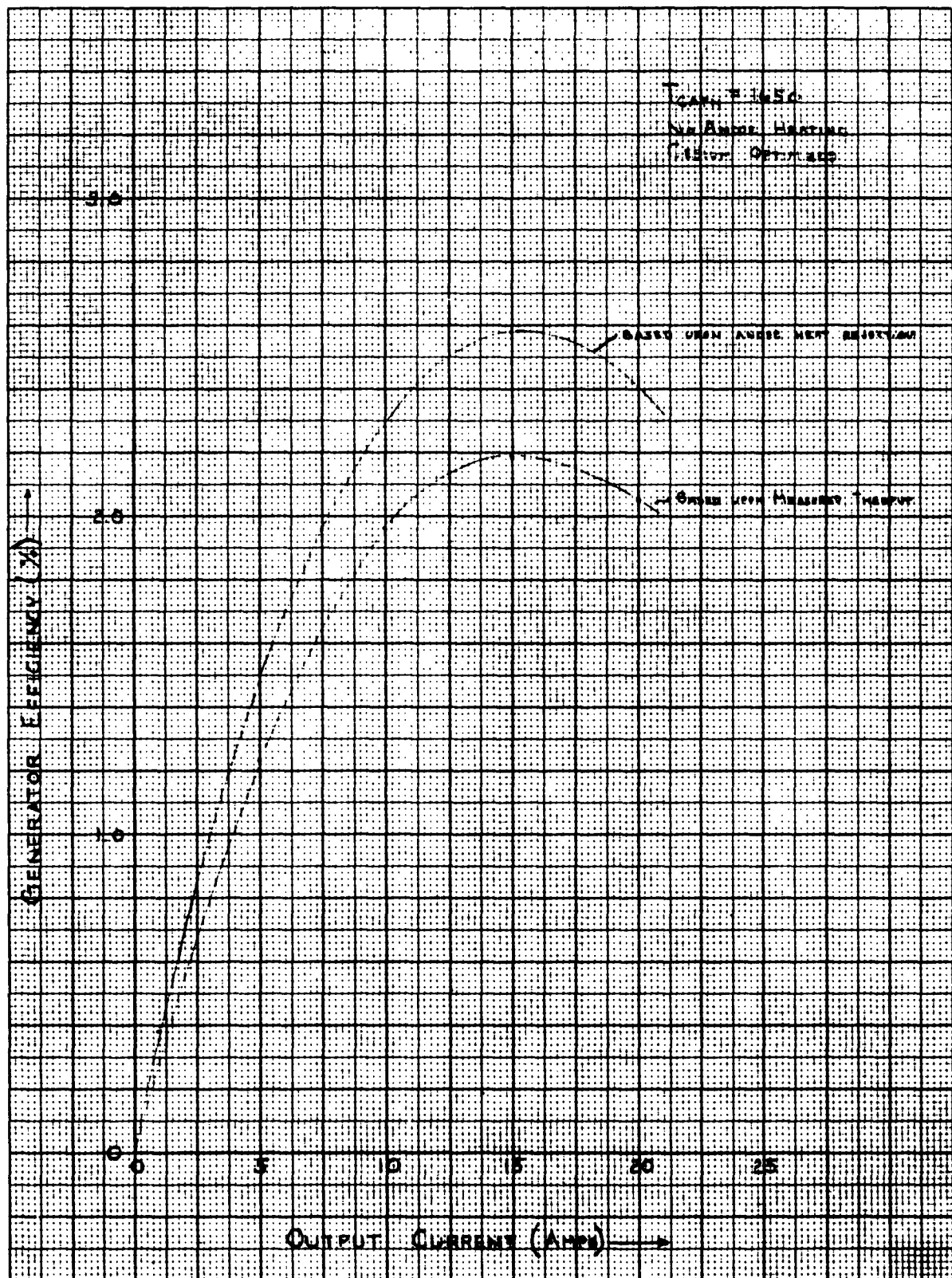
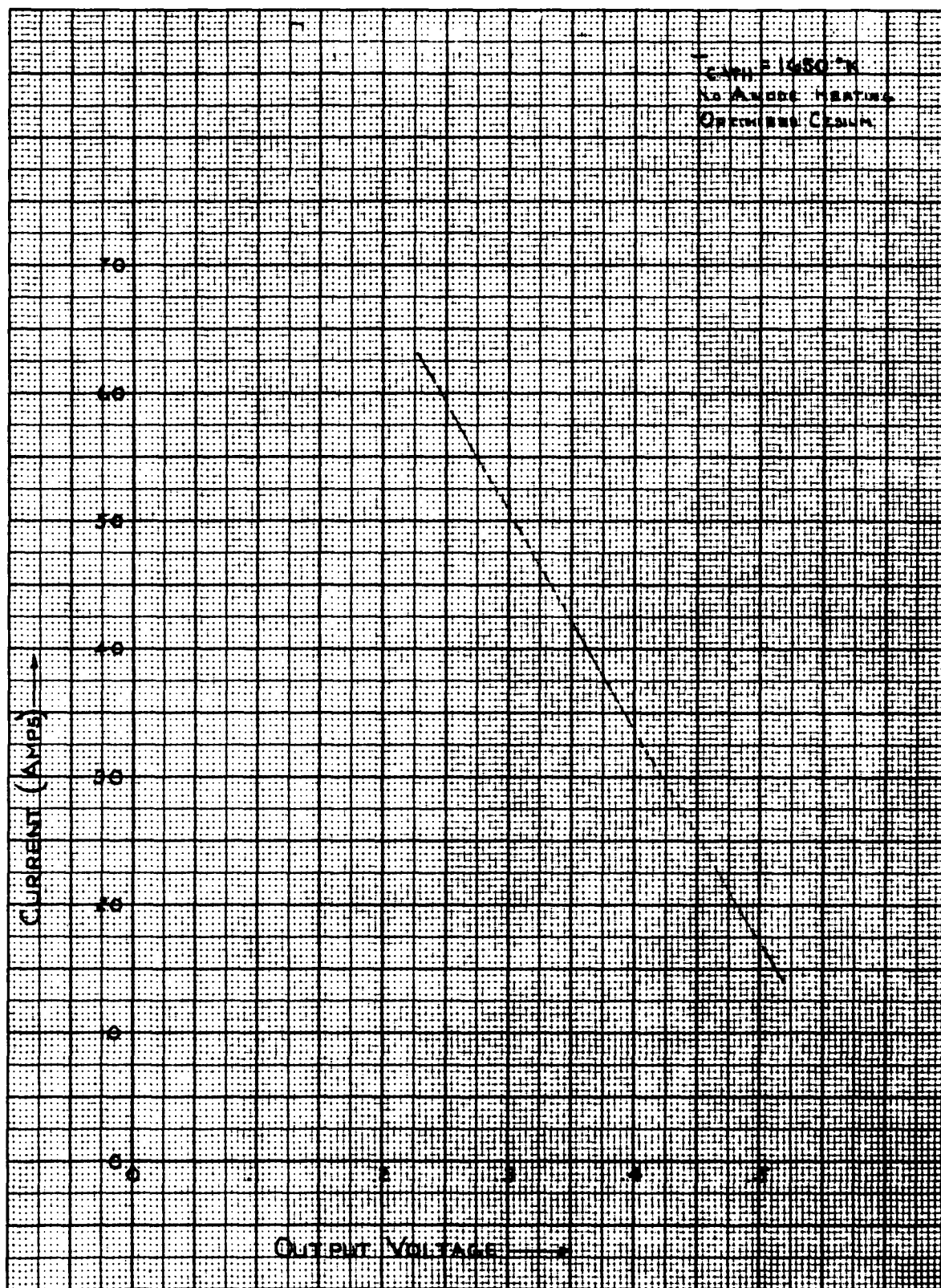Figure 86. Predicted Efficiency with 43, 46, and 47 In Series

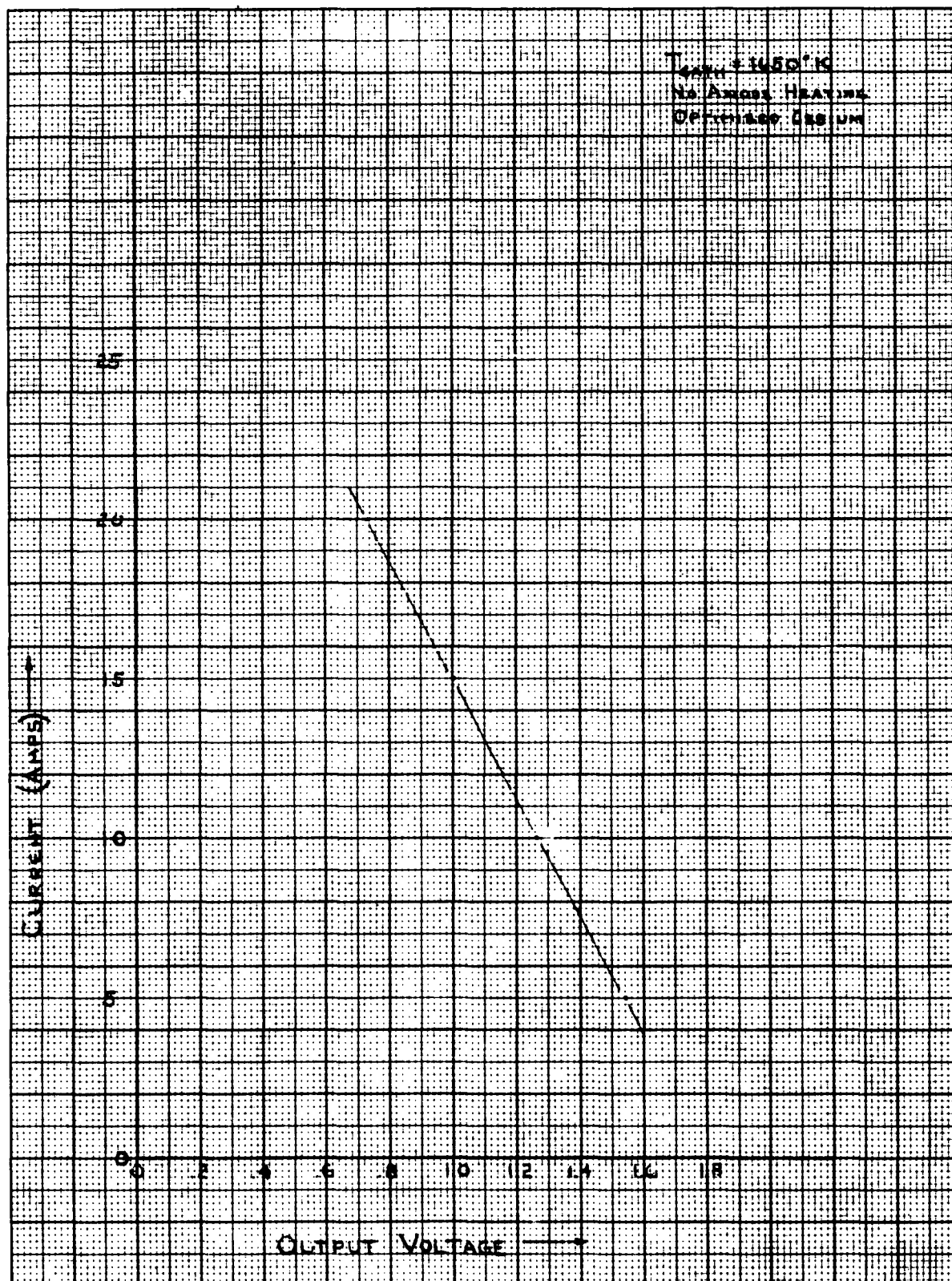Figure 87. Predicted E-I Characteristics with 43, 46, and 47 In Parallel

Figure 88.   Predicted E-I Characteristics with 43, 46, and 47 In Series
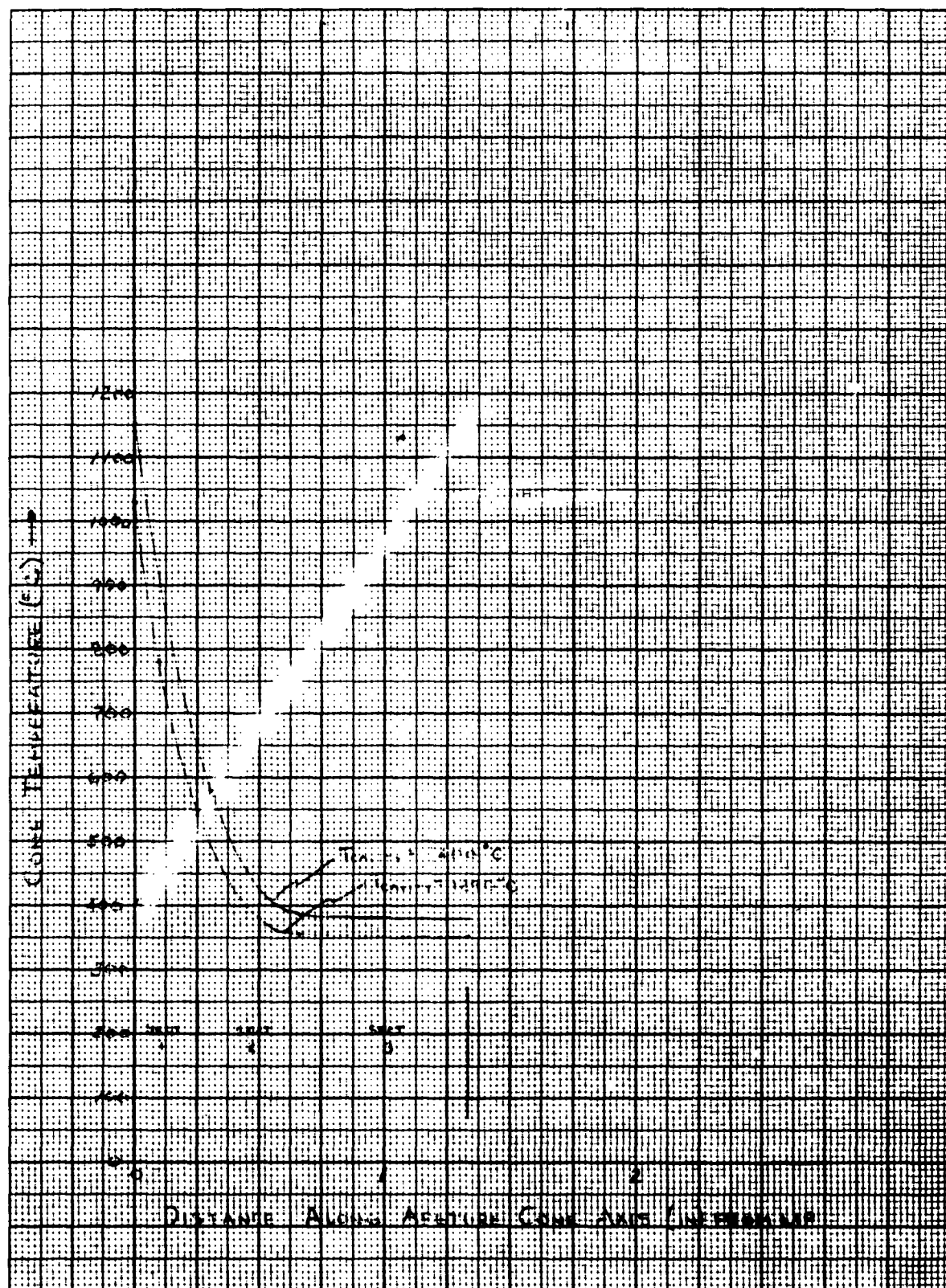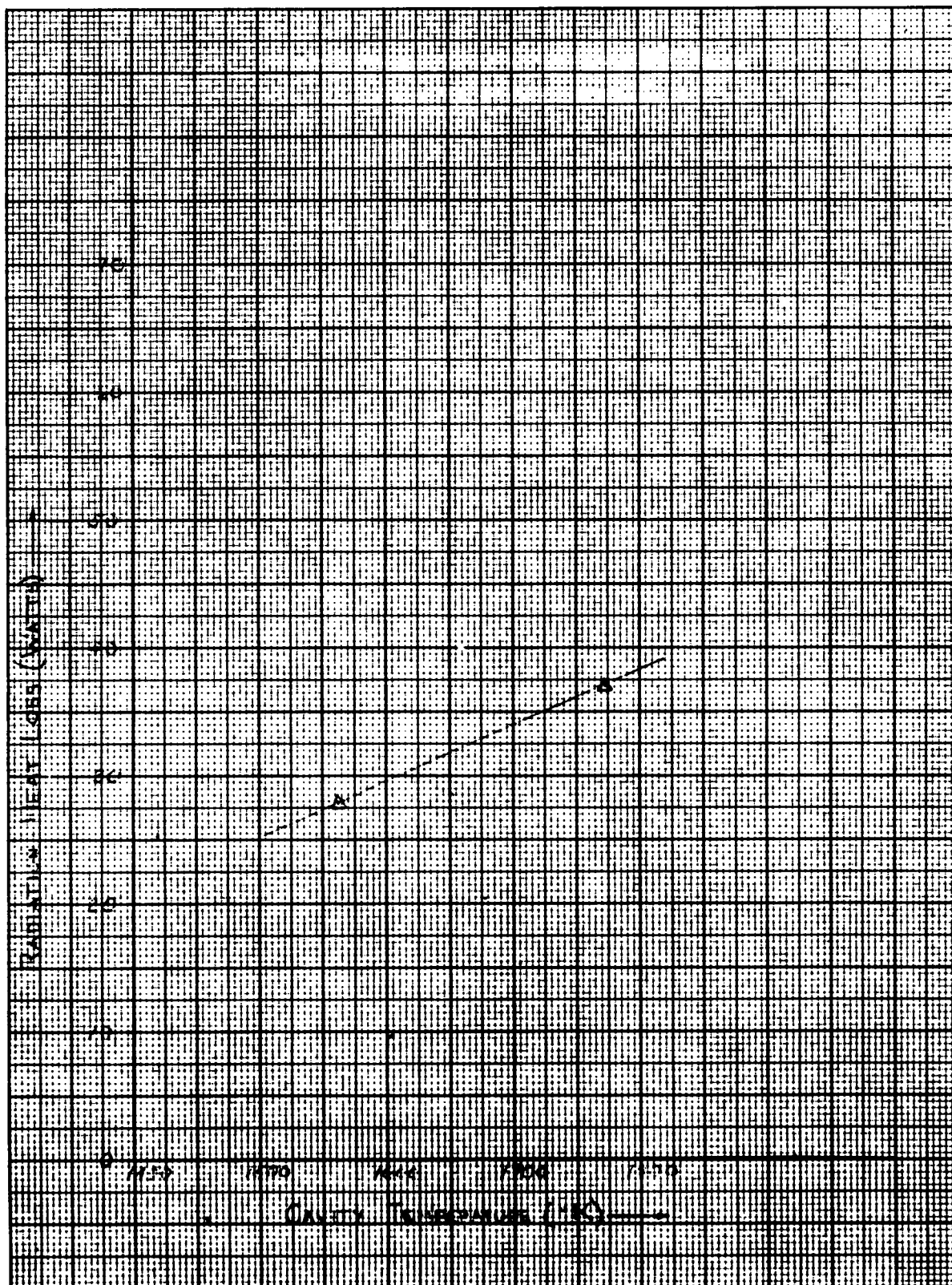
Figure 89. Aperture Cone Temperature Profile

Figure 90. Heat Losses from Aperture Cone

118

Table 1 $T_c = 1290^{\circ}C$

	$T_i(^{\circ}C)$	$T_i(^{\circ}K)$	$A(cm^2)$	T_i^4	AT_i^4
Section 1-	780	1053	11.92	1.230×10^{12}	14.70×10^{12}
Section 2-	430	703	34.40	2.440×10^{11}	8.40×10^{12}
Section 3-	353	626	56.70	1.535×10^{11}	8.70×10^{12}

$$Q = 27.90 \text{ watts}$$

Table 2 $T_c = 1400^{\circ}C$

	$T_i(^{\circ}C)$	$T_i(^{\circ}K)$	$A(cm^2)$	T_i^4	AT_i^4
Section 1-	900	1173	11.92	1.890×10^{12}	22.60×10^{12}
Section 2-	450	723	34.40	2.720×10^{11}	9.37×10^{12}
Section 3-	382	655	56.70	1.840×10^{11}	10.42×10^{12}

$$Q = 37.10 \text{ watts} \qquad 42.39 \times 10^{12}$$

8.2 CVG Run No. 1, (September 1, 1962)

Solar testing of the Cavity Vapor Generator was started at 9:42 A.M., September 1, 1962. Control shutters were gradually opened, over a time interval of approximately one hour, until cathode temperatures reached an average of 1388°C. Open circuit voltages were 1.45, 0.44, and 1.04 for converters No. 45, 46, 47 respectively. A vibration excited by either the vacuum pumps or the automatic tracking caused the cesium heater wire to No. 47 converter to open. Preliminary data was taken on the remaining two converters as follows and the test was shut down to repair the open circuit.

DATA POINT	AVERAGE CATHODE TEMP. °C	I AMPS	No. 45		No. 46		CIRCUIT	
			VOLTS	WATTS	VOLTS	WATTS	VOLTAGE	WATTS
1-5	1370	10.1	.253	2.53	.310	3.10	.563	5.63

8.3 CVG Run No. 2, (September 2, 1962)

CVG Generator Run No. 2 was performed with the generator assembly modified to provide additional support of the cesium heater bus bars, correcting the vibration condition which broke a wire to No. 47 converter cesium heater during Run No. 1. Converters No. 45, 46, and 47 were installed for Run No. 2.

Converter No. 45 would not energize and gave indication of being shorted. Modification of the external circuitry to eliminate converter No. 45 was performed and the test was continued, obtaining data on Converters No. 46 and 47 connected in series. Equilibrium performance data is summarized in the following Table:

DATA POINT	AVERAGE CATHODE TEMP. °C	I AMPS	No. 46		No. 47		CIRCUIT	
			VOLTS	WATTS	VOLTS	WATTS	VOLTAGE	WATTS
2-6	1402.5	15.0	.285	4.275	.400	6.000	.685	10.275
2-8	1487.5	15.0	.378	5.670	.455	6.825	.833	12.495

A non-equilibrium run at maximum current was performed with results as follows:

DATA POINT	AVERAGE CATHODE TEMP. °C	I AMPS	No. 46		No. 47		CIRCUIT	
			VOLTS	WATTS	VOLTS	WATTS	VOLTAGE	WATTS
2-8A	1487.5	23.5	.315	7.402	.313	7.355	.628	14.759

In an effort to determine whether a thermal cycle would clear the short in Converter No. 45, the system was shut down, cooled, and restarted in the after-noon. Converter No. 45 did not respond and a check point data run was made on No. 46 and No. 47 with results as follows, prior to shutting down:

DATA POINT	AVERAGE CATHODE TEMP. °C	I AMPS	No. 46		No. 47		CIRCUIT	
			VOLTS	WATTS	VOLTS	WATTS	VOLTAGE	WATTS
3-1	1460	15	.335	5.025	.425	6.375	.760	11.400

Solar energy available and supplied to the cavity for the generator data runs tabulated above is shown in the following Table:

DATA POINT	SOLAR INSULATION WATTS/FT^2	SHUTTER CLOSURE ANGLE-DEG.	COLLECTOR EFFICIENCY	GENERATOR INPUT ENERGY-WATTS
2-6	84.94	12.5	.420	700.5
2-8	87.53	0	.565	970.3
2-8A				
3-1	82.99	0	.565	920.1

8.4 CVG Run No. 3 (September 13, 1962)

A complete inspection of the generator was made in an effort to determine the cause of the apparent short in No. 45 converter or its circuitry. A circuitry short between the anode and cathode leads apparently caused by rotation of the feed through at the base plate was found. The leads on all converters were modified to correct this problem and the generator was re-installed with Converters No. 45, 46, and 47.

During the warm-up period the cathode temperature of No. 45 lagged behind that of both of the other converters, such that at design temperature and open cir-cuit the cathode temperatures were, No. 45-1335°C, No. 46-1410°C, and No. 47-1420°C. No. 45 converter could not be made to energize and all indications pointed to an internal short in the converter, large enough to establish a thermal energy conductance short as well as an electrical short.

Data was taken on Converters No. 46 and No. 47 at variable current settings with results as shown in the following Table prior to shutting down the system preparatory to replacing Converter No. 45.

DATA POINT	AVERAGE CATHODE TEMP. °C	I AMPS	No. 46		No. 47		CIRCUIT	
			VOLTS	WATTS	VOLTS	WATTS	VOLTAGE	WATTS
4-5	1397	20.0	.234	4.68	.250	5.00	.484	9.68
4-6	1390	15.0	.285	4.27	.326	4.89	.611	9.16
4-7	1395	10.0	.370	3.70	.410	4.10	.780	7.80

8.5 <u>CVG Generator Run No. 7 (Performance and Energy Balance. Comparison with Predicted Performance)</u>

Final system testing began on 12 September with converters No. 45, 46, and 47 wired in series. However, converter No. 45 would not develop open circuit voltage; therefore, data was taken with only 46 and 47 in series, with 45 removed from the generator circuit. On 21 September the generator was moved from the vacuum system and converter No. 45 was replaced by converter No. 42. During testing of this system all tubes developed open circuit voltage. However, for No. 42 this voltage was very low. When the load was connected, tube No. 42 failed to conduct and acted like a high impedance load. The system was immediately shut down in order to save tubes No. 46 and 47 for further testing. At this point the resistance of tube No. 42 was measured at 300 K ohms indicating that this tube had somehow opened and no longer contained cesium. At this point the generator was again removed from the vacuum system and tube No. 43 was installed in place of No. 42 on Friday, 21 September. Testing was then further hampered by bad weather, until the afternoon of 24 September when successful operation was performed with 3 converters in series. Sufficient time was available to obtain only 5 data points before the sun was no longer able to be tracked due to its low elevation.

The five points were taken at open circuit, 10 amps. and 15 amps. Time did not afford the optimization of cesium temperatures on power output; therefore, the cesium temperatures used were close to those obtained by laboratory testing. Calculations have been made on the various subsystem efficiencies and an overall energy balance for each point has been made. These calculations are shown on the attached Table 5. Here it can be noticed that the converter power outputs are very close to those measured during laboratory testing, with the result being that the predicted power outputs are very close to those actually measured during the final system test. This same holds true for the overall energy balance. The converter efficiencies have been calculated by two methods: (1) heat rejection from the anode fin, and (2) those obtained by laboratory testing at the same output current level and cathode temperatures. In most instances these agree quite faborably. Generator efficiencies have also been calculated. First by dividing input power into power output, and secondly, in a similar manner by defining input power to be exclusive of the re-radiation and reflection loss. The collector subsystem efficiencies have also been investigated. Here the collector reflectivity, shadow area, quartz plate reflectivity, and transmissivity losses are all charged to this subsystem. The electrical power output obtained during this run was 14.25 watts at a cathode temperature of 1663°K (1390°C). The generator efficiency, excluding aperture losses, was 3.89 including aperture losses, 2.018%.

8.6 <u>CVG Run 8 (Test Results and Performance Computation)</u>

On September 27, 1962, the final test to be described in this report was conducted. The original tubes 46 and 47 were still operable prior to this test, and converter 43, which had performed well in Run 7 described in the preceding paragraph, was used.

TABLE 5.

CVG FINAL SYSTEM PERFORMANCE

Converter No.	Caynode Temp. °C	Converter Output Voltage Volts	Converter Output Current Amps	Converter Output Power Watts	Collector Interacepted Power Watts	Overall System Efficiency %			Cavity Temp (Avg) °K	Calculated Radiation Loss Watts	Generator Radiation Loss Watts	Core Aperture Watts	Anode Fin Root Temp °K	Cavity Reflection Watts	Calculated Power Into Generator Watts	Palculated Power Into AT 1200K Watts		Cesium Reservoir Temp °C	Cooling Electron Converter	Reflector Watts		
43	—	2.090	0	0									588	28				—	0	28	0	
46	1380	2.025	0	0									618	43				—	0	45	0	
47	1420	2.150	0	0									598	40				—	0	40	0	
Total System		6265	0	0	1582.5	0	37.41	0	1698	200	110	34		111	73	528	—	0		111		
43	—	.4025	10	4.025										53				328	9.90	—	7.59	
46	1380	.3770	10	3.770										73				318	9.90	—	8.17	
47	1380	.3750	10	3.750										75				328	9.90	—	5.00	
Total System		1.1545	10	11.545	1578.0	.732	41.40	1.770	1685	195	108	33		201	86	623	645	3.375				
43	—	.4070	10	4.070									728	53				328	9.90	41	8.90	7.64
46	1355	.3800	10	3.800									743	73				318	9.90	70	5.47	5.81
47	1355	.3850	10	3.850									783	75				328	9.90	66	5.12	6.17
Total System		1.1820	10	11.820	1567.2	.755	41.40	1.825	1694	198	109	33		201	97	622	645	3.450			105	
43	—	.3200	15	4.800									733	59				331	14.18	55	8.73	8.14
46	1355	.3000	15	4.500									763	82				335	14.18	80	5.62	5.49
47	1355	.2850	15	4.280									743	84				333	14.18	72	5.56	5.09
Total System		.905	15	13.580	1522.0	.693	44.40	1.922	1694	200	109	34		225	91	638	684	3.690			207	
43	—	.325	15	4.875									733	59				334	14.18	55	8.90	8.17
46	1390	.315	15	4.725									763	82				334	14.18	80	5.91	5.77
47	1380	.310	15	4.650									748	84				334	14.18	74	6.28	5.66
Total System		.950	15	14.250	1581.0	.837	44.40	2.048	1693	197	109	33		225	93	638	684	3.899				

TOTAL ELAPSED TIME OF TEST IN SERIES = 29 MINUTES

TEST DATE 24 SEPTEMBER 1962

122

This test resulted in the highest generator efficiency including aperture losses, reported in this report of 2.24% at a cathode temperature of 1773°K (1500°C), and the highest output power reported in this report of 21.25 watts.

Table 6 summarizes the generator performance for this run.

Tables 7 and 8 are copies of the data sheets recorded during the run. All points are static, at both thermal and electrical equilibrium

TABLE 6. PERFORMANCE CONVERTERS 43, 46, AND 47 IN SERIES

Data Point Number	6	12
Electrical Output - Watts	14.56	21.25
Voltage Output - Volts	.97	1.214
Current - Amps	15.0	17.50
Cathode Temperature - °K	1668	1773
Cathode Temperature - °C	1395	1500
Generator Efficiency - including aperture losses %	1.895	2.24
Generator Efficiency - excluding aperture losses %	3.16	3.74

9.0 EXPECTED FUTURE PERFORMANCE

The thermal information which has been obtained from the calorimetric tests in the Philadelphia vacuum test with a resistance heater has been used to estimate anticipated generator thermal performance. Due to the low power of the converter used on the present program, the performance characteristics have been based upon a regression analysis and reproduced here in Figure 91. Close correspondence between peak power from this regression analysis and Reference 7 is also seen between 1600 and 2000°K in Figure 92. Thus, with the thermal data from the generator testing on the Cavity Vapor Generator Program coupled with the electrical data an efficiency for the system can be computed and is shown in Figure 91. Efficiency at various cathode temperatures as a function of current is plotted.

To predict the expected operation of a space system, this generator performance can now be coupled with the calorimetric test information from the Phoenix testing on a sixty degree rim angle searchlight. A 45° collector performance would be superior to this measured characteristic. The predicted collector input based on data from Reference 1 minus the aperture losses as a function of aperture diameter at several cathode temperatures is plotted in Figure 93. This peak energy divided by the total input energy results in a plot of collector efficiency as a function of cavity temperature at several mis-orientation values and is plotted in Figure 94, converted for a solar constant of 130 w/ft^2. This efficiency when multiplied by the predicted generator efficiency results in the system efficiency. Plots of these efficiencies are shown in Figure 95 and reveal that the efficiency of the system is

TABLE 7.

TABLE 8.

8

TEST TYPE CYC GEN RUN 8

DATE [illegible]

ARIZONA TAPE NO. ___

DATA POINT NO.	TIME OF DAY	[illegible] RED	[illegible] BLACK	[illegible] RED	[illegible] BLACK	[illegible] RED	[illegible] BLACK	CAVITY [illegible] RED	CAVITY [illegible] BLACK	CAVITY [illegible] RED	SEAL #46 CH.1	SEAL #45 CH2	PAN DIA #46 CH3	PAN MIDDLE #46 CH4	PAN EDGE #46 CH5	[illegible] CH6	[illegible] CH7	SEAL CYP 47 CH8	PAN DIA #47 CH9	[illegible] CH10	[illegible] CH11	[illegible] CH12	[illegible] CH13	[illegible] 47 CH14	PAN EDGE #46 CH15	[illegible] CH16	SEAL #46					CHAMBER VACUUM PRESSURE	SHUTTER POSITION DEGREES	CHAMBER WATER FLOW, POUNDS/HOUR	AVERAGE CHAMBER TEMPERATURE °F	SOLAR INSOLATION WATTS/FT²	ENERGY INTO GENERATOR-WATTS
8		—	1486	1392	1370	—	—	344	344	360																						26 [illegible]	18°			[illegible]	1632.6 765.3
9	1:29		1500	1460	1465	-	-	331	329	333		436	436	440	460	380	475	465	465	370	375	375	360	430	505	503	500					1.2 [illegible]	6°		58/70	[illegible]	1669.5 812.8
10	1:28		1470	1375	1375	-	-	338	335	340		445	525	450	460	465	480	470	470	420	420	360	375	350	510	380	520					54 10	10°		58/72	[illegible]	1646.8 764.1
11	1:15		1570	1500	1500			345	345	352		440	500	440	455	400	500	430	430	410	415	330	385	345	510	385	510					50	0			[illegible]	1689.0 952.8
12	1:21		1600	1500	1500			350	358	360		455	520	460	470	425	510	510	510	435	440	370	390	260	530	400	525					70	0			[illegible]	[illegible] 1279.9
13	1:43		1550	1460	1450			365	348	363		465	525	465	480	425	510	516	510	415	450	380	400	380	530	405	530					80	0			2.2 [illegible]	[illegible] 913.2
14	1:47		1550	1450	1450			358	363	363		465	525	465	480	425	510	515	510	410	415	380	375	380	530	405	525					80	0			[illegible]	[illegible] 925.4
15	1:53		1500	1460	1460			340	344	341		465	525	465	460	425	515	515	515	445	445	380	400	380	530	410	530					80	0		58/70	[illegible]	[illegible].5 883.7

8°

TEST TYPE CYC GEN RUN 8

[illegible] SOLAR TEST FACILITY

DATA POINT NO.	TIME OF DAY	[illegible]	[illegible]	[illegible]	[illegible]	[illegible]	[illegible]	[illegible]	[illegible]	[illegible]	[illegible]	WATTS	WATTS	WATTS	WATTS	WATTS	CYP #45 [illegible] AMPS	CYP #45 [illegible] VOLTS	CYP #45 [illegible] WATTS	CYP #46 [illegible] AMPS	CYP #46 [illegible] VOLTS	CYP #46 [illegible] WATTS	CYP #47 [illegible] AMPS	CYP #47 [illegible] VOLTS	CYP #47 [illegible] WATTS	
8	12:28	.331	.295	.231						20					3.94		2.7	7.6		2.3	6.2		2.8	6.7		
		.342	.237	.188	.667					20					2.34		2.7	7.0		2.3	5.9		2.5	6.0		
10	12:5[illegible]	.315	.188	.190	.593					20					4.86		2.6	6.8		2.3	5.9		2.4	5.4		# 7
11	1:15	.474	.481	.456	1.419					15					2.120		2.8	7.5		2.5	7.0		3.0	7.8		
12	1:21	.407	.410	.357	1.214					12.5					2.125		3.0	8.2		2.5	6.8		2.9	7.3		
13	1:43	.287	.295	.311	.893					20					1.78		2.9	7.6		2.3	6.2		2.7	6.7		
14	1:47	.251	.287	.284	.822					20							3.0	8.0		2.4	6.6		3.0	7.4		
15	1:53	.309	.313	.321						20							2.6	6.9		2.3	5.5		2.8	6.8		SHUT DOWN 1:56

128

increasing as the cathode temperature increases and that the optimum is some-
where above 2000°K. This cathode temperature, however, is so high as to cause
serious concern for system life and reliability. Thus, a compromise between
life, reliability and system performance will probably be reached in the region
of cathode temperatures between 1800°K and 2000°K. It is also evident that effi-
ciencies comparable with other methods of solar conversion are obtainable, pro-
viding it is possible to obtain the proper electrical energy density in a realistic
system. It is also evident that considerable attention should be placed on a thorough
attempt to improve generator performance, since this is still lower than desired.
Future programs should also attempt to examine the weight trade-offs, since
separate studies (see Reference 4) have indicated system specific weights of 40#/Kw,
at a cathode temperature of 1800°K and a system efficiency of 8.8%. Although this
is higher than the present study would indicate (7.8%) advances in converter insu-
lation technology should improve the performance to this point, within the next
two years.
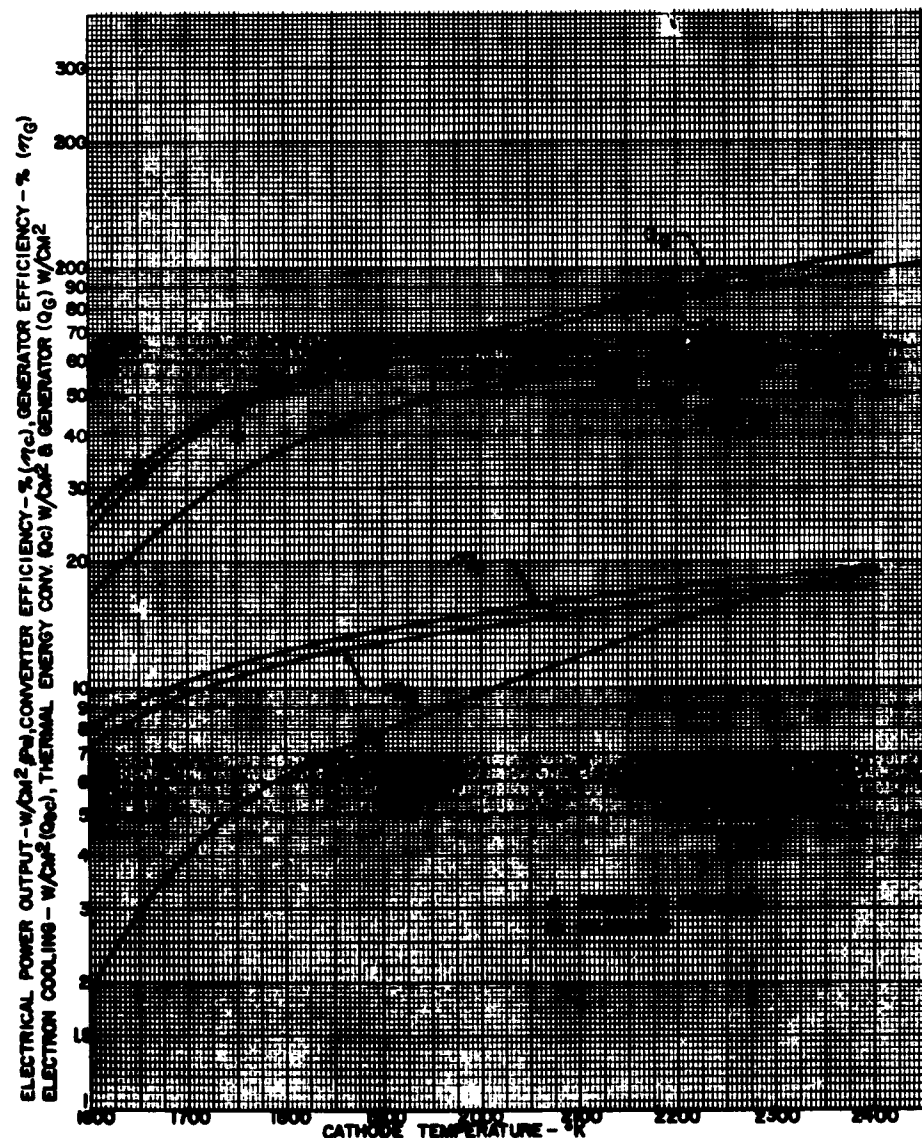
Figure 91. Performance Characteristics vs. Cathode Temperature

126
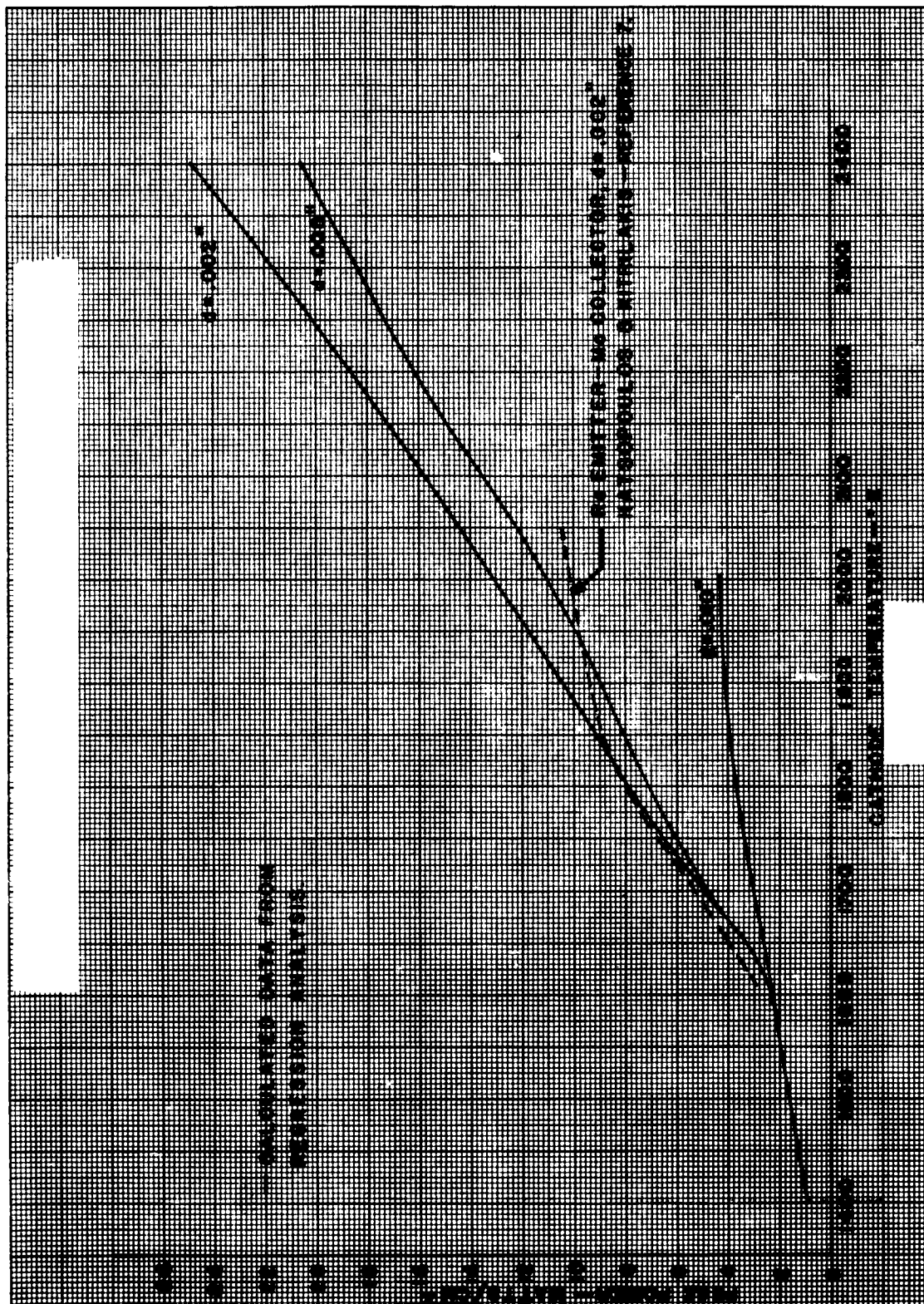
Figure 92. Peak Power vs. Cathode Temperature
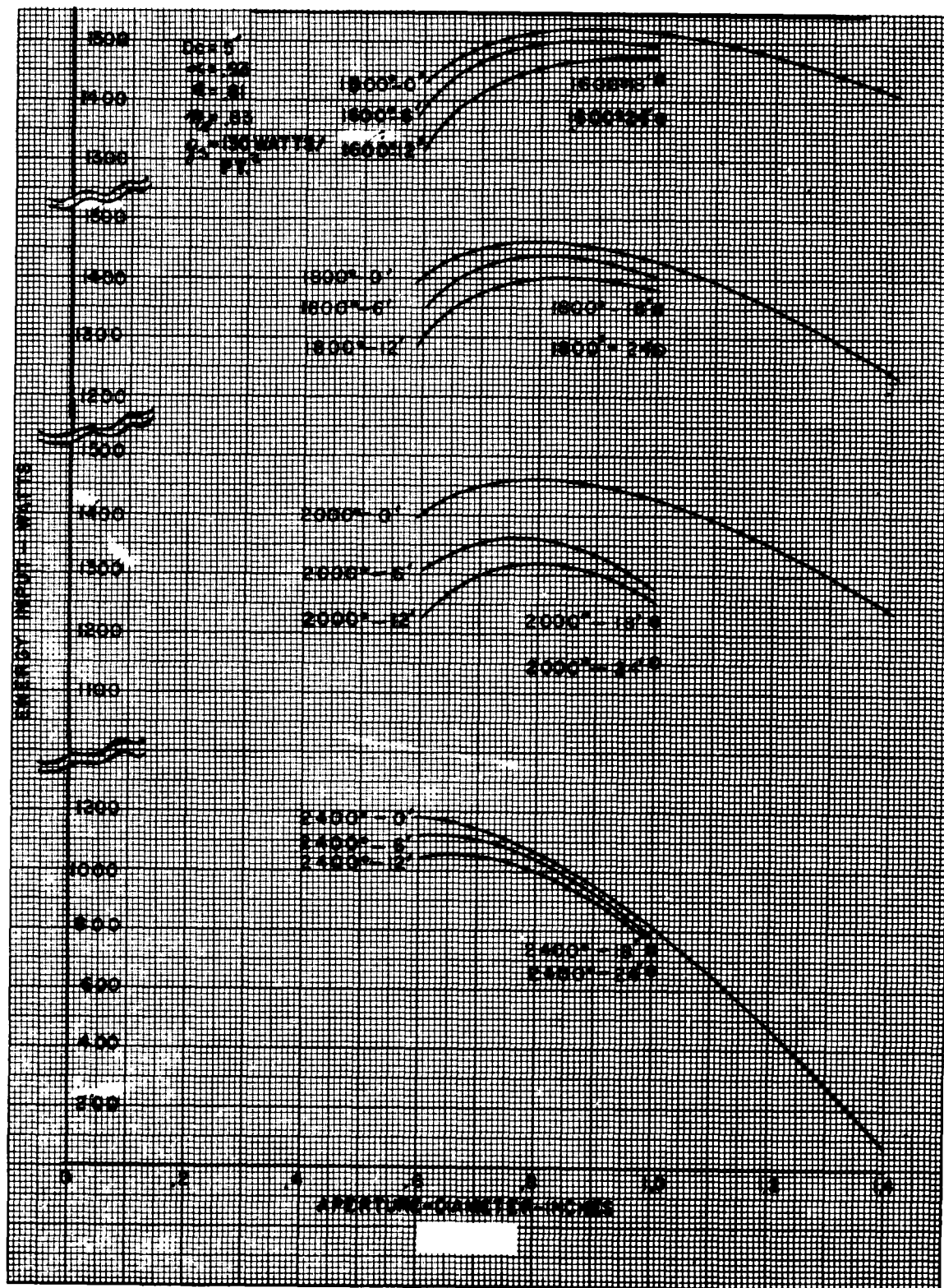
Figure 93. Energy Available vs. Aperture Diameter

128

Figure 94. Collector Efficiencies vs. Cavity Temperature
Including Reflections and Reradiations

COLLECTOR EFFICIENCY
η_R = .92
α = .93
ϵ = .81
βe = 6'
η_{sh} = .93

COLLECTOR EFFICIENCY
η_R = .92
$\alpha = \epsilon$ = 1
η_{sh} = .93
βe = 6'

COLLECTOR EFFICIENCY
η_R - CVG - .83
α = .93
ϵ = .81
βe = 6'
η_{sh} = .93

GENERATOR EFFICIENCY
SYSTEM EFFICIENCY — η_R = .92, α = .93,
ϵ = .81, βe = 6', η_{sh} = .93

SYSTEM EFFICIENCY
η_R = .83
α = .93
ϵ = .81
βe = 6'
η_{sh} = .93

SYSTEM EFFICIENCY
η_R = .92
$\alpha = \epsilon$ = 1
η_{sh} = .93
βe = 6'

FIGURE 95

EFFICIENCY — %

CATHODE TEMPERATURE — °K

Figure 95. System Efficiencies vs. Cathode Temperature

130

NOMENCLATURE FOR SECTION 9.0

T^* — Equivalent generator exterior temperature, $^\circ K$

A_1 — Area of 1st side of the generator, cm^2

A_2 — Area of second side of the generator, cm^2

A_n — Area of nth side of the generator, cm^2

T_1 — Temperature of 1st side of the generator, $^\circ K$

T_2 — Temperature of second side of the generator, $^\circ K$

T_n — Temperature of nth side of the generator, $^\circ K$

Q_t — Thermal energy input, watts

I = Converter current, amps

n = Efficiency, %

P_o = Electrical power output, watts

T_c = Cathode temperature, $^\circ K$

T_f = Anode fin temperature, $^\circ K$

$Q_{c|}$ = Thermal energy density into converter, watts/cm^2

Q_g — Thermal energy density into generator, watts/cm^2 of cathode area.

Q_{ec} — Electron cooling energy density of the cathode, watts/cm^2

n_c — Converter efficiency, %

n_g — Generator efficiency, %

Pe — Electrical output energy density, watts/cm^2

d — Cathode to anode gap, inches

D — Collector diameter, feet

a — Cavity absorbtivity, dimensionless

ϵ — Cavity emissivity, dimensionless

n_r — Collector reflectivity, dimensionless

$^1 \beta_e$ — Orientation error

131

η_s = Ratio of unshadowed area to total collector area.

q_s = Solar Intensity, watts/ft^2

10.0 INTEGRAL THERMAL ENERGY STORAGE (TES) THERMIONIC CONVERTER UNIT

10.1 Introduction

The objectives of this program were:

1) Construction of a vapor thermionic converter with built-in thermal energy storage capacity.

2) Demonstration of at least 100 hours life with a conversion efficiency of at least 10%.

3) Demonstration of increased reliability due to individually packaged converter and storage device.

4) Indication of increased converter heat receiver performance as a result of minimized temperature gradients possible with an integral converter storage device.

The program as outlined above represented a most ambitious effort for the funding allocated. Originally there was some optimism that the above studies could be delved into to a sufficient degree to allow final fabrication and test of an integral converter storage device. However, the technology of thermal storage materials had not developed to a point where sufficient data was available to accomplish the life or fabrication goals of this program. Considerable insight was gained as to the problem areas involved and this in itself made the attempt well worthwhile.

10.2 Fabrication and Test Program

Two units were completely fabricated in this effort. The first of these was built with a hemispherical TES container and a conical fin mounted as an integral part of the converter cathode (see Figures 96 and 97). This unit was made using molybdenum container and $C_aO-Al_2O_3$ for thermal storage.

The problem encountered with this first unit were:

1) Fabrication of the heavy molybdenum cone as an integral fin on the converter.

2) Preparation and insertion of the TES material.

3) Final closure of the TES container (electron-beam weld techniques were used).

This unit was placed on test and upon reaching the oxide melting temperature, the TES container leaked and the molten oxide subsequently reacted with and shorted the heater of the calorimeter.
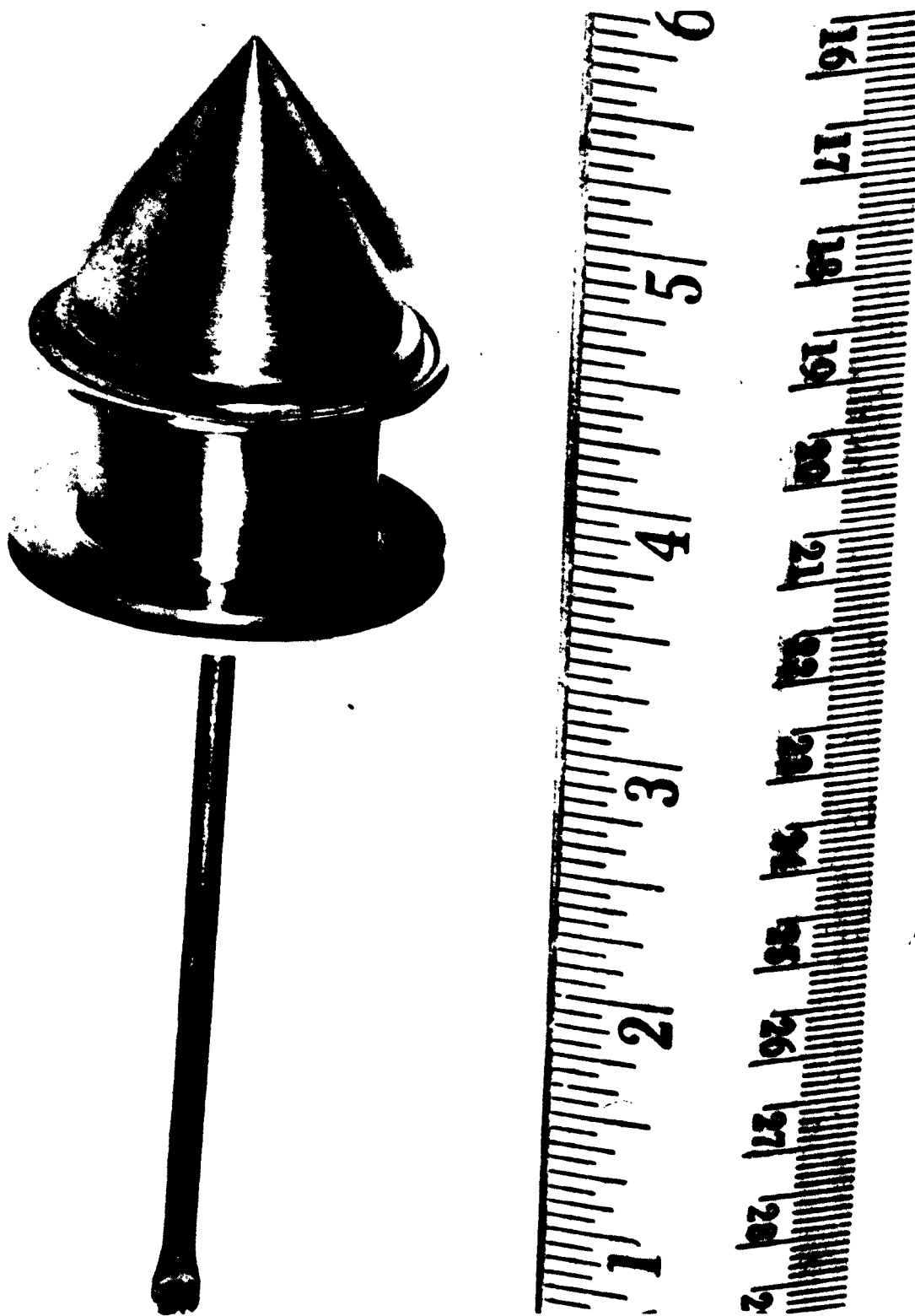
Figure 96. Converter with Fine — Intergral Thermal Storage Demonstration Unit

133

Figure 97. First Integral Thermal Storage Converter
Demonstration Unit

A second redesigned cylindrical unit was fabricated and charged with TES
material (Al_2O_3 - $3M_gO$ = $4T_1O_2$ m. p. 1910^OK). This unit is shown during fabrica-
tion, prior to test and failure in Figures 98, 99, and 100.

The oxide block was tightly fitted into the container and having a larger
coefficient of expansion than the molybdenum (container) it split the container upon
heat-up. The molten oxide (especially T_1O_2) being exposed to open vacuum re-
sulted in considerable foaming which is shown. With insufficient funds, no further
attempts were made to fabricate additional test units.

10.3 Conclusions

The tests have shown that great care must be taken in fabrication of these
devices and that all of the chemical and physical properties need to be determined
more exactly before TES material can be integrated with thermionic converter de-
vices. It will also be necessary to provide facilities for handling and preparing
TES mixtures containing beryllia (B_eO) since mixtures with this oxide are much
more attractive compatibility and energy storage-wise.

The integration of thermionic converters and thermal storage containers
being of essentially similar metals should now be accomplished without difficulty.
The major problems lie in mechanics of preparing, handling and utilizing thermal
storage materials.

134

Figure 98. Second Integral Thermal Storage Converter
Unit Prior to Test

Figure 99. Integral Unit Failure After Removal of Heater
and Shielding Fixture

Figure 100. Close-up View of Failed Unit Showing
Thermal Storage Material

REFERENCES

1. Calibration of Solar Concentrator for use in Power System Research, by Floyd A. Blake, ARS Space Power Conference, September 1962.

2. Energy Conversion Systems Reference Handbook, Volume II - Solar-Thermal Energy Sounds by D. H. McClelland and C. W. Stephens, WADD Technical Report 60-699, Volume II.

3. Thermionic Converter - Design Status and Forecast by E. A. Baum and A. O. Jensen, Atlantic City Power Systems Converence, April 1961.

4. Thermionic Space Power Generations by David L. Purdy, AIEE Winter Meeting, January 1962, #CP62-456.

5. Thermionic Energy Conversion by V. C. Wilson, ARS Space Power Systems Conference, September 1960.

6. The Cesium Vapor Thermionic Converter - observed Dependence of Performance on Cesium Pressure, Spacing, Emitter Temperature and Emitter Material, by Sotiris Kitrilakis and George N. Hatsopoulos - Interagency Thermionic Power Conversion Conference, May 1962.

1. Thermionic conversion
2. Space power systems
3. Solar energy conversion

I. AFSC Project 8173
   Task 817305-14
II. Contract No. AF33 (616)-8394
III. General Electric Co. Missile & Space Div.
IV. D. L. Purdy
    R. C. Keyser
    F. A. Blake
    J. F. Williams
V. Is available for OTS
VI. Not in ASTIA collection

Aeronautical Systems Division, Flight Accessories Laboratory, Directorate of Aeromechanics, Deputy for Technology, Wright Patterson Air Force Base, Ohio. Rpt. No. ASD-TDR-62-899. CAVITY VAPOR GENERATOR PROGRAM. Final Rpt. December 1962, 140 p. incl illus., tables   Unclassified Report

A description of the theoretical study, design, and test of a thermionic generator; utilizing solar energy concentrated by means of a parabolic collector. The generator produced 21.25 watts at a cathode temperature of 1773°K in solar test with a five foot diameter, sixty degree rim angle, parabolic collector.

Expected future performance of solar thermionic systems are discussed.

1. Thermionic conversion
2. Space power systems
3. Solar energy conversion
   I. AFSC Project 8173 Task 817305-14
   II. Contract No. AF33 (616)-8394
   III. General Electric Co. Missile & Space Div.
   IV. D. L. Purdy
       R. C. Keyser
       F. A. Blake
       J. F. Williams
   V. Is available for OTS
   VI. Not in ASTIA collection

Aeronautical Systems Division, Flight Accessories Laboratory, Directorate of Aeromechanics, Deputy for Technology, Wright Patterson Air Force Base, Ohio. Rpt. No. ASD-TDR-62-899. CAVITY VAPOR GENERATOR PROGRAM. Final Rpt. December 1962, 140p. incl illus., tables   Unclassified Report

A description of the theoretical study, design, and test of a thermionic generator; utilizing solar energy concentrated by means of a parabolic collector. The generator produced 21.25 watts at a cathode temperature of 1773°K in solar test with a five foot diameter, sixty degree rim angle, parabolic collector.

Expected future performance of solar thermionic systems are discussed.

Aeronautical Systems Division, Flight Accessories Laboratory, Directorate of Aeromechanics, Deputy for Technology, Wright Patterson Air Force Base, Ohio. Rpt. No. ASD-TDR-62-899. CAVITY VAPOR GENERATOR PROGRAM. Final Rpt. December 1962, 140 p. incl illus., tables   Unclassified Report

A description of the theoretical study, design, and test of a thermionic generator; utilizing solar energy concentrated by means of a parabolic collector. The gen-

erator produced 21.25 watts at a cathode temperature of 1773°K in solar test with a five foot diameter, sixty degree rim angle, parabolic collector.

Expected future performance of solar thermionic systems are discussed.

1. Thermionic conversion
2. Space power systems
3. Solar energy conversion
   I. AFSC Project 8173
      Task 817305-14
  II. Contract No. AF33
      (616)-8394
 III. General Electric
      Co. Missile &
      Space Div.
  IV. D. L. Purdy
      R. C. Keyser
      F. A. Blake
      J. F. Williams

  V. Is available for
     OTS
 VI. Not in ASTIA collection

Aeronautical Systems Division, Flight Accessories Laboratory, Directorate of Aeromechanics, Deputy for Technology, Wright Patterson Air Force Base, Ohio. Rpt. No. ASD-TDR-62-899. CAVITY VAPOR GENERATOR PROGRAM. Final Rpt. December 1962, 140 p. incl illus., tables   Unclassified Report

A description of the theoretical study, design, and test of a thermionic generator; utilizing solar energy concentrated by means of a parabolic collector. The generator produced 21.25 watts at a cathode temperature of 1773°K in solar test with a five foot diameter, sixty degree rim angle, parabolic collector.

Expected future performance of solar thermionic systems are discussed.

1. Thermionic conversion
2. Space power systems
3. Solar energy conversion
I. AFSC Project 8173 Task 817305-14
II. Contract No. AF33 (616)-8394
III. General Electric Co. Missile & Space Div.
IV. D. L. Purdy
    R. C. Keyser
    F. A. Blake
    J. F. Williams
V. Is available for OTS
VI. Not in ASTIA collection